Role of primary cilia-mediated signaling in human and mouse models of Autosomal Dominant Polycystic Kidney Disease

By

Luciane Martins Silva
M.S. Clinical Analysis, Federal University of Rio de Janeiro, Brazil, 2008
B.S. Pharmacy, Federal University of Rio de Janeiro, Brazil, 2006

Submitted to the graduate degree program in Anatomy and Cell Biology and the Graduate Faculty of the University of Kansas in partial fulfillment of the requirements for the degree of Doctor of Philosophy.

_____

Chair: Dr. Pamela Tran

_____

Dr. James Calvet

_____

Dr. Brenda Rongish

_____

Dr. Katherine Swenson-Fields

_____

Dr. Darren Wallace

_____

Dr. Christopher Ward

Date Defended: November 16, 2018

The dissertation committee for Luciane Martins Silva certifies that this is the approved version of the following dissertation:

Role of primary cilia-mediated signaling in human and mouse models of Autosomal Dominant Polycystic Kidney Disease

Chair: Dr. Pamela Tran

Date Approved: December 5, 2018

Abstract

Primary cilia are non-motile microtubule-based organelles that extend from the apical plasma membrane of most vertebrate cells and mediate signaling pathways. Mutations in ciliary genes often result in renal cyst formation, yet, the mechanisms connecting primary cilia dysfunction to renal cystogenesis are unclear. To address this gap, I have examined the role of ciliary-mediated Hedgehog (Hh) signaling in human and mouse models of the most common renal cystic disease, Autosomal Dominant Polycystic Kidney Disease (ADPKD), and have investigated initiating mechanisms of renal cystogenesis in a ciliary mouse model, *Thm1* conditional knock-out (cko) mice. Here, I show that human ADPKD renal tissue has increased Hh activator, GLI1, in the nuclei of interstitial and cyst-lining epithelial cells, indicating increased paracrine and autocrine Hh activity, respectively. Further, Hh inhibitors reduced cell proliferation and microcyst formation of ADPKD primary cells, suggesting a functional role for increased Hh signaling in human ADPKD. To extend these investigations to mouse models, I downregulated Hh signaling genetically in *jck*, *Pkd1* and *Pkd2* cko mice on mixed strain backgrounds and found a trend toward reduced kidney weight/body weight ratios in *jck* and *Pkd1* cko mice, suggesting increased Hh signaling has a role in renal cystogenesis *in vivo*. Finally, to investigate initiating mechanisms of renal cystogenesis in *Thm1* cko mice, RNA sequencing was performed on whole kidney extracts, which revealed approximately 10 genes that are upregulated in both pre-cystic and cystic kidneys. Collectively, these genes are typically expressed by renal epithelial cells, endothelial cells and immune cells, suggesting misregulation of genes and pathways in all three compartments may potentiate *Thm1* cko renal cystogenesis. Of these 10 molecules, STAT3 appears most prominently activated and present in epithelia of non-dilated, dilated and cystic tubules and in the interstitium. Interestingly, IL6 cytokine-treated *THM1* knock-down 293T human renal cells showed a more

robust second wave of STAT3 activation that is preceded by enhanced ERK activation, suggesting that *THM1* regulates STAT3 and ERK signaling. Together, these data are the first to suggest increased Hh signaling has a role in ADPKD disease progression and increased STAT3 signaling has a role in disease initiation in a ciliary mouse model. Hh and STAT3 inhibitors are FDA-approved, and therefore, these pharmaceutical therapies may potentially be repurposed to treat ADPKD.

Acknowledgments

While working as a retail pharmacist in Brazil, I became interested in applying to the Interdisciplinary Graduate Program in Biomedical Sciences (IGPBS) program within the University of Kansas Medical Center (KUMC) to pursue higher education. I could not anticipate the amazing journey ahead of me, all the people I met along the way and the experiences we exchanged. I believe everything I experienced in the past six years made me a better person.

Before I was accepted in the IGPBS, I gained research experience in Dr. Jed Lampe`s laboratory. To Dr. Lampe - thank you for opening your doors to me and allowing me to begin my path to research in your lab. Your graduate students at the time, Stephanie and Kelli, are great scientists and taught me the specifics about their projects and the experiments they were working on. I learned so much and the experience confirmed my wishes to be accepted as a PhD student.

To Dr. Pamela Tran – no words can describe how unbelievably smart and AMAZING you are. You were setting up your lab at KUMC and gave me an opportunity to become a research assistant in your lab. The work, the projects, the discussions, I enjoyed everything. I am forever grateful for your ongoing mentorship, for helping me with the IGPBS application process and for ultimately taking me in as a student when I joined the program. You believed in me, sent me to conferences, taught me how to be successful in Science. You are one of the top reasons why I made it this far, I could not have chosen a more supportive mentor, a better friend. I look forward to seeing where your career will take you and read all the papers to come. Thank you for everything you did/do for me.

To my committee members – Dr. James Calvet, Dr. Brenda Rongish, Dr. Katherine Swenson-Fields, Dr. Pamela Tran, Dr. Darren Wallace and Dr. Christopher Ward - thank you for challenging me to become a better scientist, for all the advice you have given me throughout the

years, all the support you provided to me. I admire how dedicated you are to students and to your own careers and hope to excel in my career the way you excel in yours.

To the Anatomy and Cell Biology Department – I thank Dr. Dale Abrahamson, the Chair of the Department, for always making yourself available to help students, attend presentations and for being so supportive and positive. I thank the graduate education directors, previously Dr. Peggy Petroff and currently Dr. Julie Christianson. You both help keep students on track to reach our goals. Dr. Christianson, I appreciate you supporting me by attending my presentations in addition to all the advice you gave me in my pursuit of earning a PhD. I also thank the students for the interactions, making the PhD experience a great one.

To everyone I worked with in Dr. Tran`s lab – thank you for being there for me, listening to my practice presentations, giving feedback on experiments, ideas, posters and life. To the summer students (Ram and Shwetha), teaching you over the last few summers helped me grow as a student. To Michael, I learned a lot of the animal work required for my projects from you, thank you. To Damon, you are always so calm and helpful at troubleshooting experiments. To Bailey – it is great to talk to you, you are such a positive person and I missed you in the lab when you graduated. To Wei – it has been a pleasure to work by your side and watch you become a terrific scientist. Finally, to Tana, we met not long ago but you are super helpful in the lab.

To every member of the Jared Grantham Kidney Institute, thank you for being so collaborative and for all the discussions and festivities. You make the Kidney Institute a great place to work.

To my Brazilian friends – I am thankful to have you in my life for so many years and that we can stay in touch despite the distance. Talking to each one of you always gives me a better perspective of life and helps me make important decisions.

To my family – Mom, Dad, Sister, Brother-in-law and Nephew, thank you for always believing in me, for coming to visit, cheering for me, celebrating my victories and helping me through my losses. And to my Mother-in-law, I value your friendship and the help provided with life issues, you enabled me to focus on my education.

To my wonderful husband Danny and our kids Lucas, Isabela and Lillian, you are the reason I want to be a better person, wife, mom, friend, student and why I put so much effort in my career. Danny, your support in everything I do keeps me going, makes me the happiest woman on Earth. I hope I can make you feel as proud of me as I am of you. Lucas, losing you was the hardest thing I had to go through, I learned that we never know where life will take us. I did not think I would move forward but your strength helped me. Isabela and Lillian, you are the light of my life, I want to be a good example to you. I want you both to be proud of me and want you to work hard and pursue your own dreams one day.

I dedicate this dissertation to my kids Lucas, Isabela and Lillian.

Table of Contents

Chapter One: Introduction

1.1 Primary cilia structure and assembly

Cilia are microtubule-based organelles that protrude from the apical plasma membrane of cells. Cilia are conserved across species, from one-celled organisms, such as *Chlamydomonas reinhardtii* and *Tetrahymena thermophile*, to invertebrates, such as *Drosophila melanogaster* and *Caenorhabditis elegans*, and to vertebrates and mammals [1-3]. Cilia are classified as motile, which occur as tufts on a cell and confer motility, or non-motile, which are present singularly on a cell and have a sensory role. In 1898, mammalian non-motile, primary cilia were first reported by Zimmermann, who proposed that these structures on renal epithelial cells sense fluid flow. These sensory organelles are essential for development and tissue homeostasis, and dysfunction of primary cilia results in disease, including Polycystic Kidney Disease (PKD) [4-6].

Primary cilia consist of an axoneme, comprised of nine microtubule doublets, that is ensheathed by a ciliary membrane and extends from a basal body, which is a modified centriole [7]. From the basal body, transition fibers, which enable centriole docking to the plasma membrane prior to ciliogenesis, extend to the transition zone, which acts as a ciliary gate, regulating the molecules that enter and exit the cilium [8] (Figure 1.1).

Primary cilia formation is coupled to the cell cycle, with cilia assembling when cells stop proliferating and disassembling when cells enter the cell cycle [9-11]. Prior to ciliogenesis, centrioles migrate to the apical plasma membrane and the mother centriole forms the basal body. Cilia are then synthesized and maintained by intraflagellar transport (IFT), which is the bi-directional transport of proteins along the microtubular axoneme. Anterograde IFT transports molecules from the base to the tip of cilium and is mediated largely by IFT complex B proteins (IFT172, IFT88, IFT81, IFT80, IFT74, IFT57, IFT54, IFT52, IFT46, IFT27, and IFT20) and the kinesin motor, while retrograde IFT returns molecules from the tip to the ciliary base and is

mediated by IFT complex A proteins (IFT144, IFT140, IFT139, IFT122, IFTA-1, and IFT43) and the cytoplasmic dynein motor [5, 11, 12]. Bardet-Biedl Syndrome (BBS) proteins are also important for ciliary protein transport. Eight BBS proteins form a complex called the BBSome, which interacts with Rab8, a nucleotide exchange factor, at the base of cilia, targeting vesicles to the cilium and promoting ciliary elongation [13]. Primary cilia act as mechanosensors and mediate signaling pathways, several of which are described in Section 1.4.

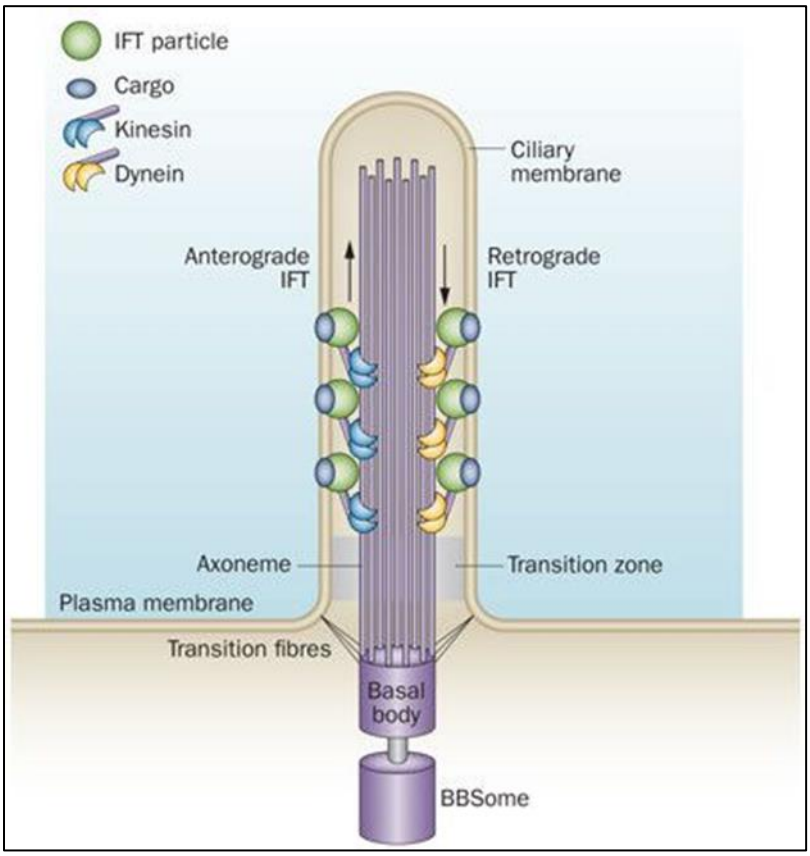

Figure 1.1: Primary Cilia structure and IFT transport.
The axoneme, transition zone and basal body are main components of the cilium. Anterograde and retrograde IFT are also represented in the image. Taken from Valente, E.M., et al., Primary cilia in neurodevelopmental disorders. *Nature Reviews Neurology*, 2013. **10**: p. 27 [14]. Image reprinted with permission from *Nature Reviews Neurology*, copyright 2013. License: 4412681159084.

1.2. Ciliopathies: Linking ciliary dysfunction to renal cystic disease

Ciliopathies are disease syndromes caused by mutations in genes that encode proteins that are important for ciliary structure and function. Since primary cilia are present on most cells throughout the body, ciliopathies affect multiple organ systems and clinical manifestations include obesity, skeletal dysplasia, and very commonly, cystic kidney disease [6] (Figure 1.2). Obesity is a cardinal feature of two ciliopathies, Bardet-Biedl Syndrome (BBS) and Alström Syndrome (ALMS) [15, 16], while skeletal dysplasia is a feature of ciliopathies like Jeune Syndrome (JATD) and Ellis van Creveld (EvC) [6, 17]. In contrast, renal cysts are featured in most ciliopathies. Treatment for ciliopathies is limited and cures are lacking [18]. Notably, certain clinical manifestations of ciliopathies are also observed in the general population. For instance, obesity affects 1 in 3 individuals in the United States [18], skeletal dysplasia affects 1 in 5,000 [19] and cystic kidney disease affects 1 in 500 worldwide [18]. Thus, studying ciliary genes and ciliary-dependent mechanisms may also contribute to better understanding of the pathogenesis of common medical burdens in the general population.

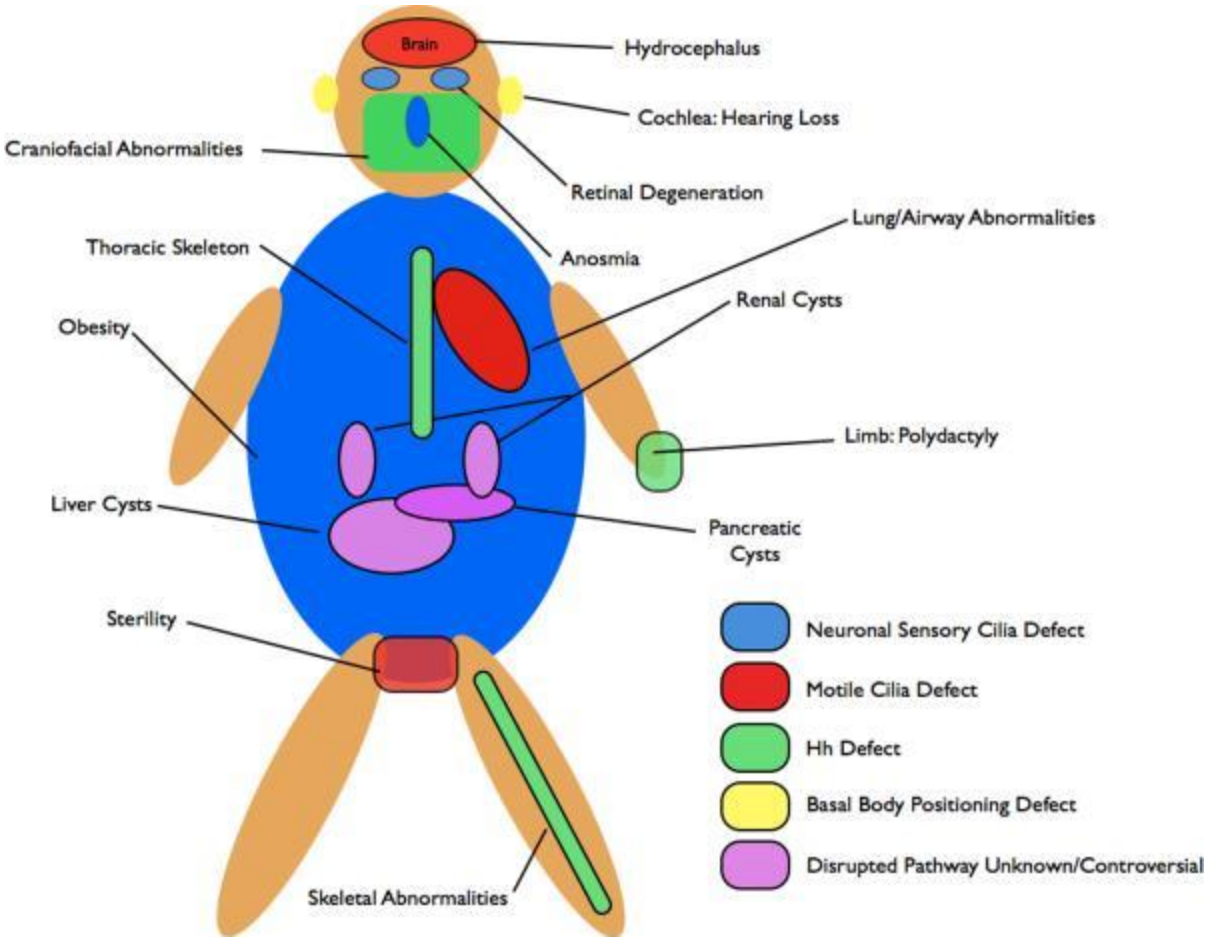

Figure 1.2 Clinical manifestation of ciliopathies.
Ciliopathies affect multiple organ systems since primary cilia are present on most cells throughout the body. Renal cystic disease is among the most common clinical manifestations in ciliopathies and is the focus of my studies. Taken from Goetz, S.C. and K.V. Anderson, The primary cilium: a signalling centre during vertebrate development. *Nat Rev Genet*, 2010. **11**(5): p. 331-44 [5]. Image reprinted with permission from *Nature Reviews Genetics*, Copyright 2010. License: 4412700063540.

1.2.1 Renal Disease

The kidneys are one of the most affected organs in ciliopathies. Renal diseases caused by ciliary dysfunction range from infantile to adult disorders and are characterized by renal cysts and fibrosis to varying extents [6]. Depending on the genes mutated, cilia-related renal diseases are classified as either non-Polycystic Kidney Disease (non-PKD) or PKD. BBS, Meckel-Gruber syndrome and nephronophthisis (NPHP) represent non-PKD diseases, while Autosomal Recessive PKD (ARPKD) and Autosomal Dominant PKD (ADPKD) comprise PKD. BBS and Meckel-Gruber Syndrome are characterized by renal dysplasia, resulting from defective differentiation of the renal parenchyma during kidney development and resulting in smaller kidneys that may have small cysts [6]. NPHP is caused by mutations in one or more of 20 genes (*NPHP1-NPHP11*, *NPHP 1L, THM1* and *SDCCAG8*) and represents the most common chronic kidney disease affecting individuals within the first three decades of life and causes end-stage renal disease in approximately 5% of patients. NPHP patients manifest cortico-medullary cysts and may present extra-renal abnormalities, such as retinal disease and fibrocystic liver disease [6]. The *NPHP* gene products, the nephrocystins, localize to primary cilia, basal bodies and centrosomes and have been found to interact with other ciliary proteins, such as BBS proteins. Finally, PKD is classified as either ARPKD or ADPKD [6]. ARPKD is a rare disease that affects 1 in 20,000 births and is caused by mutations in *PKHD1* (*Polycystic Kidney and Hepatic Disease 1*), which encodes the ciliary protein, fibrocystin. ARPKD leads to cysts being formed in renal collecting ducts, but also causes extra-renal manifestations, such as hepatic and pancreatic cysts. End-stage renal disease occurs in 30% of children with ARPKD. In contrast, ADPKD is the most commonly inherited kidney disorder, affecting 1:500 people worldwide. ADPKD is caused by mutations in *PKD1* or *PKD2* genes, which encode ciliary proteins polycystin-1 and polycystin-2, respectively. ADPKD

kidneys show cysts in all nephron segments, but most cysts are present in the collecting ducts. Cysts compress and damage surrounding renal tissue, which compromises renal function and can lead to end-stage renal disease by the 6th decade of life [20]. Since my thesis work focuses on ADPKD, I will elaborate more on this topic in Section 1.2.1.1.

There are differences between non-PKD and PKD renal cystic diseases. Non-PKD diseases are characterized by abundant renal fibrosis, resulting in reduced kidney size, while PKD patients present with massive cyst growth that increases kidney size and damages neighboring parenchyma causing fibrosis [21]. Additionally, mutation of non-PKD genes compromises cilia structure, while mutation of *PKD1* or *PKD2* generally does not. In mice, mutation of *Ift-B* genes causes absent or shortened primary cilia [22-24] and mutation of *Ift-A* genes results in shortened cilia with accumulation of proteins at the ciliary distal tip [25, 26]. In contrast, cyst-lining epithelial cells in human and mouse ADPKD kidneys generally have structurally intact primary cilia [21, 27]. However, increased ciliary length was reported on *Pkd1*$^{-/-}$ and *Pkd2*$^{-/-}$ cultured mouse renal epithelial cells [28] and on renal epithelial cells of the *Pkd1*$^{RC/RC}$ mouse, which carries a *PKD1* hypomorphic mutation that was identified in human ADPKD patients [29]. Interestingly, next-generation sequencing analysis of the genomes of 7 ADPKD patients revealed that each sample harbored truncating mutations in 5 to 15 ciliary genes, including genes associated with the basal body or centrosome, such as *PCM1*, *ODF2*, *HTT*, *CEP89* and *KIF19*, and genes required for intraflagellar transport and the transition zone, such as *IFT172*, *IFT80*, *NUP37* and *NUP62* [30]. These data suggest that ciliary genes may act as modifiers of ADPKD.

1.2.1.1 ADPKD Diagnosis

In ADPKD, renal fluid-filled cysts have been shown to develop *in utero* but grow very slowly and compromise renal function typically in adulthood [20] (Figure 1.2.1.1). Other clinical manifestations include pain, urinary tract infections, renal stones, hematuria, liver cysts, hypertension and cardiovascular complications, which are responsible for the majority of deaths [31].

The diagnosis of ADPKD is carried out by imaging studies in patients with a family history of the disease. Ultrasonography is the most common method, due to lower cost and availability, but more sensitive methods, such as computed tomography and magnetic resonance imaging, are also used. Lastly, genetic testing is an option in cases where imaging and family history do not provide certainty on the diagnosis [31].

Genetic tests include screening for mutations in *PKD1* and *PKD2*, which account for ~85% and 15% of ADPKD cases, respectively [6]. Mutation of *PKD1* results in more severe disease than mutation of *PKD2*, and is thought to be due to earlier onset of cysts [20]. Curiously, in a few reported cases, mutations in *PKD1* or *PKD2* were not found, causing speculation of the presence of a third ADPKD locus [32]. Further analysis of ADPKD families showed ~3% of genetically unresolved cases have mutations in *GANAB*, which encodes glucosidase II subunit a (GIIa). Loss of GIIa leads to defective maturation and subcellular localization of PC1 and PC2 [33]. These patients present a mild cystic phenotype.

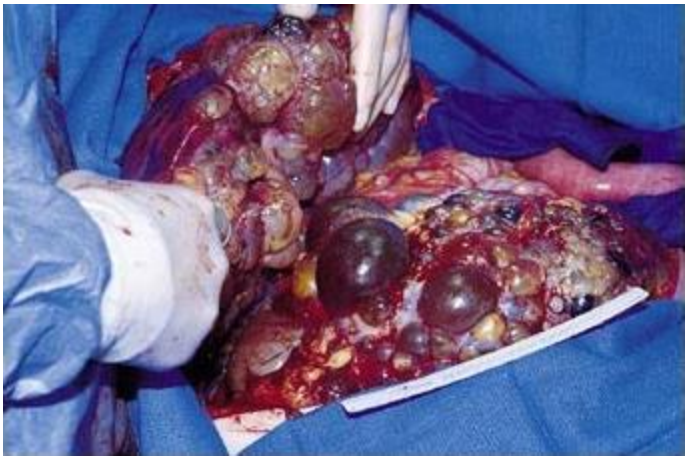

Figure 1.2.1.1 ADPKD in human. Kidneys of 45-year old man with ADPKD. Reproduced with permission from Brown, J. A., Images in clinical medicine. End-stage autosomal dominant polycystic kidney disease, 2002. Copyright Massachusetts Medical Society [34].

1.2.1.2 Polycystins are ciliary proteins

Polycystin-1 (PC1) is a large membrane protein with 11 transmembrane domains, a short cytoplasmic tail and a large extracellular region (Figure 1.2.1.2). The C-tail interacts with polycystin-2 (PC2), G proteins and proteins tethered to the cytoskeleton, while the N-terminus associates with additional proteins and carbohydrates. Since PC1 has several binding partners, PC1 is expected to have a wide range of functions, accounting for the diverse clinical manifestations that result from dysregulation of PC1 [35]. PC1 localizes to primary cilia, tight junctions, adherens junctions and other cellular compartments [35], but its localization to primary cilia has been reported to be critical for its function [36]. Further, PC1 is highly expressed in developing kidneys and is downregulated in adult kidneys [37].

PC2 is comprised of 6 transmembrane domains and a cytoplasmic C-terminus and N-terminus [35] (Figure 1.2.1.2). PC2 has homology to transient receptor potential channel subunits (TRPC) and has a nonselective cation channel activity that is permeable to calcium. PC1 and PC2 form a complex. Structural analysis of the human PC1/PC2 complex revealed one PC1 molecule interacts with three PC2 molecules [38]. The same study suggests PC1 has a segment that resembles the structure of ion channels but PC1 structure is positively charged, indicating PC1 likely does not have channel activity, unlike PC2 [38]. PC1/PC2 complex is found within the primary cilia membrane. PC2 is also present in other cellular compartments, such as the endoplasmic reticulum and mitotic spindles [35] (Figure 1.2.1.2). In the kidneys, PC2 is expressed during and after development [37]. PC2 has several binding partners, allowing for diverse functionality, which includes microtubule stabilization and calcium channel activity [37]. The function of the ciliary polycystin complex remains controversial. The polycystin complex has been reported as a flow-induced calcium modulator, since renal cells without functional PC1 or PC2 were not able to

increase intracellular Ca^{2+} in response to physiological fluid flow [39] (Figure 1.2.1.2). This finding was suggested to link ciliary dysfunction to ADPKD, since homeostatic intracellular calcium levels are reduced in renal cells of ADPKD patients [39]. However, another group reported that ciliary calcium levels did not affect intracellular calcium, suggesting that the ciliary and intracellular calcium pools are distinct [40]. Moreover, the cilium has several calcium channels, such as Tmc7, TRPV4, and PKD1, PKD2, PKD1-L1, PKD1-L2, PKD2-L1, PKD2-L2 and alpha-epithelial sodium channel, but only si-RNA for *PKD1-L1* or *PKD2-L1* in human RPE cells reduced both inward and outward ciliary currents, suggesting PC2 may not be required to allow ciliary calcium signaling [41, 42].

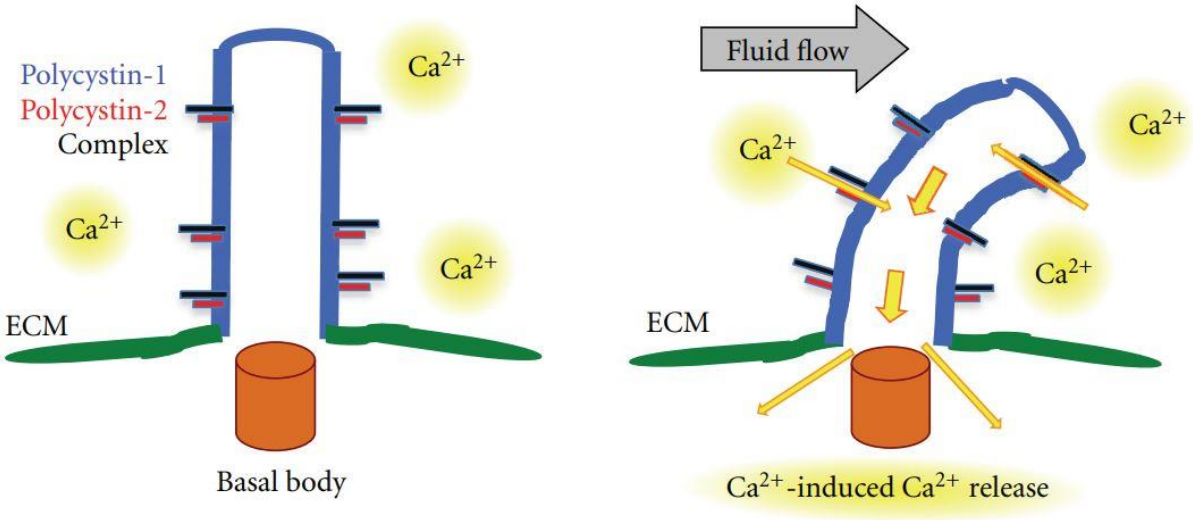

Figure 1.2.1.2 Polycystin-1 and Polycystin-2 localize to primary cilia.
PC1 and PC2 form a complex within the primary cilia membrane and have been proposed to mediate ciliary calcium signaling. Taken from Abdul-Majeed, S. and S.M. Nauli, Polycystic Diseases in Visceral Organs. *Obstetrics and Gynecology International*, 2011. **2011**: p. 7 [43]. Open Access through Creative Commons Attribution License.

1.2.1.3 Gene dosage or second-hit?

ADPKD patients inherit the disease as an autosomal dominant trait, yet mice heterozygous for *Pkd1* or *Pkd2* do not develop cysts, and only manifest the disease when the mutation is in the homozygous form. This has led to two hypotheses - gene dosage or second-hit - to explain how cyst formation is triggered and disease severity determined. These hypotheses remain controversial, as evidence exists in support of either hypothesis (Figure 1.2.1.3).

The gene dosage hypothesis proposes that the remaining functional *PKD1* or *PKD2* alleles in a patient are unable to sustain a threshold of PC1 and PC2 that is necessary to maintain renal tubular integrity, leading to cyst formation. This hypothesis is supported by studies that show that the type of mutation affects disease severity. For example, mice with an incompletely penetrant hypomorphic mutation (R3277C) in *Pkd1*, which has been identified in ADPKD patients, show different levels of disease severity when combined with different *Pkd1* alleles. $Pkd1^{RC/RC}$ develop slowly-progressive disease, while $Pkd1^{RC/-}$ mice show rapidly-progressive renal cystogenesis [29]. Additionally, $Pkd1^{+/-};Pkd2^{+/-}$ mice also develop cysts, supporting the notion that a polycystin threshold is necessary to maintain tubular stability [44]. More recently, human *PKD1* was shown to have abnormal patterns of splicing that truncate the PC1 protein, resulting in a novel smaller PC1 product and reduction of full-length PC1 [45]. These events do not occur in mouse, and the inherent decreased levels of full-length PC1 may cause humans to be more susceptible to cyst formation in the kidneys. Thus, these findings could account for why ADPKD develops in humans when a mutation is on 1 allele, but only develops in mice carrying mutations on both alleles.

However, only 2-3% of nephrons are affected in ADPKD patients and cysts are monoclonal, suggesting a second event or second-hit is necessary for cysts to form [20]. This hypothesis is

supported by several findings. Renal epithelial cells have a high rate of somatic mutations, implicating secondary mutations in the loss of functional PC1 or PC2 [46].

Further, the "developmental switch" phenomenon in mice, in which deletion of *Pkd1*, *Pkd2* or other cystogenic gene before postnatal day (P)14, when kidneys are not yet fully developed, causes aggressive, rapidly-progressing renal cystic disease, while gene deletion after P14 results in very mild, slowly-progressive disease, suggests loss of PC1 is not the only important event in this disease [47]. Lastly, the observation that metanephric *Pkd1*-null kidneys develop cysts *in vivo* and yet cyst formation does not occur naturally when these kidneys are cultured *ex vivo* suggests elements in addition to *Pkd1* loss are required for cystogenesis [48].

A speculation that combines these two hypotheses suggests that reduction of polycystins below a threshold may initiate cyst formation, while a somatic mutation may aid in cyst expansion [44]. Lastly, a third-hit hypothesis proposes that the environment contributes to severity of the disease by stimulating cellular processes such as inflammation and cell proliferation, which in turn stimulates cyst expansion [44].

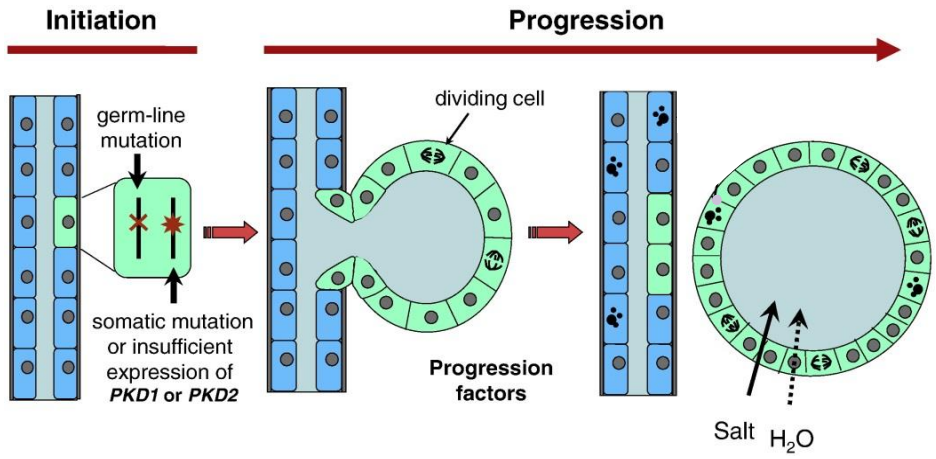

Figure 1.2.1.3 Cyst Formation in ADPKD.
Schematic showing disease initiation involving a germ-line mutation and a somatic mutation or insufficient expression of *PKD1* or *PKD2*. Cysts form as a result of increased cell division. Swelling of the renal tubule pinches off from the tubule wall to form a cyst that continues to grow due to persistent fluid secretion. Modified from Open Access Wallace, D.P., Cyclic AMP-mediated cyst expansion. *Biochim Biophys Acta*, 2011. **1812**(10): p. 1291-300 [49]. Image reprinted with permission from *Biochimica et Biophysica Acta*, Elsevier, copyright 2010. License: 4413111068148.

1.2.1.4 cAMP/Ca^{2+} signaling in ADPKD renal cystogenesis

ADPKD cells in cystic tubules have low levels of intracellular calcium (Ca^{2+}) and increased levels and abnormal function of cAMP, an important ubiquitous second messenger, which are central to disease processes [49]. A few mechanisms that lead to increased cAMP levels have been proposed. One is that decreased intracellular Ca^{2+} results in dysregulation of calcium-regulated adenylate cyclases (ACs) and phosphodiesterases (PDEs), which in turn, leads to increased production of cAMP [49]. Another proposed mechanism involves arginine vasopressin (AVP), a hormone active in the collecting ducts and distal nephron. AVP binds vasopressin V2 receptors, stimulates cAMP production, which activates protein kinase A (PKA), inducing higher water absorption back into circulation through aquaporin water channels [49]. In ADPKD cells, cAMP activates the mitogen-activated protein kinase/extracellular signal-regulated kinase 1/2 (MAPK/ERK1/2) pathway, increasing cell proliferation, and activates the cystic fibrosis transmembrane conductance regulator (CFTR) to induce fluid secretion, enabling cyst growth [48, 50]. Importantly, reducing Ca^{2+} levels in normal renal cells resulted in a PKD phenotype [51] and restoring intracellular Ca^{2+}levels prevented the aberrant proliferative response to cAMP in cultured ADPKD primary renal cells [52]. These studies further support the critical role for calcium homeostasis in maintaining renal tubular integrity.

1.2.1.5 Dysregulated ciliary length may contribute to renal cystogenesis in ADPKD

In addition to the polycystin complex localizing to primary cilia, cAMP and PKA are also found at relatively high basal levels within the cilium, where adenylate cyclases and cAMP are thought to regulate ciliary length and PKA is thought to regulate GLI processing and Hedgehog signaling [53, 54]. Ciliary length misregulation is suggested to be a contributing factor to renal

cystogenesis in disease models. Primary cilia of *jck* and *Pkd1*$^{RC/RC}$ mutant mice are lengthened [29, 55, 56], and pharmacological shortening and genetic ablation of cilia in *jck* mutant and *Pkd1/2* cko mice, respectively, attenuated the renal cystic disease [57, 58]. *In vitro* studies with mammalian epithelial cells showed that decreased intracellular $Ca^{2+}$and increased cAMP levels, followed by PKA activation, increase ciliary length [59]. Interestingly, ciliary length of renal tubule cells is modulated during renal injury and repair [60, 61], and *Pkd1* and *Pkd2* heterozygous mice are sensitive to acute ischaemia-reperfusion renal injury [62, 63]. The connection between ciliary length and disease models is not well understood, but ciliary length seems to be a dynamic process that needs to be closely regulated to sustain renal tubular integrity.

1.3. Murine models of renal cystic disease

Mouse models are valuable to elucidate the molecular mechanisms that lead to renal cystogenesis and to uncover new therapeutic targets against ADPKD. There is no model that recapitulates human ADPKD completely but the combination of studies using several models has helped advance research in this field. Here, I will describe the murine models that are relevant to my work.

1.3.1 *Pkd1* and *Pkd2* orthologous mouse models of human ADPKD

Several mutant alleles of *Pkd1* and *Pkd2* have been generated in mice in attempt to mimic the human disease. Since homozygous deletion of *Pkd1* and *Pkd2* is embryonically lethal, conditional, hypomorphic and overexpression alleles have also been generated [64]. Conditional alleles are advantageous in that deletion can be cell- or tissue-specific and/or temporally regulated depending on the promoter chosen to drive the Cre recombinase [64]. Cre recombinase is derived

from P1 bacteriophage and recombines two directly or inversely oriented 34 bp loxP sites on double-stranded DNA [65]. Commonly used promoter-Cre recombinases to study PKD are the *Ksp (Cdh16)-Cre*, which is expressed in the distal tubule, loop of Henle and collecting duct, and the *Rosa26-Cre^{ERT}*, which is expressed ubiquitously upon induction by tamoxifen. This type of inducible Cre recombinase was instrumental in identifying the "developmental switch" phenomenon, in which *Pkd1/2* deletion before kidneys have fully matured at P14 leads to rapidly progressing, severe renal cystic disease, while *Pkd1/2* deletion after P14 results in slowly progressing, mild disease [47]. Since ADPKD progresses slowly, mouse models that take longer to reach end-stage renal disease may resemble the human disease more closely. However, molecular mechanisms and pathways leading to renal cystogenesis in rapidly progressing models can be studied in a much more timely manner (3 weeks vs. 1 year) and have shown to also play a role in the human disease, indicating that both slow and fast progressing models have utility.

1.3.2 *Nek8 $^{jck/jck}$* mouse model

In mice, a nucleotide substitution of valine for glycine at amino acid 488 in the C-terminal domain of NEK8 results in cystic kidney disease in a mouse model called *juvenile cystic kidney disease* (*jck*)[66] (Figure 1.3.2). NEK8 is a serine/theorine kinase and is 1 of 11 mammalian Never in Mitosis Gene A-related kinases (NEK) [67] (Figure 1.3.2). *jck* mice have been reported to develop renal cysts by postnatal day 3 [66] and share several similarities with human ADPKD. *jck* mice have a relatively slowly-progressing disease, developing ESRD around 4 months of age, and cysts develop from several segments of the nephron, including the distal tubule, collecting duct and loop of Henle [56]. Additionally, cAMP levels in the kidney correlate with disease progression, and the cystic epithelia show overexpression and mislocalization of EGFR. These

factors lead to activation of B-Raf and ERK which contributes to cell proliferation, as seen in human ADPKD [52, 56]. Further, *jck* males have more aggressive cystic kidney disease than mutant females [56], a gender dimorphism that is also observed in human ADPKD [68]. Because of these similarities, *jck* mice have been considered a useful model to investigate human ADPKD.

NEK8 localizes to centrosomes during interphase of dividing cells and to the proximal region of cilia in ciliated cells [69, 70]. In contrast, the *jck* mutation causes NEK8 to mislocalize along the entire length of primary cilia [71] and to increase ciliary length [56]. NEK8 is activated upon exit of the cell cycle when primary cilia are formed, but *Nek8* knock-down does not affect ciliogenesis [69]. NEK8 also regulates G2/M proteins, indicating a role for NEK8 in the cell cycle [72]. Lastly, a GFP-NEK8 construct was localized to the nucleus [69, 73], where it was shown to be important for the ATM and Rad3-related (ATR) -mediated replication stress response. Cells without functional NEK8 show increased double strand breaks which accumulate due to reduced replication fork rates, increasing DNA damage [74].

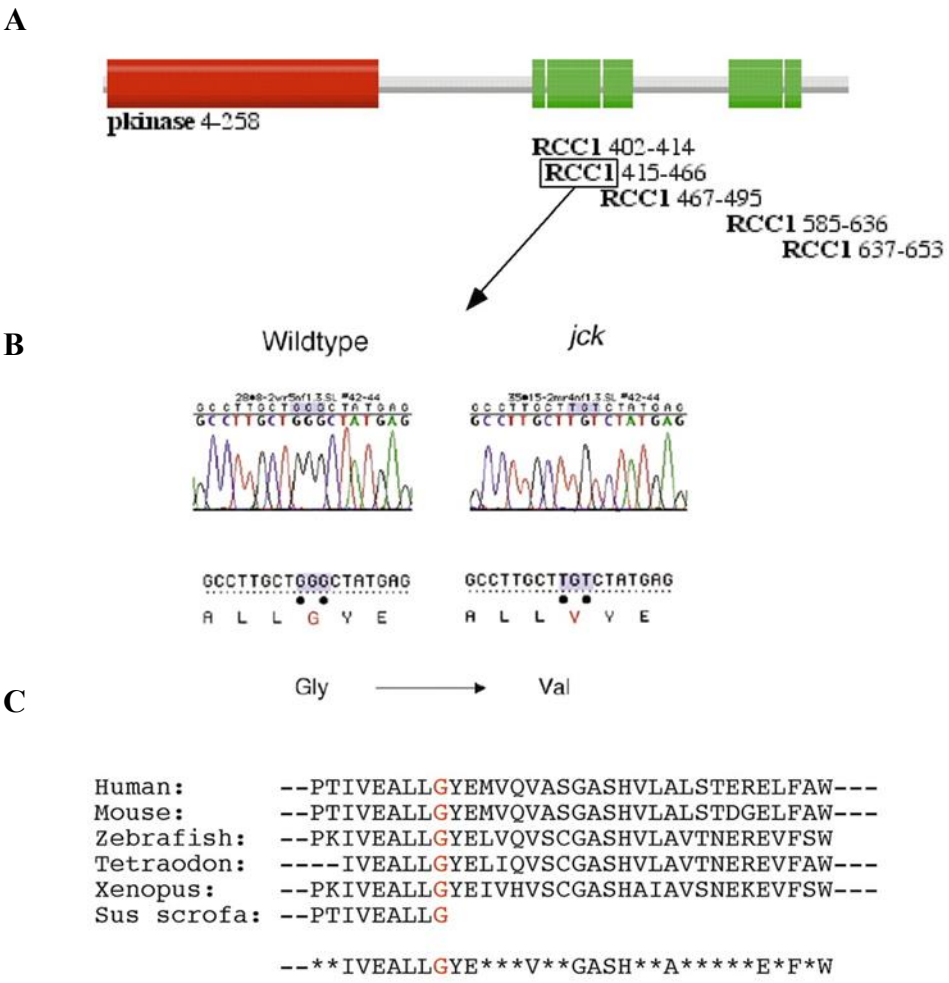

Figure 1.3.2 *Nek8* gene mutation in *jck* mice.
A) Protein domain structure of the murine NEK8 protein. B) A Gly-to-Val substitution at amino acid 448 occurs in *jck* mutant mice. C) Region containing the *jck* mutation is conserved across species. Regulator of chromatin condensation (RCC). Image republished with permission from The Company of Biologists Ltd, from A defect in a novel Nek-family kinase causes cystic kidney disease in the mouse and in zebrafish [67]. *Development and Disease*, Copyright 2002; permission conveyed through Copyright Clearance Center, Inc. License: 4413721365839.

1.3.2.1 Renal disease associated with *NEK8*

Nephronophthisis (NPHP) is an autosomal recessive kidney disease that is caused by germline mutations in the human *NEK* family of genes. NPHP causes renal cysts and fibrosis, progressing to end-stage renal disease (ESRD) in the first 3 decades of life [75]. NPHP accounts for 2.4% to 15% of ESRD in children [76]. *NEK8* has also been implicated in cancer. A missense mutation in *NEK8* was identified in a patient with pancreatic cancer [77], and *NEK8* was shown to be overexpressed in human breast tumors [72].

1.3.2.2 Relationship between NEK8 and Polycystins

Two studies have investigated the relationship between NEK8 and the polycystins. In one study, NEK8 was demonstrated to interact with PC2 but not with PC1 [71]. Additionally, the *jck* mutation was shown to lead to misregulated phosphorylation of PC2, increased ciliary localization of the polycystins and increased PC1 and PC2 levels in whole kidney extracts [71]. In the second study, single mutant embryonic kidney cultures of $Pkd1^{-/-}$ or $Nek8^{jck/jck}$ mice demonstrated that the level of the mutated gene plays a role in severity of cystogenesis, with more mutated alleles increasing cystogenesis [78]. Cysts formed in *Pkd1*-null or $Nek8^{jck/jck}$ single mutant embryonic kidney explants displayed dysfunctional cell-cell junctions, altered desmosomal protein expression and reduced E-cadherin levels, like ADPKD epithelia. *Nek8* mutant cells show increased PC1 within the cilium while *Pkd1* mutant cells show increased NEK8 within the primary cilia, indicating an association between the proteins [78]. Importantly, $Pkd1^{+/-}$; $Nek8^{jck/+}$ double heterozygous mice developed renal cysts in adulthood, unlike single heterozygous animals, suggesting NEK8 and PC1 mechanisms converge to induce renal cystogenesis [78].

1.3.3 *Thm1* mouse model

In an ethylnitrosourea (ENU)-derived mouse mutagenesis screen for late developmental phenotypes, the *alien* (*aln*) mutant which exhibits polydactyly, craniofacial and neural tube defects was identified [79]. The *aln* phenotype is caused by a glutamine to proline change at residue 15 in THM1 (Tetratricopeptide repeat-containing Hedgehog Modulator 1; also known as TTC21B), which causes the absence of THM1 protein [80]. *aln* mice die shortly after birth, and thus, a conditional allele of *Thm1* is necessary to investigate THM1 function post-natally [80] (Figure 1.3.3). Global deletion of *Thm1* at E17.5 or P0 causes renal cystic disease by 6 weeks of age, with cysts deriving from proximal tubules, Loop of Henle and collecting ducts [80] (Figure 1.3.3.1). Consistent with other ADPKD mouse models, *Thm1* conditional knockout (cko) mice show increased kidney to body weight ratio (KW/BW), increased cAMP levels, and increased blood urea nitrogen (BUN) levels, indicative of compromised renal function [80]. In contrast, global deletion of *Thm1* at 5 weeks of age causes mild cystic kidney disease, consistent with the developmental switch, and the more prominent phenotype in these mice is obesity, due to hyperphagia or over-eating, indicating a role for THM1 in regulating appetite [81].

THM1 is orthologous to *Chlamydomonas* IFT-A component, IFT139. THM1 localizes throughout the ciliary axoneme in a punctate manner and THM1 deficiency causes shortened cilia with accumulation of proteins at the distal ciliary tip, reflecting the role of THM1 in mediating retrograde IFT [25].

Epistasis analyses between *aln*, and Hh components, *Smo* and *Gli2*, revealed that THM1 acts as a negative regulator of Hh signaling downstream of the SMO signal transducer but upstream of GLI2 transcription factor [25]. In cystic kidneys of *Thm1* cko mice, increased Hh activity is also observed. Culture of E13.5 *aln* kidneys with cAMP, to induce renal cyst formation, together

with either control DMSO, or with Hh inhibitors, Gant61 or Sant2, showed that the Hh inhibitors reduced *aln* renal cystogenic potential [80]. Further, genetic downregulation of Hh signaling by *Gli2* deletion in *Thm1*,*Gli2* double conditional knock-out mice reduced renal cystogenesis, suggesting increased Hh signaling has a role in *Thm1*-mutant renal cystogenesis [80].

1.3.3.1 Disease associated with *THM1*

Mutations in *THM1* were identified in ~5% of ciliopathy patients, rendering *THM1* the most commonly mutated IFT gene. Mutations in *THM1* cause disease, such as NPHP, also act to modify diseases, such as Bardet Biedl Syndrome (BBS), in which patients have been identified to harbor mutations on both alleles of a *BBS* gene in addition to a heterozygous pathogenic mutation in *THM1* [82]. Additionally, *THM1* mutations have been found in patients with Joubert Syndrome, a disorder of the cerebellum [83]. Cerebellar architecture requires Hh signaling, and interestingly, *Thm1*-deficient Bergmann glia cells showed decreased levels of GLI1, a Hh target that reflect Hh activity, suggesting that *Thm1* acts as a positive regulator, rather than a negative regulator, of the pathway in these cells [83]. These studies demonstrate that regulation of Hh signaling by THM1 and/or ciliary proteins is context-dependent.

Lastly, a missense mutation in *THM1* was the first ciliary mutation identified in patients with familial focal segmental glomerulosclerosis (FSGS). FSGS affects podocytes and mature podocytes lack cilia [84]. This study showed that knock down of *Thm1* in podocytes leads to cytoskeletal alterations and abnormal cell migration and suggested that THM1 plays an extra-ciliary role in mature podocytes [84].

Figure 1.3.3: Protein structure of THM1
THM1 protein is comprised of 1,317 amino acids and predicted by Pfam (http://pfam.wustl.edu/) to have 11 TPR motifs. Modified from paper: Tran, P.V., et al., THM1 negatively modulates mouse sonic hedgehog signal transduction and affects retrograde intraflagellar transport in cilia. *Nat Genet*, 2008. **40**(4): p. 403-410 [25]. Reprinted with permission from *Nature Genetics*, copyright 2008. License: 4413181193600.

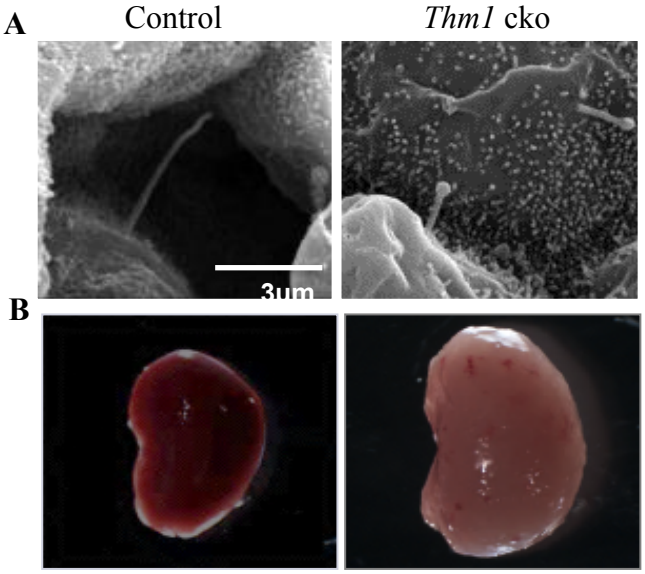

Figure 1.3.3.1: Deletion of *Thm1* results in ciliary phenotype and renal cystic disease in mice A) Scanning electron micrographs of primary cilia in collecting ducts. *Thm1* cko mice have shortened primary cilia with a bulb-like distal tip. B) *Thm1* cko mice at P42 (6 weeks of age) have renal cystic disease. *Thm1* was deleted at E17.5. Image from Tran, P.V., et al., Downregulating hedgehog signaling reduces renal cystogenic potential of mouse models. *J Am Soc Nephrol*, 2014. **25**(10): p. 2201-12 [80]. Reprinted with permission from *Journal American Society of Nephrology*, copyright 2014. License: 4413180797361.

1.4. Ciliary-mediated signaling pathways

1.4.1 Primary cilia as mechanosensors of flow-induced calcium signaling

Supporting Zimmerman's proposition from the 1800's that primary cilia of renal epithelial cells act as mechanosensors, flow-induced bending of primary cilia of renal epithelial cells increased intracellular calcium by increasing Ca^{2+} entry through Ca^{2+} channels and by releasing Ca^{2+} from intracellular Ca^{2+} stores [85]. Depletion of PC1 or PC2 abolished flow-induced increase in intracellular Ca^{2+}, leading to the proposition that the ciliary-localized polycystin complex mediates flow-induced Ca^{2+} signaling [39, 86]. More advanced imaging technology further demonstrated that bending of cilia on renal epithelial cells increased ciliary Ca^{2+} and, subsequently, increased cytosolic Ca^{2+} [86, 87]. However, these findings and theories have become controversial because of reports from another group, who demonstrated that bending of primary cilia did not increase ciliary Ca^{2+}, and moreover, increased ciliary calcium minimally affected intracellular Ca^{2+} levels in their system. Conversely, increases in intracellular Ca^{2+} elevated ciliary Ca^{2+} pools. Ciliary Ca^{2+} concentrations were also shown to be approximately 5-fold higher than intracellular Ca^{2+} concentrations, suggesting that these two calcium pools are independent of each other [40, 88]. In addition to PC2, other TRP channels that can mediate calcium signaling localize to primary cilia [89, 90]. Studies from the same group that negated flow-induced ciliary Ca^{2+} signaling showed that TRP channels encoded by *Pkd1L1* and *Pkd2L1* generate ciliary calcium currents, while the polycystins did not [41]. These conflicting results could be due to the use of different cell models and imaging techniques. These contradictory data suggest that the function of primary cilia and the polycystin complex as mechanosensors to induce ciliary calcium signaling requires further investigation.

1.4.2 Hedgehog Signaling

The mammalian Hedgehog (Hh) pathway is fundamental for development and tissue homeostasis and is the best characterized, cilia-mediated pathway [91]. Hh signaling was first identified in *Drosophila melanogaster*, which revealed core signaling components conserved across species. Hh ligand is modified and released to activate the Patched (PTCH) receptor, a large multipass transmembrane transporter-like protein, and consequentially, the Smoothened (SMO) signal transducer, ultimately causing post-translational modification and activation of Cubitus/Glioma (Cu/GLI) transcription factors [92].

In mammals, many of the Hh signaling events occur at the primary cilium [93]. The pathway is initiated by one of three Hh ligands, Indian (*Ihh*), Dessert (*Dhh*) or Sonic Hedgehog (*Shh*). Hh ligands are lipid-based proteins that undergo post-translational modifications to be secreted by producing cells and transported [94, 95]. Hh ligands have tissue-specific roles. *Ihh* plays a role in bone development, *Dhh* in spermatogenesis and *Shh* is essential for neuronal cell fate in embryonic development [96]. During mouse development, *Shh* is first produced by cells in the notochord and the floor plate, but as development progresses, other cell types produce and release Hh ligands [96]. Upon ligand binding to the PTCH receptor present in the ciliary membrane, PTCH exits the cilium, and concomitantly, Smoothened (SMO), which is a member of the G protein-coupled receptors (GPCR), translocates to the primary cilium and is activated. In canonical Hh signaling, SMO activates GLI transcription factors (GLI1, GLI2 or GLI3), which then translocate from the cilium to the nucleus to modulate transcription of Hh target genes, thus controlling cell proliferation, differentiation and cell fate (Figure 1.4.2). While GLI1 is an obligate transcriptional activator that functions in its full-length form, GLI2 and GLI3 can function as activators in their full-length form or as repressors upon cleavage of their C-terminal activation domain. GLI2 is

thought to function mainly as an activator, and GLI3 as a repressor [93, 97-99]. A series of phosphorylation and ubiquitylation events beginning with phosphorylation by protein kinase A (PKA) dictate the cleavage and activity of GLI proteins [91]. The ratio between the active and repressive forms of GLI transcription factors regulate canonical Hh signaling output in a tissue-dependent matter [100]. Interestingly, Hh signaling can be activated independently of GLI transcription factors in a noncanonical pathway. The activation and role of non-canonical Hh signaling are less well-defined than canonical Hh signaling [101].

In mice, mutations in *Ift* genes result in embryonic phenotypes associated with dysregulated Hh signaling, demonstrating a central role of primary cilia in regulating the Hh pathway. Mutations in most *Ift-B* genes, which are required for anterograde IFT, result in absent or shortened primary cilia, and cause a loss of Hh signaling. This was shown in *Ift172*[22], *Ift88*[22], *Ift52*[23], and *Ift57*[24] mutant mice, which exhibit a loss of caudal neural tube ventral markers [93], which require Hh signaling [25]. In contrast, mutations in *Ift-A* genes, such as *Thm1*[25] and *Ift122*[26], which are important for retrograde IFT, cause shortened cilia with accumulation of proteins in a swollen, bulb-like distal tip. These mutants also show upregulation of Hh signaling, with expansion of ventral-specific markers in the caudal neural tube [93]. Collectively, these data suggest opposing roles for *Ift-A* and *Ift-B* genes in regulating Hh signaling, or that *Ift-A* and *Ift-B* together finely tune regulation of signaling pathways.

The mechanisms by which IFT complexes and individual IFT proteins modulate Hh signaling remain incompletely understood, but individual IFT proteins are also likely to have distinct roles. *aln* mutant embryos which lack THM1, show increased Hh signaling, and presence of GLI full-length proteins and SMO in mutant cilia [25]. However, mouse embryonic fibroblasts (MEF) derived from complex A *Ift144*-null mice did not show ciliary localization of SMO, even

when cells were treated with a small molecule Hh activator and SMO agonist, SAG, suggesting different IFT complex A proteins have distinct roles in regulating transport of Hh signaling components within cilia [102].

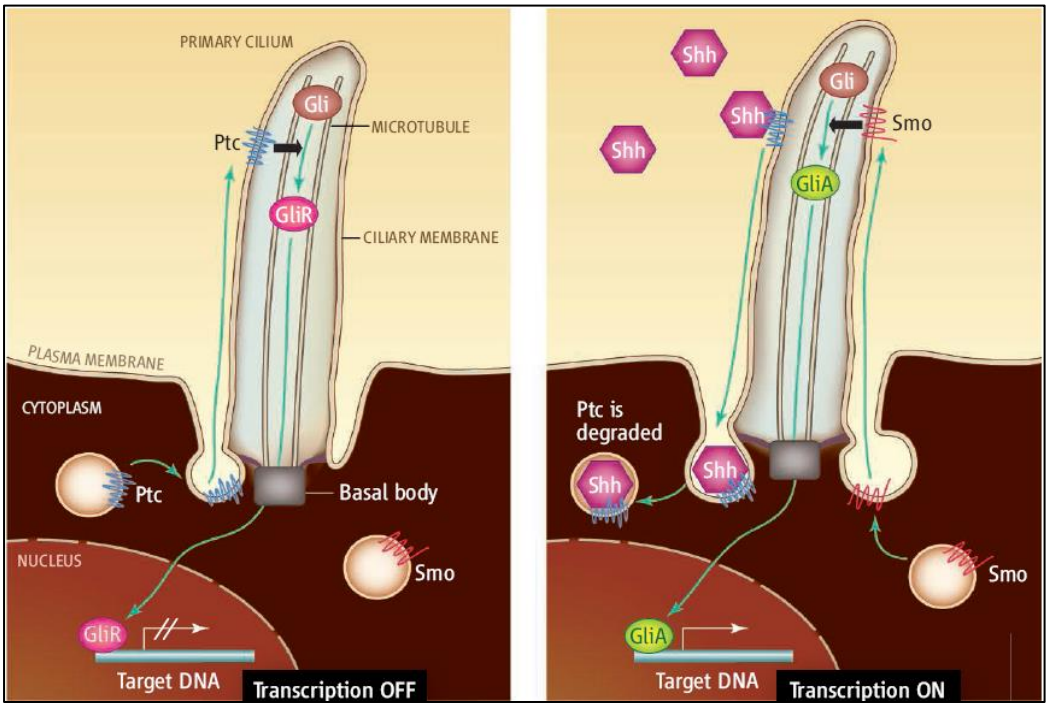

Figure 1.4.2: Mammalian Hedgehog Signaling.
Diagram on the left: Hh pathway in the absence of Hedgehog stimulus. PTCH receptor is present in the ciliary membrane, preventing GLI transcription factors from being activated. Diagram on the right: Hh pathway in the presence of Hh ligand. Hh-bound PTCH exits the cilium, and SMO enriches in the cilium, where it is activated leading to activation of the GLI transcription factors. Image from Christensen ST, Ott CM., A ciliary signaling switch. *Cell signaling*, 2007. 20; 317:330 –331[103]. Reprinted with permission from AAAS.

1.4.2.1 Hh signaling in the kidney

Shh and *Ihh* ligands are expressed in renal tubular epithelial cells [104]. Hh signaling is active in embryonic kidneys and dampened after development. In mice, *Shh* deficiency or pharmacological inhibition of SMO compromised renal organogenesis by decreasing levels of GLI1, GLI2 and GLI3A:Gli3R, and in turn, expression of kidney patterning genes and cell cycle regulators [105]. Importantly, elimination of *Gli3* in $Shh^{-/-}$ mice allowed kidneys to develop normally and restored expression of affected genes [105]. These results are thought to be due to the role of GLI3 in regulating nephron formation [106].

Hh signaling is a developmental pathway that is usually activated during organogenesis and downregulated following organ development. In contrast, inappropriate activation of the Hh pathway in adulthood is commonly associated with disease. Adult mice that underwent unilateral ureteral obstruction (UUO) developed renal fibrosis, which was associated with increased *Gli1*, *Gli2* and *Gli3* mRNA expression, suggesting increased Hh activity [104]. Interestingly, SHH and IHH ligands were present in renal epithelial cells, while GLI1 and GLI2 were found in the interstitium, suggesting paracrine Hh signaling in this model [104]. Enhanced Hh activity has also been suggested to play a role in renal cystic disease. Increased *Gli1* transcripts have been shown in cystic kidneys of several mouse models, including *Arl13b*, *Ift140*, *Glis2*, *Thm1, jck* and *Pkd1* [80, 107-109] and genetic downregulation of the Hh pathway reduced renal cystogenesis in *Thm1* conditional knock-out mice [80]. Additionally, Hh inhibitors reduced renal cystogenic potential of *jck* and *Pkd1* mutant embryonic kidneys cultured with cAMP [80]. Moreover, transcriptome analysis of human ADPKD kidneys showed increased expression of Hh signaling components [110].

1.4.2.2 Hh signaling in other diseases

Increased Hh signaling is also associated with several cancers, such as basal cell carcinoma, medulloblastoma, lung, and renal cell carcinoma [111, 112]. Tumor cells release Hh ligand, which activates the pathway in the surrounding areas, promoting tumorigenesis. The pathway also promotes proliferation of cancer stem cells and is associated with promoting tumor invasiveness [111]. Interestingly, *in vitro* inhibition of Hh signaling reduced cell proliferation of renal carcinoma cells [112]. Several synthetic Hh antagonists are being tested in clinical trial for cancer [111].

1.4.2.3 Hh modulators

High-throughput screening for Hh modulators using various cell types has identified small molecule regulators of the pathway. SAG, a SMO agonist, activates the pathway by binding to SMO [113]. Cyclopamine, a Hh antagonist that interacts with SMO, prevents its activation, yet still allows SMO translocation to the primary cilium, illustrating that SMO ciliary translocation and activation are separate events [113-115]. In contrast, another SMO antagonist, Sant2, prevents Shh-induced SMO translocation to the cilium [113]. Itraconazole has been used as an anti-fungal therapy since 1988 and was discovered to antagonize SMO in the 2000s [116]. Itraconazole inhibits Hh by binding to SMO, on a different site than cyclopamine [116]. GDC-0449 is a SMO antagonist that is approved by the Food and Drug Administration (FDA) and is indicated to treat basal cell carcinoma, while ongoing studies aim to expand its recommendation for other diseases [117, 118]. Finally, Hh antagonists that inhibit targets downstream of SMO have also been identified. Gant61 is a hexahydropyrimidine that inhibits Hh signaling by interfering with the DNA binding activities of GLI1 and GLI2 [113, 119].

1.4.3 Other ciliary-mediated pathways

Since most vertebrate cells have primary cilia but not all cells have active Hh signaling, the possibility that primary cilia can mediate other signaling pathways was raised [5]. Indeed, Wnt and LKB1/AMPK signaling are pathways whose components have been localized to the cilium [5, 90].

Wnt signaling is conserved among species and plays a role in cell migration and development. Both canonical (β-catenin-dependent) and non-canonical (β-catenin-independent) Wnt signaling pathways are activated when ligand binds to frizzled receptors. In the canonical Wnt pathway, binding of the ligand to receptor increases levels of the transcription factor β-catenin. *Inversin* (INVS) is located at the base of the cilium and is increased in whole inner medullary collecting duct (IMCD) cell extract when flow is applied, *in vitro*. INVS inhibits canonical Wnt pathway but is required for non-canonical Wnt signaling, acting as a switch between canonical and non-canonical Wnt signaling, [90, 120]. Kidney specific inactivation of *Kif3a*, a ciliary protein, in mice results in cystic kidney disease and increased Wnt signaling activity, suggesting a link between cilia and Wnt signaling [121]. However, mutations in *Ift* ciliary genes in mice do not cause phenotypes that resemble Wnt signaling dysregulation [5], suggesting that primary cilia may be more important for Hh signaling than Wnt signaling during mouse embryogenesis [122].

Upon fluid flow, ciliary-localized liver kinase B1 (LKB1), a tumor suppressor kinase, phosphorylates AMP-activated protein kinase (AMPK), a molecule that senses energy levels. Upon phosphorylation, AMPK accumulates at the base of primary cilia, and downregulates the mammalian target of rapamycin (mTOR) pathway [123]. mTOR pathway plays a role in cell metabolism and growth and is upregulated in epithelial cells that line the cyst walls of human ADPKD kidneys [124]. Importantly, rapamycin, an mTOR inhibitor, and metformin, an AMPK

activator, attenuated renal cystic disease in PKD animal models [124-127]. However, clinical trials with mTOR inhibitors were unsuccessful in delaying disease progression [128-130].

1.5. Loss of primary cilia partially rescued cystic kidney disease in a mouse model

Paradoxically, loss of primary cilia in *Pkd1* and *Pkd2* conditional knock-out mice attenuates renal cystogenesis, which led to the proposal that a ciliary-dependent cyst-promoting mechanism occurs when polycystins are deficient [58]. Recently, ciliary PC1 was found to interact with a ciliary complex comprised of LKB1-ANKS3-NEK7-NPHP1, which suppresses expression of *Ccl2*, which encodes MCP1 (monocyte chemoattractant protein) and consequently regulates inflammation [131]. *Pkd1*,*Ccl2* mutant mice showed reduced renal cystogenesis, suggesting that the immune reaction triggered by CCL2 may link primary cilia to renal cystic disease [131]. Thus, these studies suggest *Ccl2* promotes PKD via a primary cilia mechanism and presents as a likely effective therapeutic target for ADPKD.

1.6. Drug therapy for ADPKD

The economic burden of ADPKD is estimated at several billions of dollars/year worldwide [132]. Drug therapy represents a good strategy to improve quality of life and reduce costs within the healthcare system. However, the molecular mechanisms underlying disease initiation and progression are not well understood, which makes development of drugs that effectively slow disease progression challenging. Several pharmaceutical approaches have been tested in clinical trials, including somatostatin analogs, mTOR pathway inhibitors, anti-hypertensives and regulators of the renin-angiotensin system, but most have not shown significant disease attenuation [128, 129, 133-135]. Only Tolvaptan, a selective arginine vasopressin V2 receptor antagonist, has

shown to significantly delay disease progression and is the only Food and Drug Administration (FDA)-approved drug for ADPKD. Tolvaptan decreases cAMP levels, which in turn decreases fluid secretion and cell proliferation [136]. The clinical success of Tolvaptan has led to clinical trials that focus on high water intake to mimic the effect of Tolvaptan [137]. Investigating and discovering cilia-mediated mechanisms leading to renal cystogenesis may provide novel drug targets and enhance therapy for PKD.

1.7. Study Significance

In this dissertation, *in vitro* and *in vivo* studies investigate cilia-mediated pathways that may play a role in initiation and progression of renal cystogenesis. In Chapter 2, I examine Hedgehog (Hh) signaling, an established cilia-dependent pathway, in ADPKD human primary cells and tissues. I have found that Hh inhibitors reduced *in vitro* proliferation and microcyst formation of ADPKD cells and that Hh activity is enhanced in cystic areas of ADPKD tissues, compared to normal human kidney tissues. These data suggest a role for Hh signaling in human ADPKD. While enhanced Hh activity plays an important role in various cancers and in renal fibroses, the pathway remains largely unexplored in PKD. In Chapter 3, using a genetic approach, I explore Hh signaling in ADPKD mouse models *jck, Pkd1 cko* and *Pkd2 cko,* on a mixed strain background. My data show Hh signaling may play a role in disease progression in most mouse models analyzed. In Chapter 4, I investigate initiating mechanisms of renal cystogenesis in *Thm1* cko mice using RNA-Sequencing. My data reveal upregulated STAT3 signaling in pre-cystic *Thm1* cko kidneys, while *in vitro* studies using *THM1* kd human kidney 293T cells show a dysregulated response to IL-6, which activates STAT3 signaling. Taken together, these studies are the first to implicate a functional role for Hh signaling in ADPKD progression and a role for

STAT3 in renal cyst initiation, proposing these pathways as therapeutic targets. Several Hh and STAT3 inhibitors are FDA-approved and could be used in future ADPKD studies.

Chapter Two: Inhibition of Hedgehog signaling suppresses proliferation and microcyst formation of human Autosomal Dominant Polycystic Kidney Disease cells

Previously published as an open access article as: Silva LM, Jacobs DT, Allard BA, Fields TA, Sharma M, Wallace DP, et al. Inhibition of Hedgehog signaling suppresses proliferation and microcyst formation of human Autosomal Dominant Polycystic Kidney Disease cells [138]. Scientific reports. 2018;8(1):4985.

2.1 Abstract

Autosomal Dominant Polycystic Kidney Disease (ADPKD) is caused by mutation of *PKD1* or *PKD2*, which encode polycystin 1 and 2, respectively. The polycystins localize to primary cilia and the functional loss of the polycystin complex leads to the formation and progressive growth of fluid-filled cysts in the kidney. The pathogenesis of ADPKD is complex and molecular mechanisms connecting ciliary dysfunction to renal cystogenesis are unclear. Primary cilia mediate Hedgehog signaling, which modulates cell proliferation and differentiation in a tissue-dependent manner. Previously, we showed that Hedgehog signaling was increased in cystic kidneys of several PKD mouse models and that Hedgehog inhibition prevented cyst formation in embryonic PKD mouse kidneys treated with cAMP. Here, we show that in human ADPKD tissue, Hedgehog target and activator, Glioma 1, was elevated and localized to cyst-lining epithelial cells and to interstitial cells, suggesting increased autocrine and paracrine Hedgehog signaling in ADPKD, respectively. Further, Hedgehog inhibitors reduced basal and cAMP-induced proliferation of ADPKD cells and cyst formation *in vitro*. These data suggest that Hedgehog signaling is increased in human ADPKD and that suppression of Hedgehog signaling can counter cellular processes that promote cyst growth *in vitro*.

2.2 Introduction

Autosomal Dominant Polycystic Kidney Disease (ADPKD) is among the most commonly inherited, life-threatening diseases, affecting 1:500 adults worldwide. ADPKD is characterized by the formation and growth of fluid-filled cysts in the kidneys, which compress neighboring tubules, resulting in renal injury and fibrosis. Many of these patients progress to end stage renal disease (ESRD) by the 6th decade of life. The molecular mechanisms underlying ADPKD are complex, involving misregulation of multiple signaling pathways and aberration of multiple cellular processes, including increased cell proliferation, fluid secretion, apoptosis and incomplete differentiation of tubular epithelial cells [35]. Most ADPKD cases result from mutations in *PKD1* or *PKD2*, which encode polycystin-1 (PC1) and polycystin-2 (PC2) transmembrane proteins, respectively. PC1 and PC2 localize to the primary cilium, a non-motile sensory organelle, and form a functional complex that is thought to mediate signaling pathways [39, 139].

Mutation of most ciliary genes causes renal cystic disease [140]; however, the role of ciliary dysfunction in renal cystogenesis remains unclear. Paradoxically, genetic ablation of primary cilia in *Pkd1* and *Pkd2* conditional knock-out mice attenuated PC-mediated renal cystogenesis, which led to the proposal that an undefined cilia-dependent signaling pathway promotes PC-deficient cyst formation [58]. Consistent with these data, pharmacological shortening of primary cilia in *Nek8*$^{jck/jck}$ mouse mutants, which model ADPKD, ameliorated *Nek8*$^{jck/jck}$ renal cystic disease [141].

The Hedgehog (Hh) signaling pathway is among the best characterized ciliary-mediated pathways. Hh signaling controls cell proliferation, differentiation and cell fate, and is essential for development and tissue homeostasis [91]. In the canonical pathway, binding of Hh ligand to the Patched (PTCH1) receptor at the cilium promotes ciliary exit of PTCH1 and ciliary entry and

activation of the Smoothened (SMO) signal transducer [142, 143]. The signal is transduced ultimately to the Glioma (GLI) transcriptional factors and final mediators of the pathway, whose activity is also regulated at the cilium.

Cilia are formed by intraflagellar transport (IFT), the bi-directional transport of protein cargo along the ciliary axoneme by IFT-B and -A complexes. In mice, loss of most IFT-B proteins causes absent or stunted cilia and the inability to respond to the Hh signal [144]. In contrast, loss of the IFT-A proteins, THM1 (TTC21B) and IFT122, results in accumulation of proteins in bulb-like structures at the distal tip of shortened cilia and enhanced activation of the Hh pathway [25, 26].. Deletion of *Ift-B* or *-A* genes in the kidney or globally during late embryogenesis causes renal cysts [107, 121, 145].

Hh signaling has been reported to promote renal proliferative diseases, including renal cell carcinoma [112, 146] and fibrosis [147], and several studies suggest Hh signaling may also influence cystogenesis [80, 108, 148, 149]. Cystic kidneys of several mouse models have shown upregulation of *Gli1*, a transcriptional target of the Hh pathway [80, 107-109], and Hh inhibition reduced cAMP-mediated cysts of cultured embryonic kidneys of several PKD mouse models [80]. Further, a transcriptome analysis of human ADPKD kidneys revealed increased expression of Hh signaling components [110]. Thus, we sought to extend our analyses of Hh signaling in renal cystogenesis to human ADPKD. To this end, we examined Hh status in human ADPKD renal tissue and primary cystic epithelial cells and assessed the effect of Hh modulators on ADPKD cell proliferation and cyst formation *in vitro*.

2.3 Methods

2.3.1 ADPKD tissue and primary cells

Human ADPKD and NHK tissues and primary cells were obtained from the PKD Biomarkers and Biomaterials Core at the University of Kansas Medical Center (KUMC)[150]. ADPKD kidneys were obtained from the KU hospital and hospitals participating in the Polycystic Kidney Research Retrieval Program with the assistance of the PKD Foundation (Kansas City, MO) and the Biospecimen Shared Resource (BSR) at KUMC. These kidneys were removed solely for clinical purposes and de-identified prior to being submitted to the Repository; therefore, the use of the materials is not considered human subjects research. The protocol for the use of ADPKD tissue for research was approved by the Institutional Review Board at KUMC. These patients were below the age of 60 years. Since the majority of the ADPKD cases is caused by mutation in *PKD1* and has an earlier onset of ESRD compared to patients with *PKD2* mutation (54 vs 74 years)[151] all of the primary ADPKD cells were likely derived from *PKD1*-mutant kidneys. Normal regions of human kidneys, confirmed by histological examination, were obtained from nephrectomy specimens through the BSR at KUMC. Normal kidneys withheld from transplantation due to poor perfusion characteristics and anatomical abnormalities were obtained from the Midwest Transplant Network (Kansas City, KS).

The protocol used to generate NHK and ADPKD primary renal epithelial cells has been detailed previously[50, 152-155]. Samples are retrieved from the renal cortex of NHK individuals and from the epithelium of surface (cortical) cysts of ADPKD individuals. Cells from several cysts are pooled together. Preparative steps, such as collagenase treatment and keeping cell passage numbers ≤2, which collectively keep lines fibroblast-free, are identical between NHK and ADPKD cells. The majority of ADPKD and NHK cells have been shown to stain positively for

Dolichos biflorus agglutinin, suggesting that most cells derive from collecting ducts [50, 153]. The Core provides approximately 1-2 million primary cells each of 1 NHK and 1 ADPKD line on a weekly basis to investigators.

2.3.2 qPCR

RNA was extracted using Trizol (Life Technologies) and RNA integrity was verified by the Genome Sequencing Facility at the KUMC. RIN values ranged from 8-10. One microgram of RNA was converted into cDNA using Quanta Biosciences qScript cDNA mix (VWR International). The analysis was made using Quanta Biosciences Perfecta qPCR Supermix (VWR International) and a BioRad CFX Connect Real-Time PCR Detection System. Primers used are described in Table 2. qPCR was performed on RNA lysates of three ADPKD and three NHK cell lines.

2.3.3 Western blot

Protein extracts were obtained by homogenizing frozen kidney tissue with Passive Lysis Buffer (Promega) cointaining proteinase inhibitor cocktail (Pierce) using Bullet Blender Bead Lysis tubes (MidSci) and a Bullet Blender Storm 24 (Next Advance) set at Speed 10 for approximately 10 minutes, centrifuging lysates at 4°C at maximum speed for 1 minute, and collecting the supernatant. Western blot was done as described [80], using primary antibodies for GLI1 and βactin (Cell Signaling Technology). Extracts from six NHK and five ADPKD frozen renal tissue samples were examined for GLI levels.

2.3.4 Immunohistochemistry

Human ADPKD and NHK renal tissue sections were deparaffinized in xylene and rehydrated through an ethanol series to distilled water. Antigen retrieval was performed by steaming tissue sections for 25 minutes in Sodium Citrate Buffer (10mM Sodium Citrate (Fisher Scientific), 0.05% Tween 20 (Fisher Scientific) in autoclaved water, pH 6.0). To minimize background staining, sections were treated with 3% hydrogen peroxide for 30 min, washed in PBS, then blocked with 1% BSA for 1 hour. Tissue sections were then incubated with GLI1 antibody (Cell Signaling) overnight at 4°C. Following 3 washes in PBS, sections were incubated with HRP-conjugated rabbit secondary antibody (Cell Signaling) for 30 minutes. Following another 3 washes in PBS, tissues were incubated with ABC reagent (Vector Laboratories), rinsed in PBS, and then incubated with SigmaFAST DAB metal enhancer (Sigma) until desired signal/color was obtained. To determine GLI1 localization in proximal tubules or collecting ducts, sections were incubated with fluorescein-conjugated *Lotus tetragonolobulus* or *Dolichus biflorus* agglutinin for 1 hour at room temperature, washed and mounted in Vectashield containing 4,6-diamidino-2-phenylindole (DAPI) (Vector Laboratories). Staining was visualized and imaged using a Nikon 80i light/fluorescent microscope and Nikon DS-Fi1 camera. Immunohistochemistry images were converted to grayscale.

2.3.5 Immunofluorescence

Cells were then washed with PBS, fixed with 4% paraformaldehyde and 0.2% triton X-100 for 10 minutes at room temperature, washed with PBS, and blocked with 1% BSA in PBS for 1 hour, and then incubated with antibodies against SMO (generous gift from Dr. K Anderson, and purchased from Abcam), IFT52, IFT81, IFT88, IFT140, BBS2, BBS5 (Proteintech) and acetylated

α-tubulin (Sigma) overnight at 4° C. To address localization of the SMO within cilia, cells were first treated with 500nM SAG (Enzo Life Sciences) in DMSO. Following 3 washes in PBS, cells were incubated with anti-rabbit AF488 and anti-mouse AF594 (InVitrogen Technologies) for 30 minutes at room temperature. Cells were washed 3X in PBS and mounted with Vectashield containing 4,6-diamidino-2-phenylindole (DAPI) (Vector Laboratories). Immuno-labeled cells were viewed and imaged using a Leica TCS SPE confocal microscope configured on a DM550 Q upright microscope. Each ciliary antibody was examined in a minimum of three NHK and three ADPKD cell lines.

2.3.6 Cell Proliferation

ADPKD or NHK cells (15,000 cells/well) were plated in a 24-well plate (Costar) in DMEM/F12 media containing 1% FBS, ITS (Insulin, Transferrin, Selenium) culture supplement (Fisher) and Pen/Strep and grown to approximately 70% confluency. Cells were serum-starved in DMEM/F12 media containing 0.02% FBS and Pen/Strep overnight. The following morning, cells were treated with 500nM SAG, 5μM Gant 61 or Sant2 (Enzo Life Sciences), 100μM cAMP (Sigma), 100ng/mL EGF (Sigma), DMSO (Sigma) alone or in combination for 48 hours. Cells were trypsinized in 100μl of Trypsin (Gibco), and 10μl were counted in a cell counting slide (Bio-Rad) using a TC20 automated cell counter (Bio-Rad). Assays were performed in triplicate wells, using primary cells from at least three NHK and three ADPKD kidneys.

2.3.7 Viability/Cytotoxicity Assay

Following the same 48-hour treatment of NHK and ADPKD cells with Hh modulators, alone or with cAMP, as done in the cell proliferation assays, the LIVE/DEAD

Viability/Cytotoxicity Kit for mammalian cells (InVitrogen) was used according to manufacturer's instructions. Cells were imaged using a digital camera attached to an inverted microscope Nikon Eclipse TE2000-U. Assays were performed in duplicate wells, using primary cells from three NHK and three ADPKD kidneys.

2.3.8 Microcyst Assay

ADPKD and NHK cells (4,000 cells/well) were dispersed in cold Type I collagen (Advanced Biomatrix; San Diego, CA) in wells of a 96-well plate, warmed to 37˚C to enable polymerization of the collagen gel. Defined media (DMEM/F12, Pen/Strep, ITS Culture Supplement (Fisher), $5x10^{-8}$ M Hydrocortisone and $5x10^{-12}$ M Triiodothyronine) supplemented with forskolin (5 μM) and EGF (5 ng/ml), to stimulate *in vitro* cyst formation, was placed onto collagen-suspended cells, and refreshed every 2-3 days over a 7-day period. Once microscopic cysts (microcysts) were observed, media was replaced with media containing either forskolin, EGF, DMSO (Sigma), 500nM SAG, 5μM or 10μM Gant 61 or 5μM Sant2 (Enzo Life Sciences) in combination or individually. For wells treated with Hh modulators alone, wells were incubated with defined media for 4h prior to treatment with Hh modulators, to wash out initial EGF and forskolin from the collagen matrix. Following microcyst assay, culture gels were fixed in 0.5% paraformaldehyde, and microcysts were photographed with a digital camera attached to an inverted microscope Nikon Eclipse TE2000-U, objective (2x). Diameters of spherical cysts with distinct lumens were measured using Image-Pro Premier 9.2 64 bit. Assays were performed in six replicate wells, using primary cells from three NHK and three ADPKD kidneys.

2.4 Results

2.4.1 GLI1 is upregulated in human ADPKD renal tissue

We performed Western blot analysis for GLI1, a target and activator of the Hh pathway. We found increased GLI1 in ADPKD compared to normal human kidney (NHK) tissue (Figure 2.1A; 2.2-2.3). Using immunohistochemistry, we observed more intense nuclear GLI1 staining in interstitial cells and in epithelial cells lining some cysts of ADPKD tissue (Figure 2.1B; Figure 2.4). We next incubated ADPKD tissue sections with fluorescein-conjugated *Lotus tetragonolobulus* (LTL) or *Dolichos biflorus* agglutinin (DBA) lectins or with antibody against Tamm-Horsfall Protein (THP) to examine the tubular origin of GLI1+ cells. While cystic cells did not label with LTL, a marker of proximal tubules, DBA or THP staining of cystic cells suggested that the cysts originated from collecting duct or Loop of Henle tubules, respectively, and that GLI1-positive epithelial cells were present in these cysts (Figure 2.5-2.6).

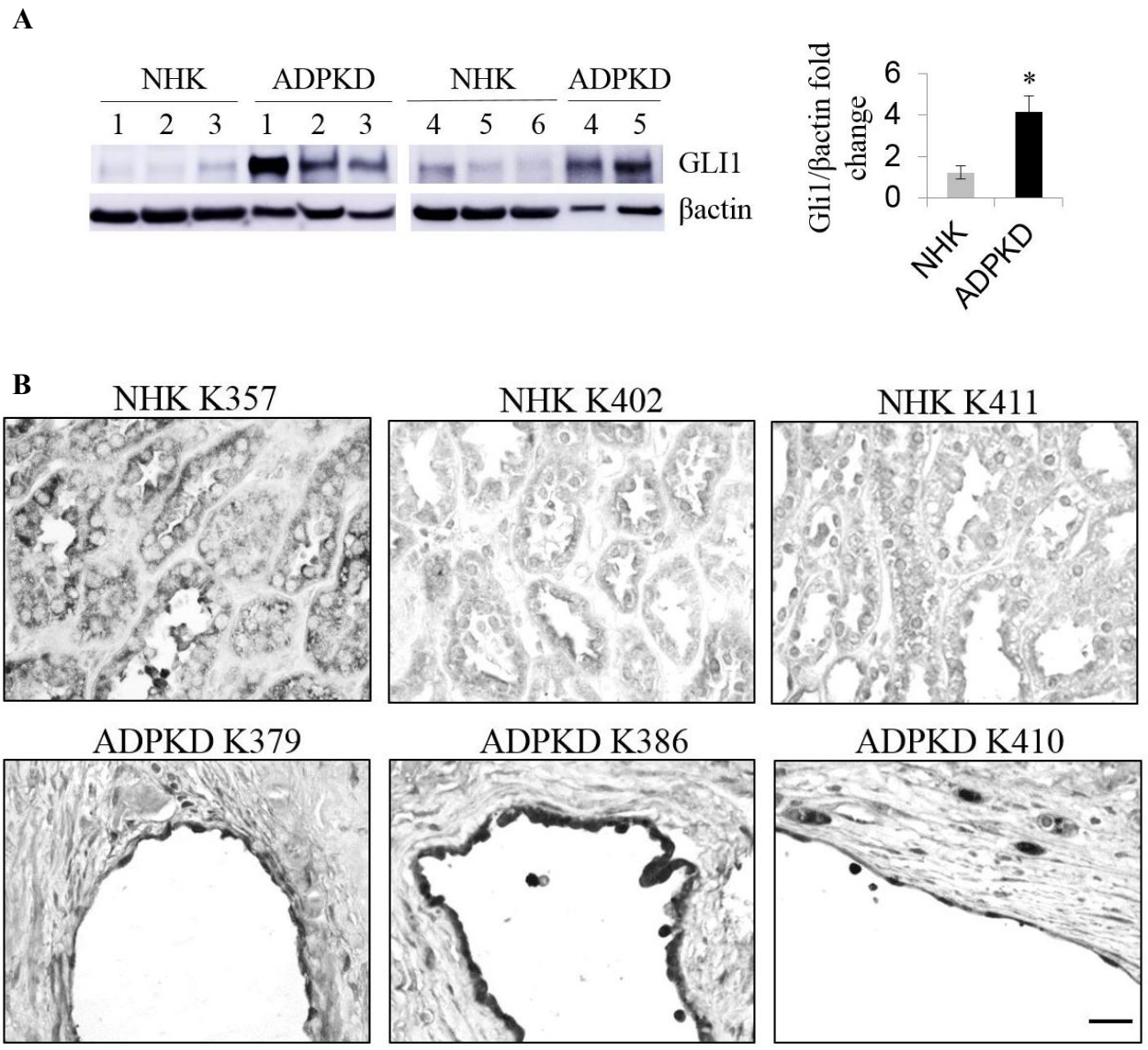

Figure 2.1: GLI1 is upregulated in human ADPKD renal tissue
A) Western blot analysis for GLI1 in normal human kidney (NHK) and ADPKD extracts of the renal cortex. Bars (mean ± SEM) are band intensity normalized to β-actin, and represented as fold change from NHK, set to 1.0. Quantification of GLI1 levels was performed on 6 NHK and 5 ADPKD tissue extracts (Table 1). Statistical significance was determined by an unpaired t-test. *P<0.05 B) Immunohistochemistry for GLI1 on NHK and ADPKD sections of the renal cortex. Scale bar = 50 μm.

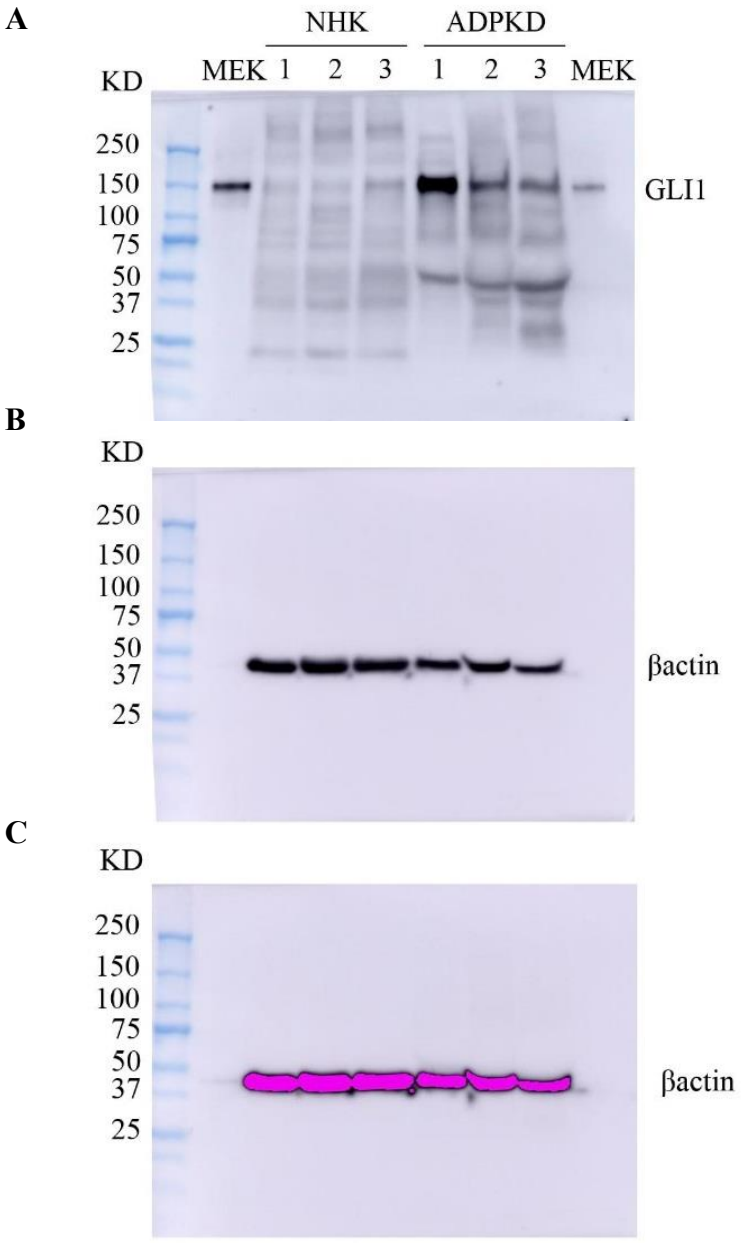

Figure 2.2: GLI1 is upregulated in human ADPKD renal tissue.
Full-length Western blots of Fig 1. Extracts of mouse embryonic kidney (MEK) were included as a positive control for GLI1 detection. Twice as much MEK extract was loaded in lane 1 than in lane 8. A) 1-minute exposure for GLI1. B) 0.5-second exposure for ß-actin. C) 40-second exposure for ß-actin. Longer exposure of ß-actin reveals presence of band in MEK extract lane 1. This low ß-actin expression indicates markedly higher GLI1 expression in mouse embryonic kidney than in human adult kidney. Pink bands indicate over-exposure.

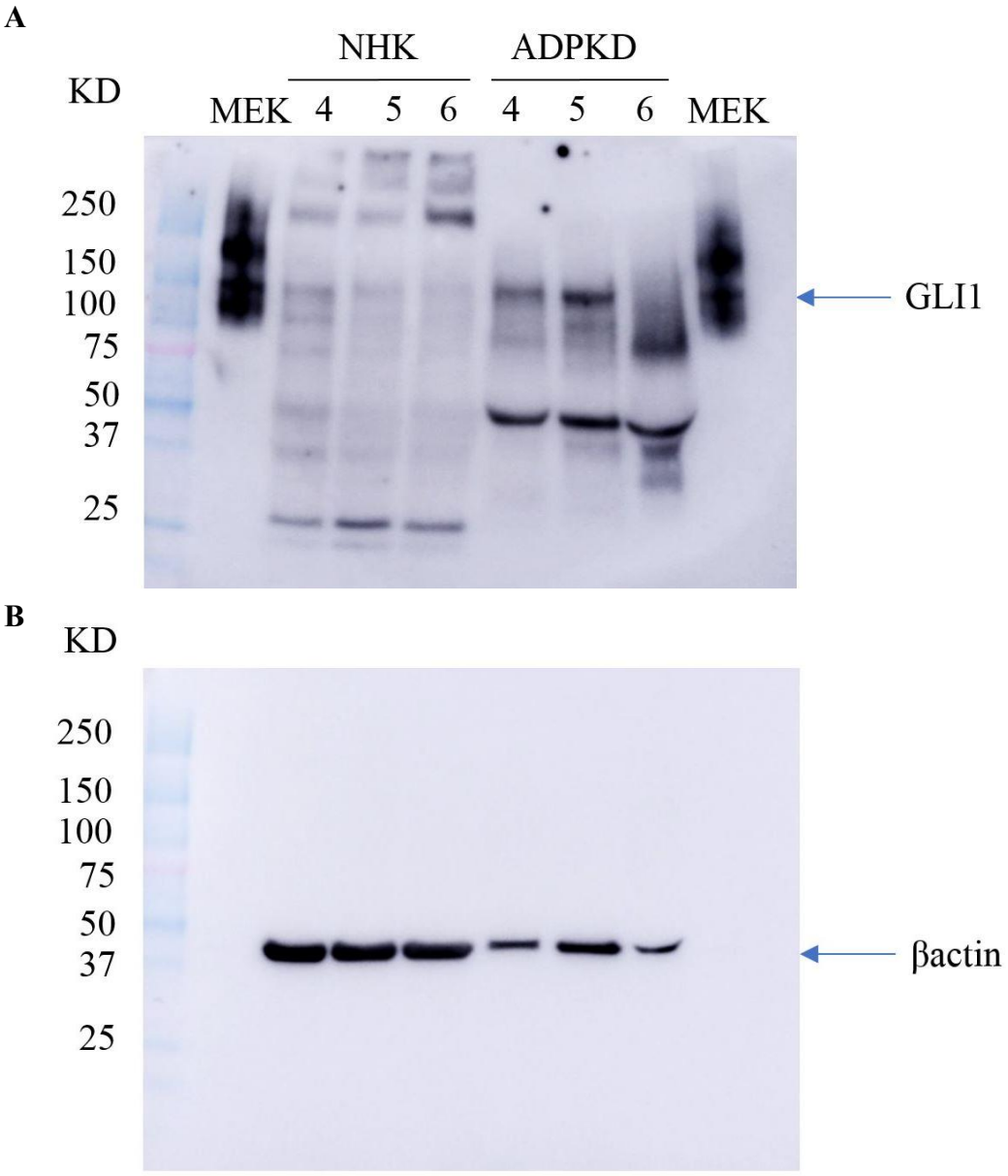

Figure 2.3: GLI1 is upregulated in human ADPKD renal tissue.
Full-length Western blots of extracts of NHK and ADPKD renal tissue, and mouse embryonic kidney (MEK), included as a positive control for GLI1 detection. A) 1-minute exposure for GLI1. ADPKD sample 6 appears degraded, and therefore, was not included in the GLI1 quantification in Fig 1A. B) 0.5 second exposure for ß-actin. Absence of ß-actin bands in MEK lanes indicates markedly higher GLI1 expression in mouse embryonic kidney than in human adult kidney.

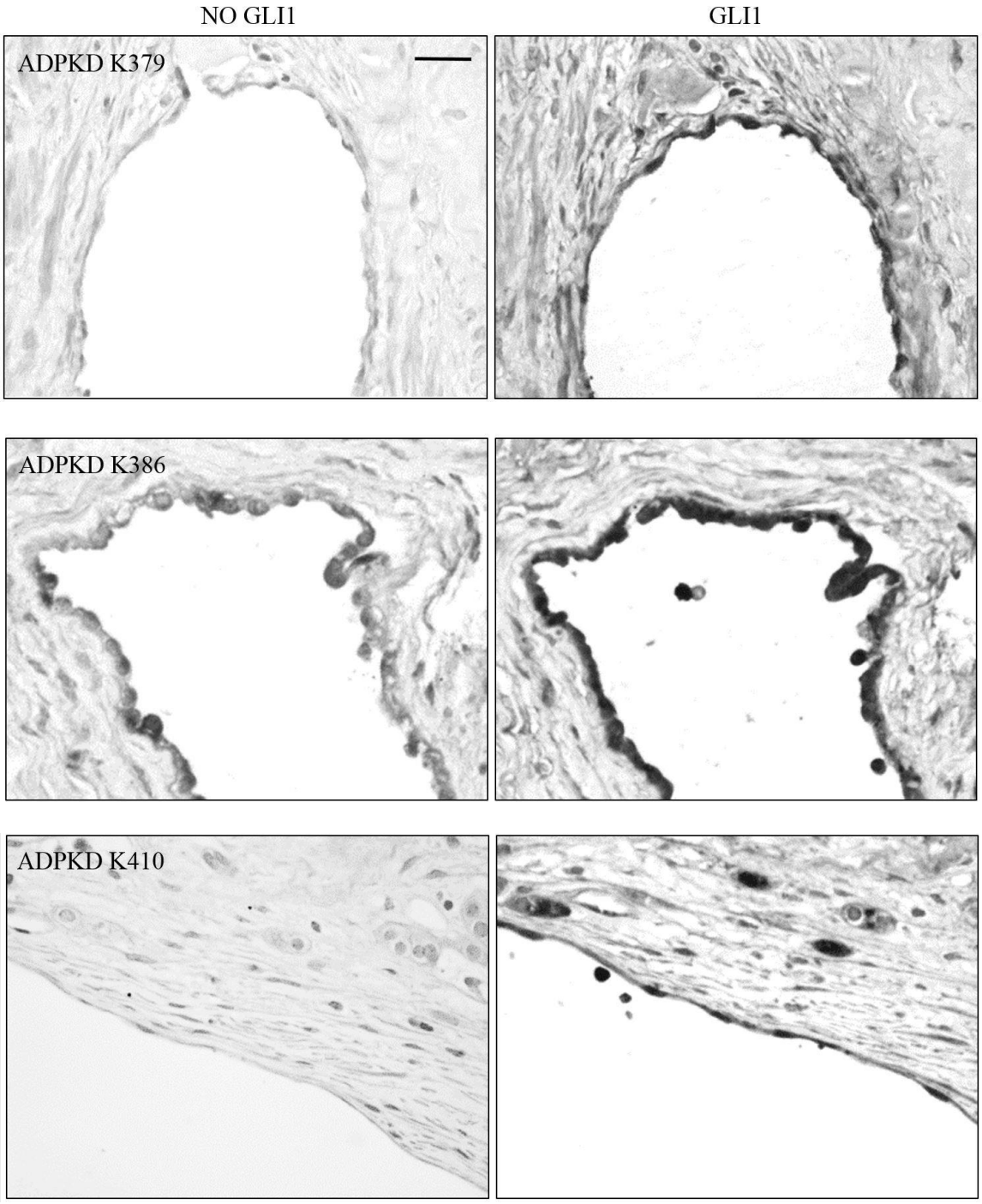

Figure 2.4: GLI1 immunohistochemistry on ADPKD tissue.
GLI1 immunohistochemistry with no GLI1 antibody control. Images obtained with a 40X objective lens. Scale bar = 50 μm.

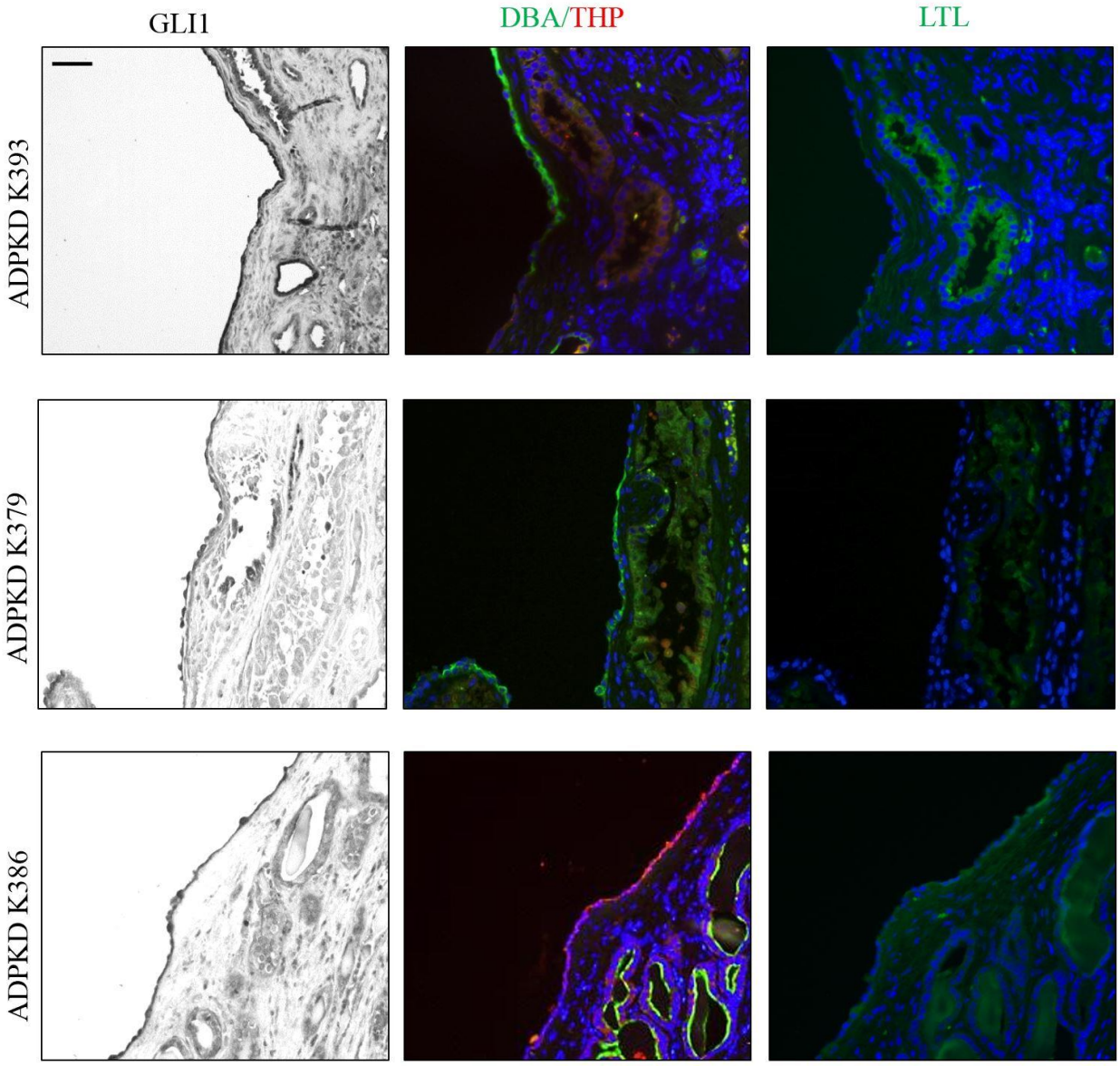

Figure 2.5: GLI1-expressing epithelial cells derive from collecting duct and Loop of Henle tubules

GLI1 immunohistochemistry and staining with DBA, LTL and THP on ADPKD sections of the renal cortex. Scale bar = 100μm.

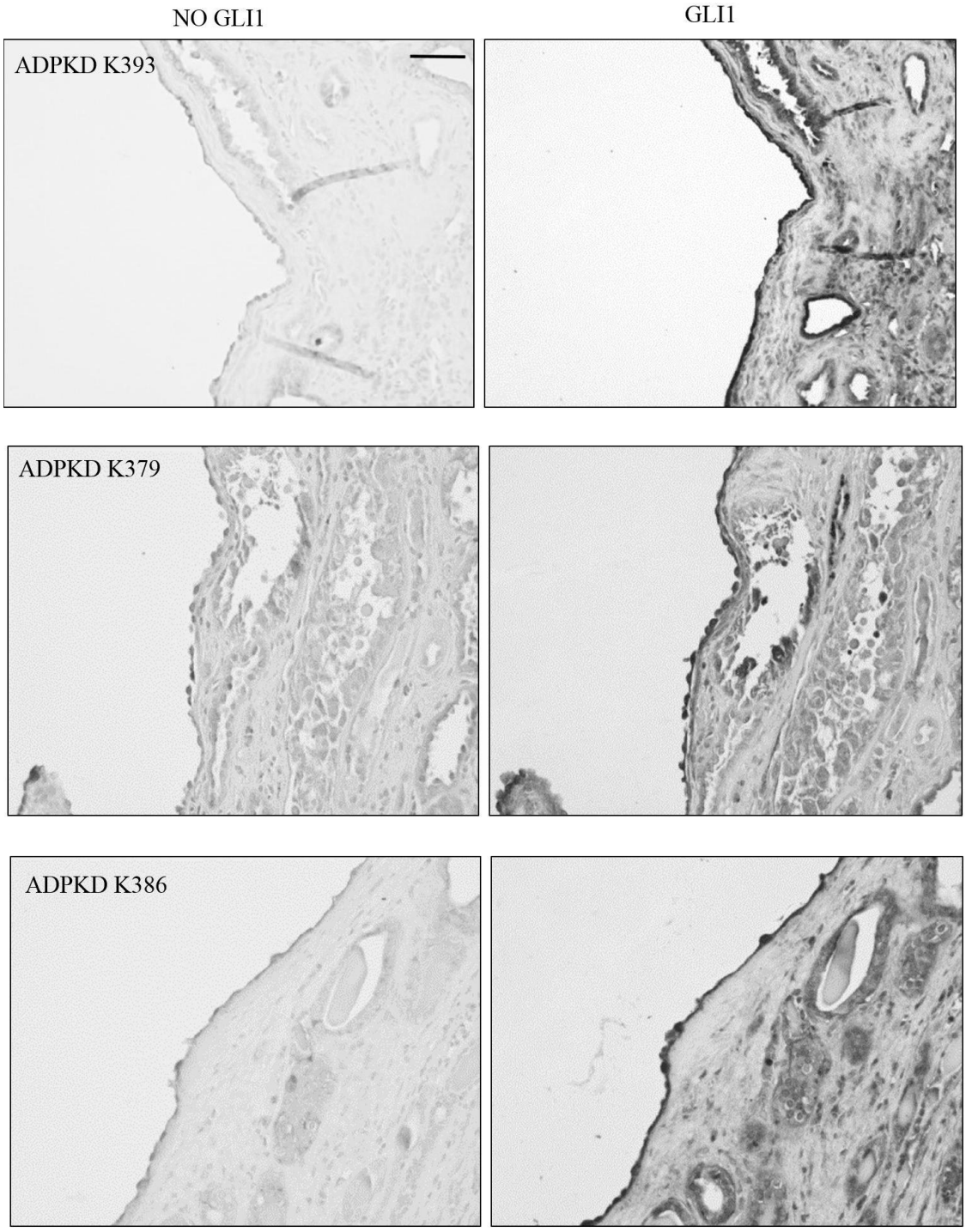

Figure 2.6: GLI1 immunohistochemistry on ADPKD tissue.
GLI1 immunohistochemistry with no GLI1 antibody control. Images obtained with a 20X objective lens. Scale bar = 100μm.

2.4.2 Ciliary trafficking and Hedgehog signaling are intact in ADPKD primary renal epithelial cells

In mice, ciliary length appears to affect PKD severity [58, 141]. Further, increased ciliary length has been reported in the *Pkd1*$^{RC/RC}$ mutant mouse, which harbors an ADPKD mutation [29], and in *Pkd1*$^{-/-}$ and *Pkd2*$^{-/-}$ - derived embryonic renal epithelial cells [55]. Since ciliary length can be modified via IFT, and IFT affects Hh signaling [144], we examined ciliary localization of IFT components in primary epithelial cells derived from the cortex of NHK kidneys or from surface cysts of ADPKD kidneys. The majority of NHK and ADPKD primary renal epithelial cells stained with varying intensities for DBA, but not for LTL or THP (Figure 2.7-2.8), suggesting most cells originate from collecting ducts, consistent with previous reports [50, 153]. In ADPKD primary cells, IFT-B components, IFT52, IFT81 and IFT88, and IFT-A component, IFT140, localized throughout the cilium, similar to their localization in NHK cells (Figure 2.9).

The BBSome is an 8-unit protein complex that shuttles protein cargo to cellular membranes and throughout the ciliary membrane and has been suggested to regulate the ciliary import and export of PC1 and PC2. *Bbs1* knock-down or expression of a dominant-negative form of Bbs3 in IMCD cells resulted in absence of PC1 in the cilium [156], while combined deficiency of *BBS4* and *BBS5* in retinal pigment epithelial (RPE) cells caused ciliary accumulation of PC2 [157]. To determine if the BBSome is conversely affected in ADPKD, we examined the localization of BBS components, BBS2 and BBS5 (Figure 2.9). Similar to the IFT proteins, the BBS proteins localized normally along the ciliary axoneme. Together, these data suggest that polycystin dysfunction does not overtly affect the ciliary trafficking machinery.

We examined Hh status in ADPKD primary renal epithelial cells. Using qPCR, we found that *GLI1*, *GLI2* and *GLI3* transcript levels were similar in NHK and ADPKD cells (Figure 2.10A).

Additionally, we examined SMO localization, which enriches in the cilium upon pathway stimulation [142]. In the absence of Hh agonist, SMO was mostly undetected in primary cilia of NHK and ADPKD cells, but following treatment with SAG, a SMO agonist, NHK and ADPKD cells showed similar ciliary enrichment of SMO (Figure 2.10B), suggesting similar Hh signaling levels. These data indicate that ADPKD primary renal epithelial cells have Hh signaling machinery and respond appropriately to Hh modulation.

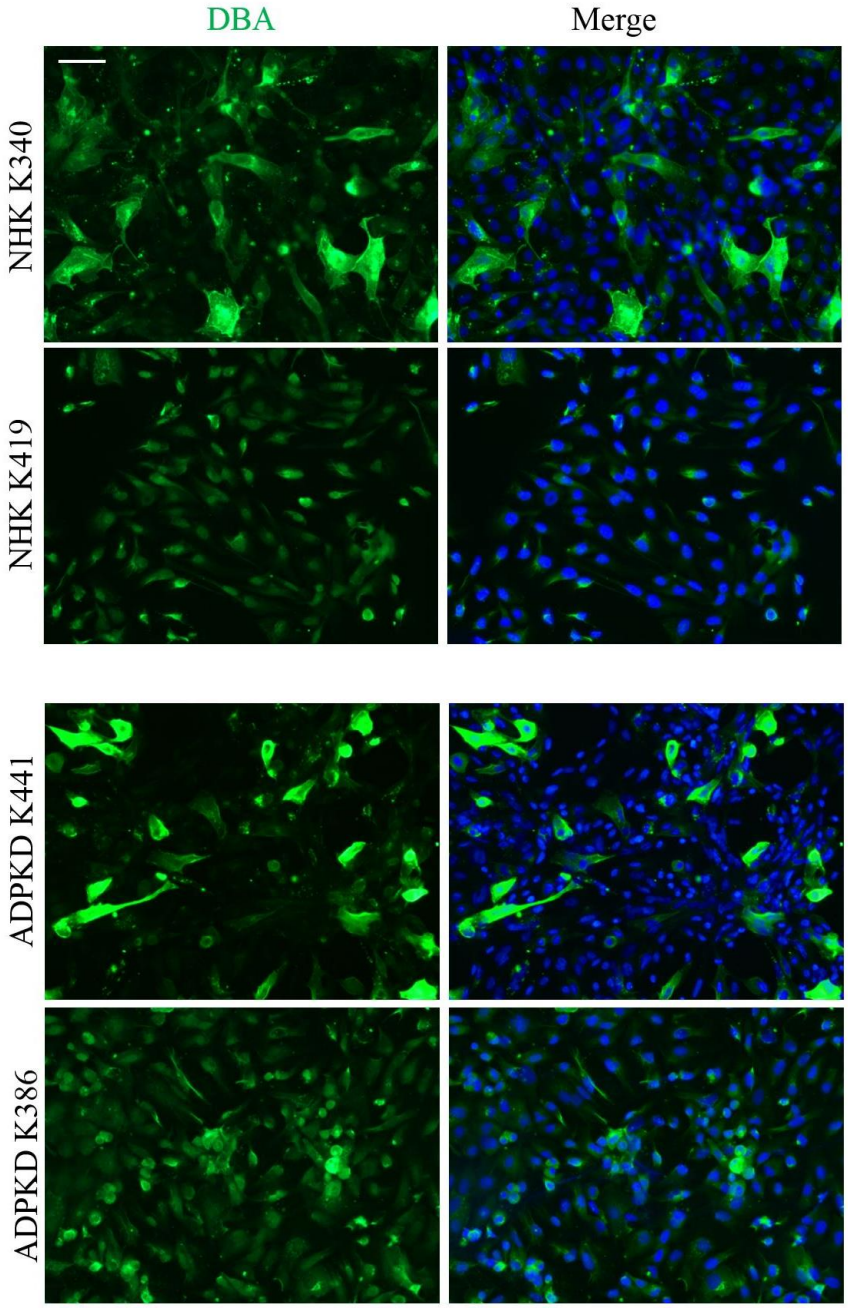

Figure 2.7: NHK and ADPKD primary renal epithelial cells are DBA-positive.
Representative staining of primary renal epithelial cells with DBA, marker for the collecting duct. Staining was performed in 5 NHK and 5 ADPKD cell lines. Scale bar = 100μm.

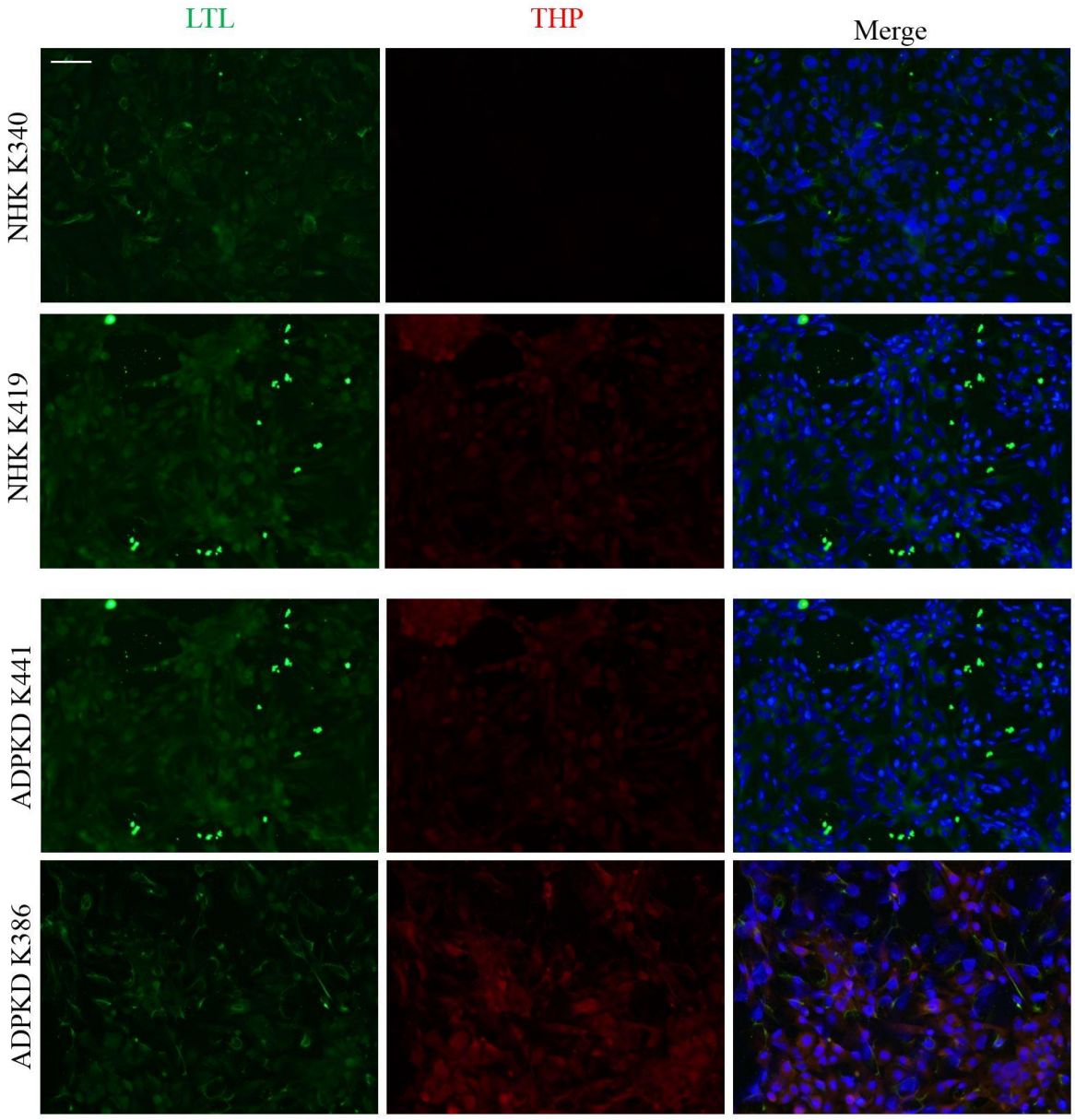

Figure 2.8: NHK and ADPKD primary renal epithelial cells are DBA-positive.
Representative staining of primary renal epithelial cells with LTL together with immunostaining for THP, which are markers of proximal tubule, and Loop of Henle, respectively. Staining was performed in 5 NHK and 5 ADPKD cell lines. Scale bar = 100μm.

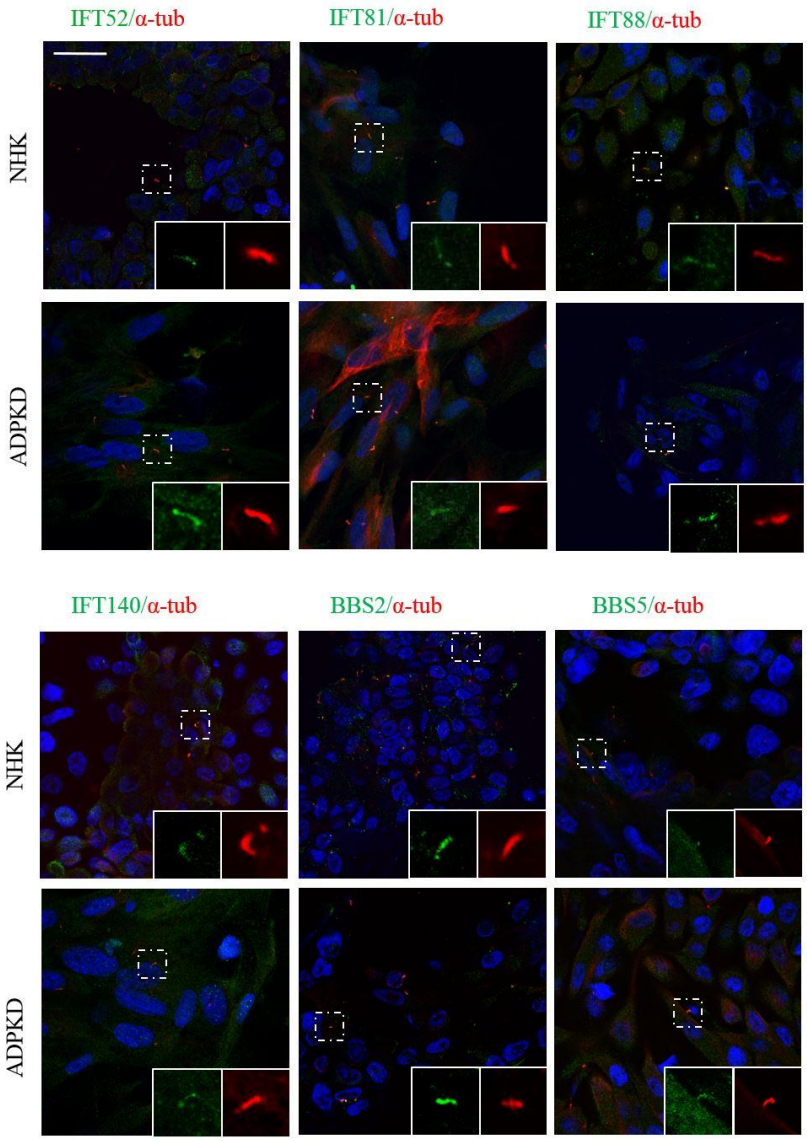

Figure 2.9: Primary cilia of ADPKD cells show normal localization of IFT and BBS proteins Immunofluorescence for IFT52 (green), IFT81 (green), IFT88 (green), IFT140 (green), BBS2 (green), and BBS5 (green) and acetylated α-tubulin (red) in NHK and ADPKD cells. Scale bar = 25 μm. Localization of each ciliary protein was examined in a minimum of 3 NHK and 3 ADPKD cell lines (Table 1).

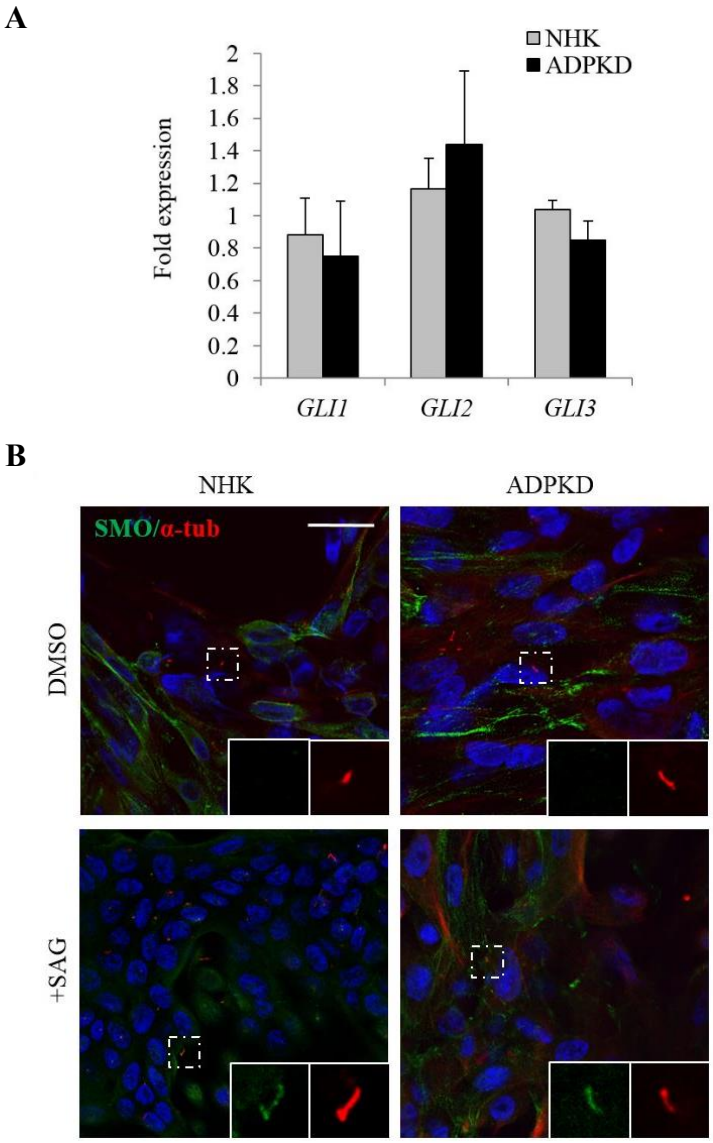

Figure 2.10: Human primary renal epithelial cells have Hh signaling machinery
A) qPCR analysis on NHK and ADPKD primary renal epithelial cells. Bars represent mean ± SEM of 3 NHK and 3 ADPKD cell lines (Table 1). B) Immunofluorescence for SMO (green) and acetylated α-tubulin (red) in presence or absence of SAG. Experiments were replicated in 5 NHK and 5 ADPKD cell lines (Table 1). Scale bar = 25 μm.

2.4.3 Hh inhibitors reduce cAMP-induced proliferation and microcyst formation of human primary ADPKD renal cells

Since Hh signaling affects proliferation of multiple cell types, we examined proliferation of ADPKD cells in response to Hh modulators. NHK and ADPKD cells were treated with SAG or with SMO or GLI antagonists, Sant2 or Gant61, respectively, alone or in combination with SAG, for 48 hours. Cell counts were then obtained. As control, cells of designated wells were treated with epidermal growth factor (EGF), which increases proliferation of both NHK and ADPKD cells[158] (Figure 2.11). In both NHK and ADPKD cells, SAG increased proliferation, and Gant61 and Sant2 reduced proliferation (Figure 2.11). Additionally, treatment with SAG together with either Gant61 or Sant2 reduced proliferation relative to SAG (Figure 2.11), suggesting specificity of the Hh modulators.

In ADPKD cells, but not in NHK cells, cAMP is mitogenic [159]. To determine if Hh inhibitors can mitigate cAMP-mediated proliferation, NHK and ADPKD cells were treated with cAMP in the presence of DMSO or a Hh modulator. As control in all experiments, cells of designated wells were treated with EGF or cAMP ascertaining that NHK and ADPKD cells increased proliferation in response to EGF and that ADPKD cells increased proliferation in response to cAMP (Figure 2.12). In NHK cells, cAMP, cAMP with DMSO, or cAMP with SAG, did not alter cell proliferation, but treatment with cAMP together with Gant61 or Sant2 reduced proliferation (Figure 2.12). In ADPKD cells, cAMP increased proliferation, and cAMP with DMSO showed similar proliferation as cAMP alone. Treatment with cAMP and SAG yielded similar cell counts as treatment with cAMP and DMSO (Figure 2.12), suggesting that SAG does not increase cAMP-mediated proliferation. However, cAMP together with either Gant61 or Sant2 reduced cell counts relative to treatment with cAMP and DMSO (Figure 2.12), suggesting that

Gant61 or Sant can offset cAMP-induced proliferation. Using a Viability/Cytotoxicity Assay that incorporates calcein AM in live cells (GFP) and ethidium homodimer-1 in dead cells (RFP), we observed that treatment of NHK and ADPKD cells with Hh modulators, alone or together with cAMP, resulted in similar proportions of live and dead cells as non-treatment, indicating that the Hh modulators did not cause cell death (Figure 2.13). Together, these data demonstrate that Hh signaling can modulate proliferation of both NHK and ADPKD epithelial cells, and moreover, that Hh inhibition can counter the mitogenic effect of cAMP in ADPKD cells.

Finally, we examined the effect of Hh modulation on microcyst formation of ADPKD and NHK cells. Microcyst formation was initiated by treatment with forskolin (FSK), which is a cAMP agonist, and EGF, which has an established role in promoting proliferation in ADPKD. Once microcysts were observed, cysts were treated with SAG, Gant61 or Sant2, alone or in combination with FSK and EGF. Continued treatment with FSK and EGF following microcyst initiation caused maximal cyst formation and growth in NHK (64.3±12.37 cysts/experiment with average cyst surface area of 18.5 ± 3.93 mm^2) and ADPKD cells (83.0 ± 16.39 cysts/experiment with average cyst surface area of 46.6 ± 21.86 mm^2) (Figure 2.14; Figure 2.15), while treatment with Hh modulators alone did not influence cyst formation or growth (data not shown). SAG together with FSK and EGF resulted in similar cyst number and size as FSK and EGF treatment, suggesting SAG does not exacerbate FSK and EGF-induced cyst growth (Figure 2.14). Conversely, treatment with Gant61 or Sant2 together with FSK and EGF, markedly reduced number and size of microcysts relative to FSK and EGF-treated cells (Figure 2.14). These data suggest that while Hh signaling is insufficient to induce cyst formation and growth, inhibition of Hh signaling within a cystic environment can mitigate cystogenic processes *in vitro*.

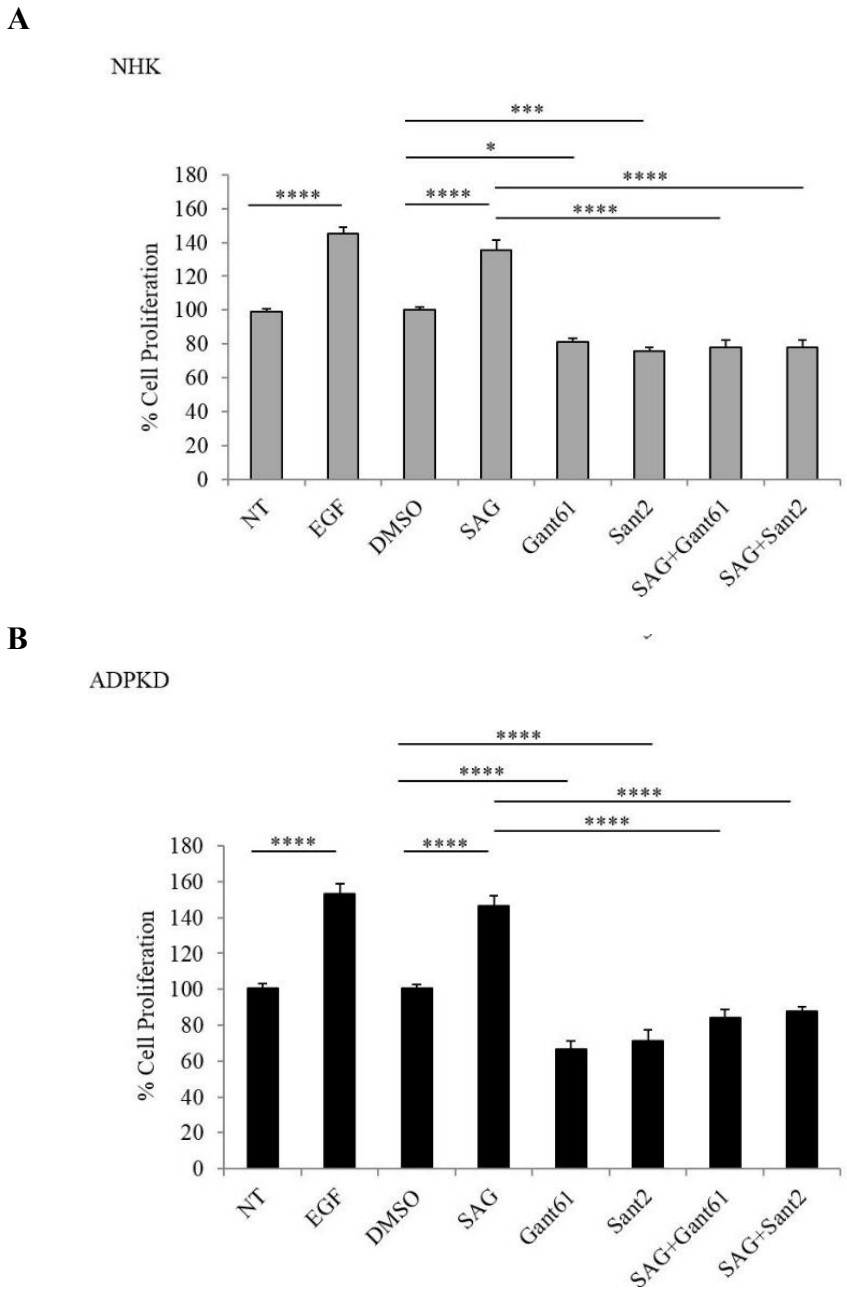

Figure 2.11: Hh inhibitors suppress proliferation of human primary renal epithelial cells
A) Percent cell proliferation of NHK and B) ADPKD cells. Cell proliferation was calculated as a proportion relative to cell number of the NT (no treatment) group, which was set at 100. NT-no treatment; EGF – epidermal growth factor; SAG – Smoothened agonist; SANT2- Smoothened antagonist; GANT61 – GLI antagonist. Bars represent mean ± SEM of 5 NHK and 4 ADPKD cell lines (Table 1). Cells of each line were plated in triplicate wells. Statistical significance was determined by ANOVA and Tukey's test. *P<0.05; ***P<0.001; ****P< 0.0001

A

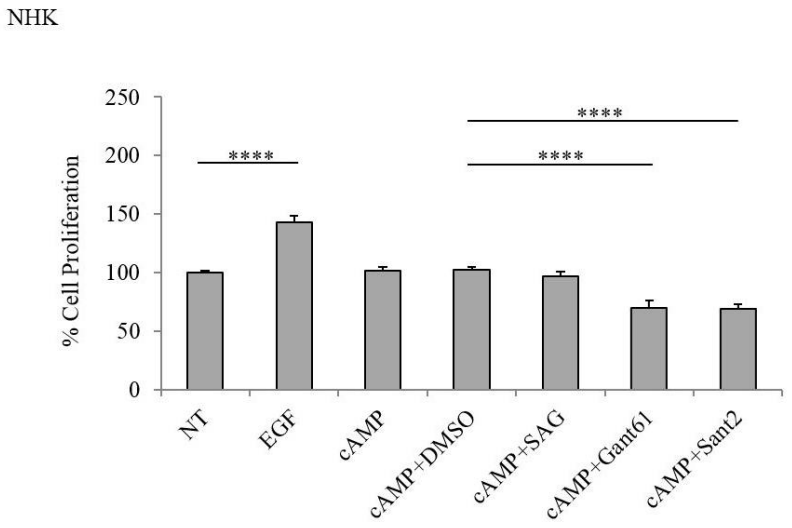

B

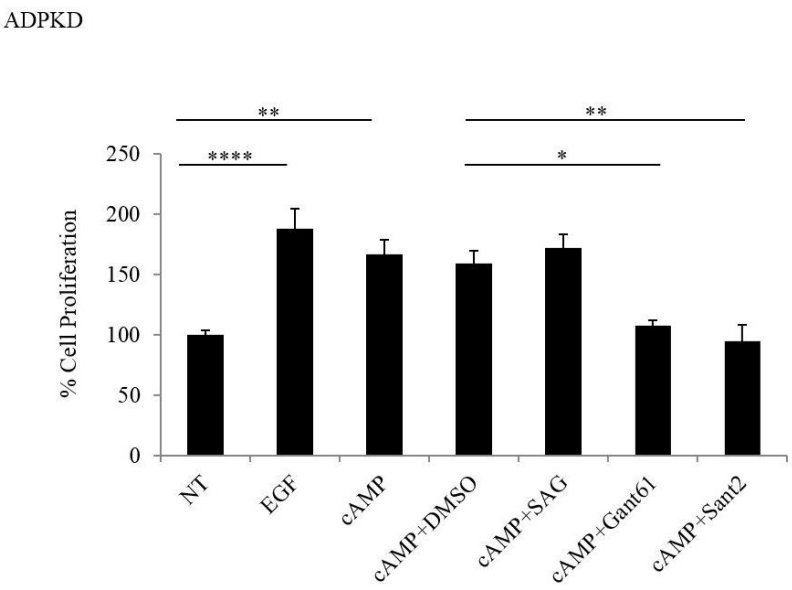

Figure 2.12: Hh inhibitors counteract proliferative effect of cAMP in human ADPKD primary renal cells

A) Percent cell proliferation of NHK and B) ADPKD cells. NT-no treatment; EGF – epidermal growth factor; SAG – Smoothened agonist; SANT2- Smoothened antagonist; GANT61 – GLI antagonist. Bars represent mean ± SEM of 3 NHK and 3 ADPKD cell lines (Table 1). Cells of each line were plated in triplicate wells. Statistical significance was determined by ANOVA and Tukey's test. *P<0.05; **P< 0.01; ****P< 0.0001

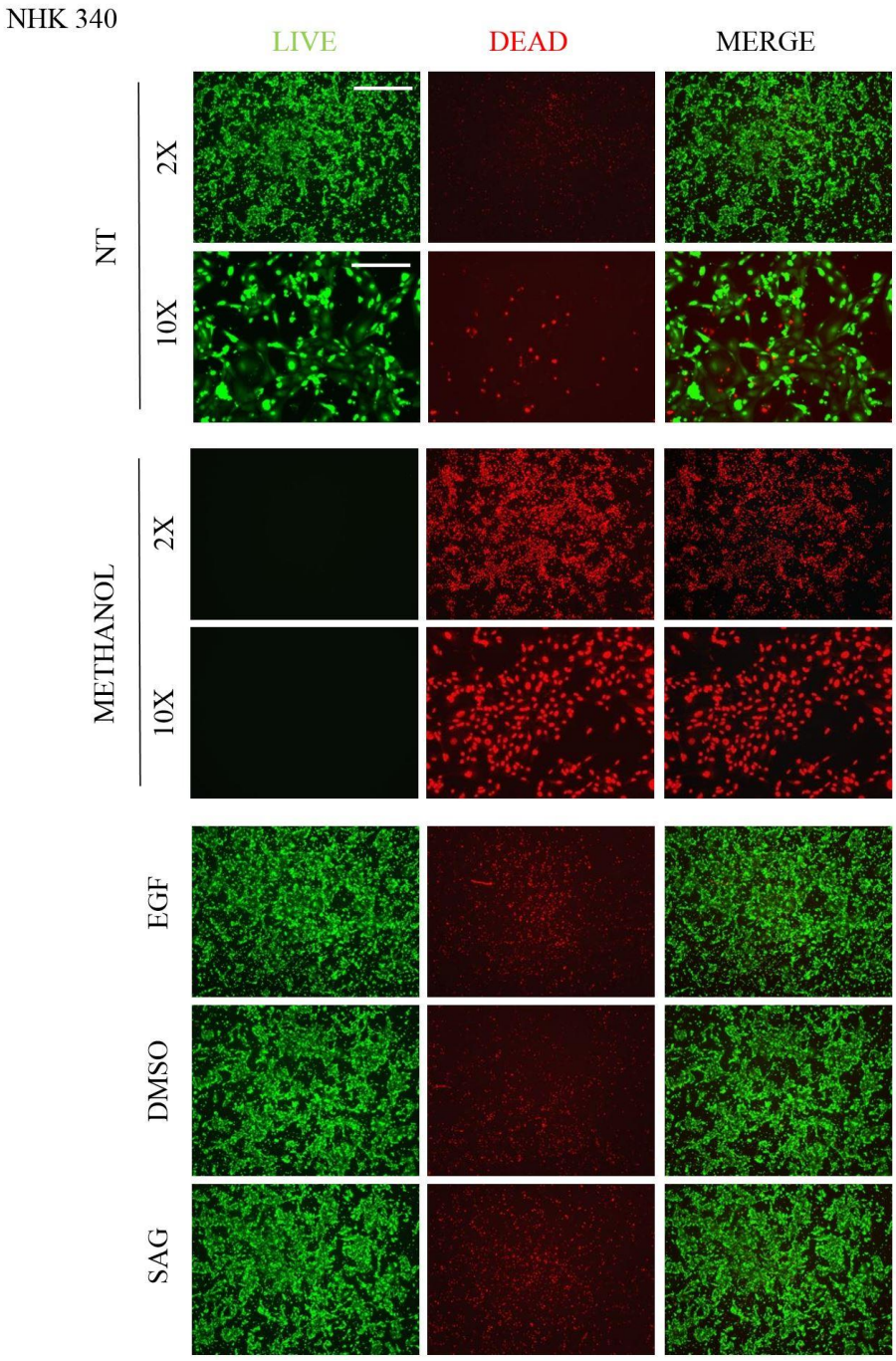
NHK 340
LIVE
DEAD
MERGE
NT
2X
10X
METHANOL
2X
10X
EGF
DMSO
SAG

NHK 340

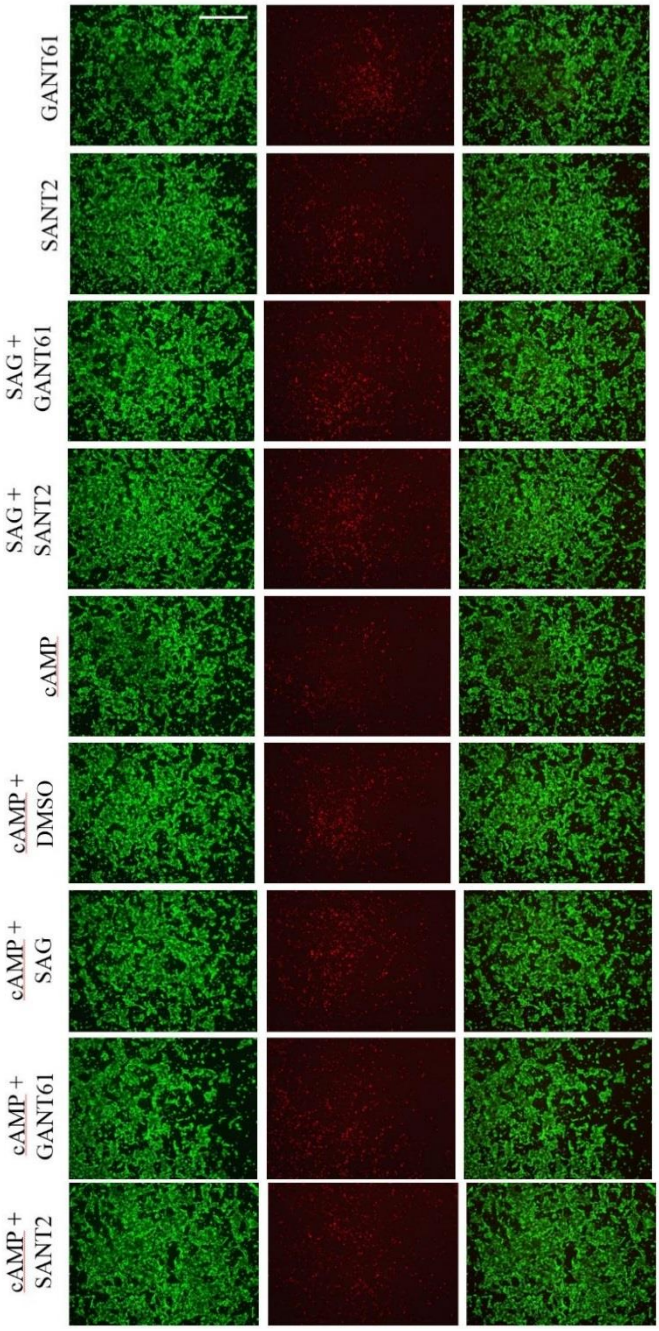
GANT61
SANT2
SAG + GANT61
SAG + SANT2
cAMP
cAMP + DMSO
cAMP + SAG
cAMP + GANT61
cAMP + SANT2

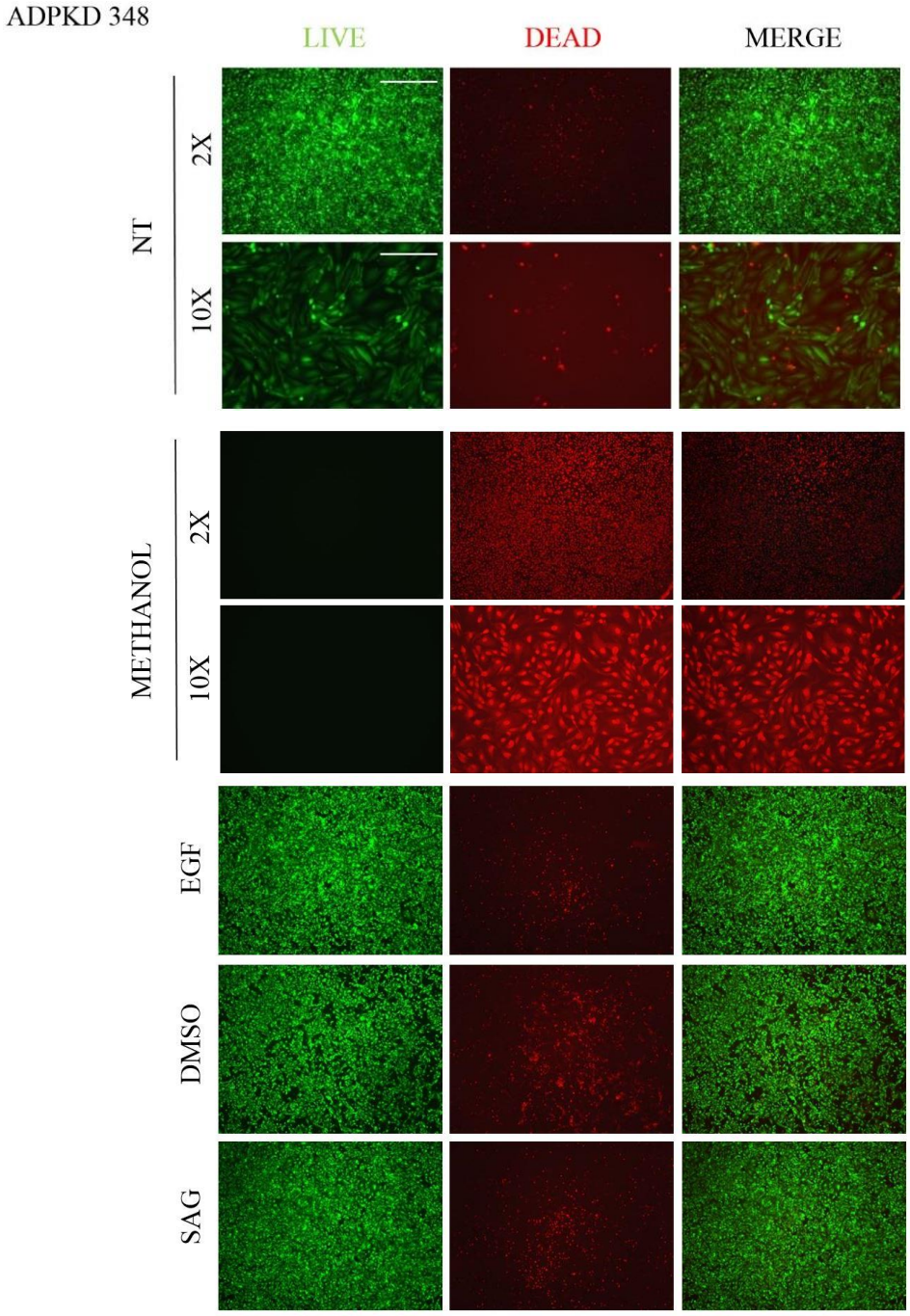
ADPKD 348
LIVE
DEAD
MERGE
NT
2X
10X
METHANOL
2X
10X
EGF
DMSO
SAG

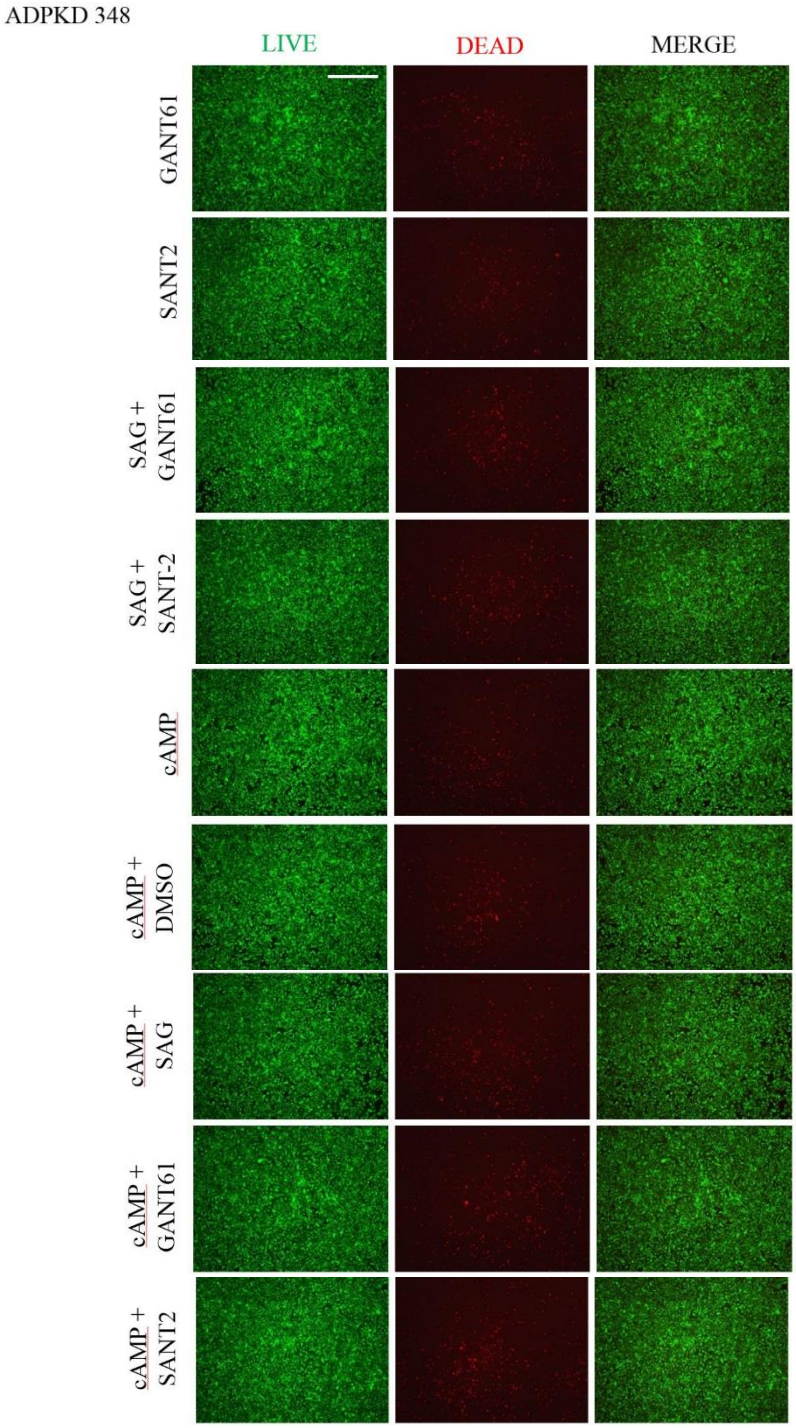

Figure 2.13: Analysis of cell viability and cytotoxicity of Hh modulators.
NHK and ADPKD cells were treated with Hh modulators, alone or together with cAMP, then analyzed for viability/ retention of calcein AM (GFP) in membranes or for non-viability/incorporation of ethidium homodimer-1 (RFP) in nuclei. NT - no treatment. Methanol – 30-minute incubation in 70% methanol was used to cause 100% cell death. Hh treatments were imaged using a 2X objective lens. Scale bar for 2X – 500µm. Scale bar for 10X - 100µm. Assays were performed in 3 NHK and 3 ADPKD cell lines.

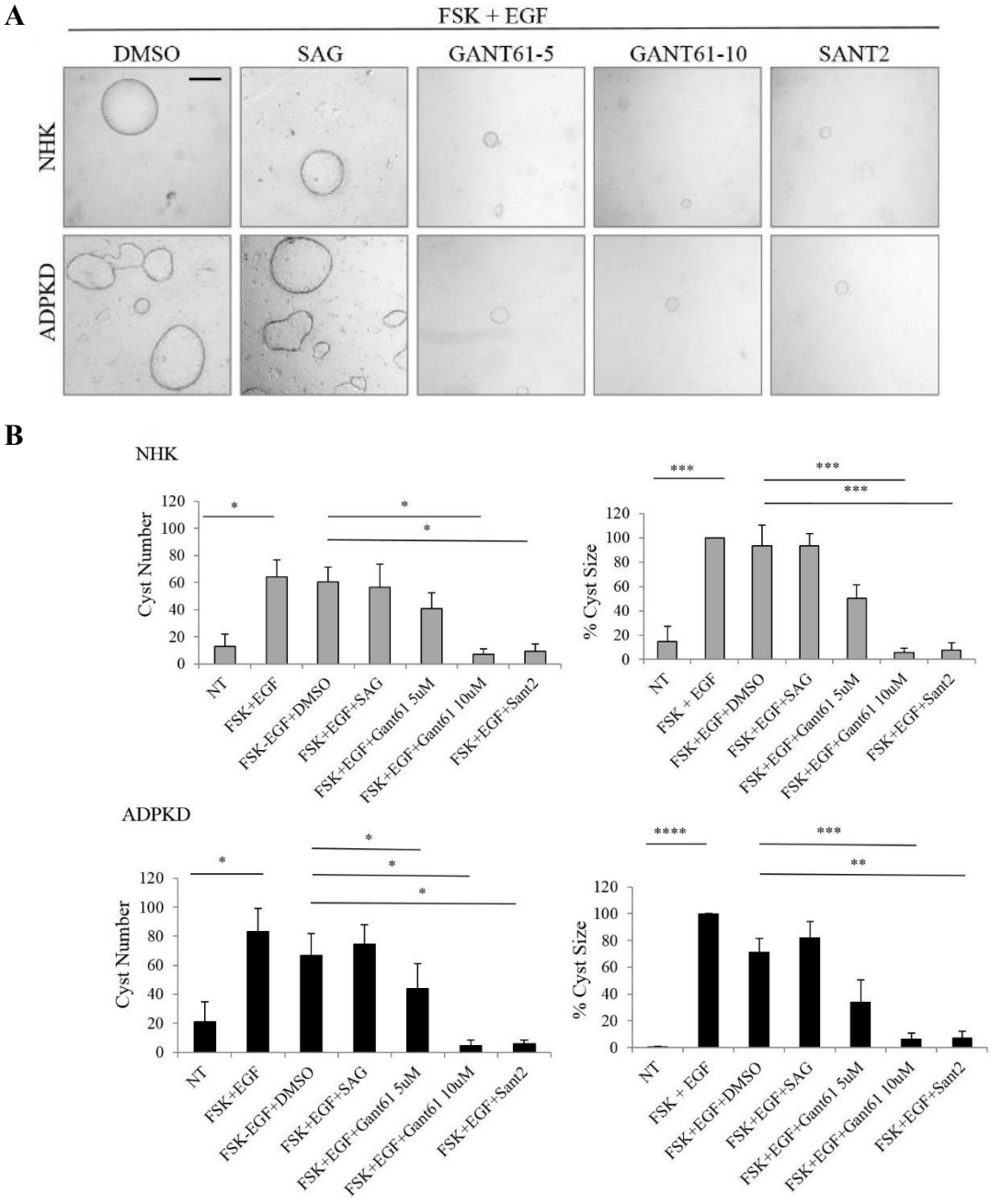

Figure 2.14: Hh inhibitors suppress microcyst formation of human primary renal epithelial cells

A) Representative images of NHK and ADPKD microcysts in the presence of DMSO or Hh modulators. Cysts were imaged and quantified using Image-Pro Premier. Gant61-5 – Gant61 at 5μM; Gant61-10 – Gant61 at 10 μM. Scale bar = 500μm. B) Quantification of microcysts. Cyst size was calculated as a proportion relative to average cyst size of FSK and EGF treatment group, which was set at 100. FSK-forskolin. Bars represent mean ± SEM of 3 NHK and 4 ADPKD cell lines (Table 1). Cells of each line were plated in six replicate wells. Statistical significance was determined by ANOVA and Tukey's test. *P<0.05; **P<0.01; ***P<0.001; ****P< 0.0001

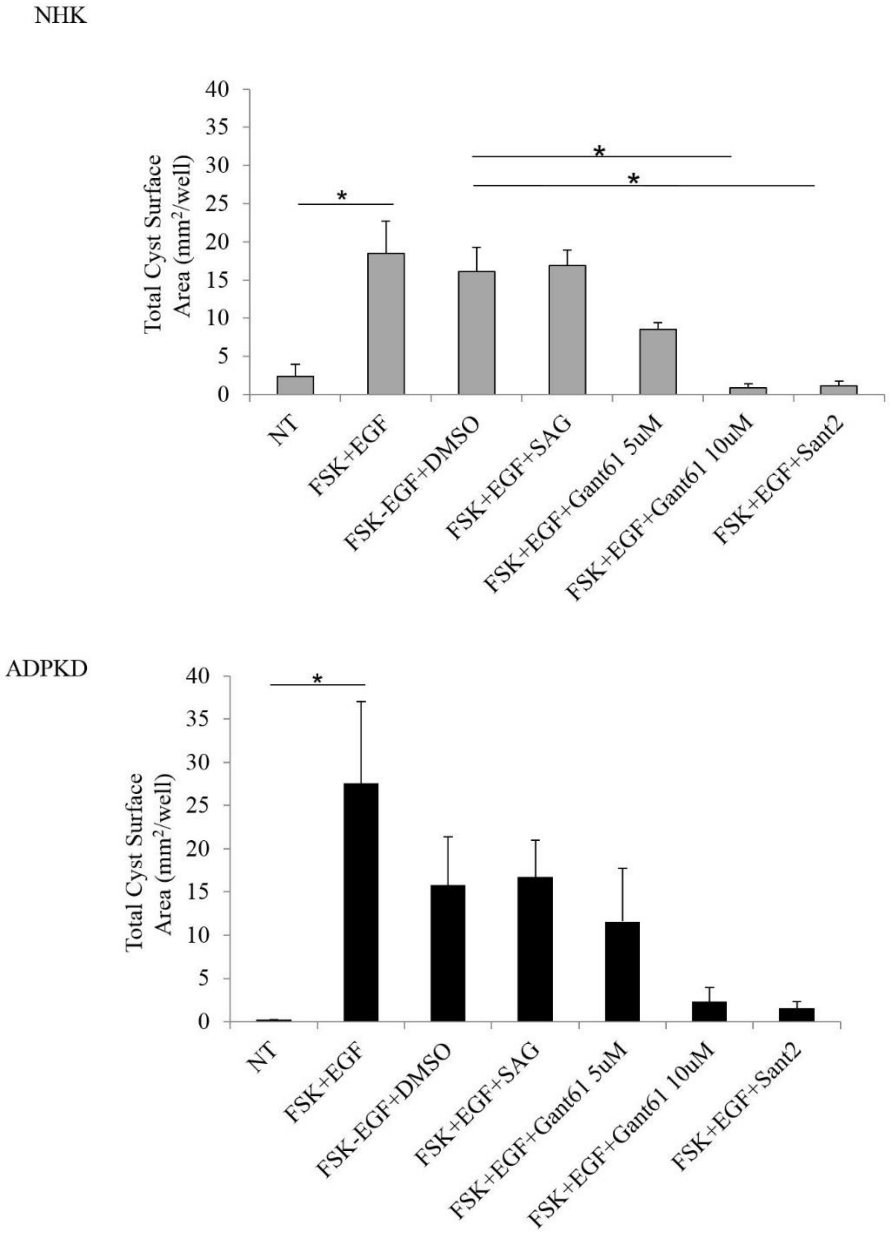

Figure 2.15: Hh inhibitors reduce FSK- and EGF-induced cyst growth.
Quantification of total microcyst surface area per well. FSK-forskolin. Bars represent mean ± SEM of 3 NHK cell lines and 4 ADPKD cell lines. Cells of each line were plated in six replicate wells. Statistical significance was determined by ANOVA and Tukey's test. *P<0.05

Table 1: Sample numbers used in experiments.

		NHK	ADPKD
Figure 1	Tissue 1	K235	K389
	Tissue 2	K241	K294
	Tissue 3	K395	K397
	Tissue 4	K364	K288
	Tissue 5	K378	K399
	Tissue 6	K388	
Figure 3	IFT52	K340	K315
		K388	K276
		K376	K354
	IFT81	K347	K428
		K362	K276
		K376	K315
	IFT88	K376	K276
		K265	K251
		K337	K315
	IFT140	K340	K276
		K376	K315
		K419	K417
	BBS2 and BBS5	K340	K276
		K388	K354
		K419	K417
	BBS5	K376	K315
Figure 4	qPCR	K337	K315
		K340	K354
		K388	K426
	SMO	K376	K339
		K337	K288
		K340	K276
		K347	K428
		K419	K417

		NHK	ADPKD
Figure 5	proliferation	K291	K276
		K337	K319
		K340	K339
		K342	K346
		K419	
Figure 6	cAMP proliferation	K250	K276
		K340	K319
		K342	K339
Figure 7	microcyst assay	K340	K276
		K342	K348
		K362	K350
			K354
Figure S5	DBA/LTL/THP	K340	K441
		K419	K386
		K325	K315
		K337	K339
		K343	K417
Figure S6	Live/Dead Assay	K340	K348
		K337	K339
		K388	K386

Table 2: qPCR primers.

GLI1-F	5’ CAG GGA GGA AAG CAG ACT GA 3’
GLI1-R	5’ ACT GCT GCA GGA TGA CTG G 3’
GLI2-F	5’ CAC GCT CTC CAT GAT CTC TG 3’
GLI2-R	5’ CCC CTC TCC TTA AGG TGC TC 3’
GLI3-F	5’ CGA ACA GAT GTG AGC GAG AA 3’
GLI3-R	5’ GTC TGT CCA GGA CTT TCA TCC T 3’
OAZ1-F	5’ CAC CAT GCC GCT CCT AAG 3’
OAZ1-R	5’ GAG GGA GAC CCT GGA ACT CT 3’

2.5 Discussion

The primary cilium is important for renal tubular integrity, but the mechanisms by which ciliary dysfunction causes or modifies renal cystogenesis are not understood. Multiple mechanisms may lead to a renal cyst, and these may compare or contrast among different renal cystic diseases. ADPKD causes enlarged kidneys with varying degrees of fibrosis and ESRD in the mid-50s, while non-PKD renal cystic diseases often reduce kidney size due to abundant fibrosis and cause ESRD in the pediatric years. In ADPKD, cilia lack polycystin but are thought to be structurally intact, while in non-PKD cystic kidney disease, cilia structure is often disrupted due to mutation of a ciliary structural component. Cilia regulate Hh signaling, and this pathway is often altered in cilia mouse mutants with or without an overt ciliary structural defect[23, 25, 26, 160-162]. Since others have reported increased *Gli1* in cystic kidneys of ciliary mutants, *Ift140* and *Arl13B* conditional knock-out mice[107, 109], and we have observed increased *Gli1* in cystic kidneys of *Nek8*$^{jck/jck}$, *Thm1* and *Pkd1* conditional knock-out mice (on mixed strain backgrounds) [80], suggesting a general role for elevated Hh signaling in renal cystogenesis, we investigated the Hh pathway in human ADPKD.

Previously, a transcriptome analysis of human ADPKD renal tissue revealed increased expression of Hh components, *PTCH1*, *GLI2* and *GAS1* [110]. Our data showing enhanced staining of nuclear GLI1 in interstitial and epithelial cells of ADPKD cystic tissue add to this. Renal tubular epithelial cells have been reported to express Hh ligand [147], thus the presence of GLI1 in both interstitial and epithelial cells suggests occurrence of paracrine and autocrine Hh signaling mechanisms in ADPKD. Paracrine and autocrine Hh signaling have been reported in other kidney pathologies. Increased paracrine Hh signaling was demonstrated in renal fibrosis [147], while elevated autocrine Hh signaling was shown in renal cell carcinoma (RCC) [112]. The

intact Hh signaling we observed in NHK and ADPKD primary renal epithelial cells also supports the presence of autocrine signaling. This is consistent with studies in IMCD cells, demonstrating GLIS2 as a negative regulator of Hh signaling [149] and showing reduced ciliary GPR161, a Hh negative modulator, in response to SAG [51], collectively indicating that the Hh signaling machinery is present in kidney epithelial cells. We anticipated increased Hh signaling in ADPKD primary renal epithelial cells similar to ADPKD renal tissue. This was not the case, which could reflect that additional cell types or signaling molecules cross-talk *in vivo* to cause upregulation of GLI1. Indeed, a caveat of *in vitro* systems is the inability to mimic all conditions present *in vivo*. Yet, *in vitro* models can be useful in understanding how cells might respond to a particular stimulus, and the primary renal epithelial cells allow functional analyses on patient-derived materials, which cannot be done at the tissue level.

Our data show that Hh inhibitors can abate cAMP-mediated proliferation in ADPKD cells and FSK and EGF-induced cystogenesis *in vitro*. Previously, we observed that Gant61 and Sant2 reduced the cAMP-mediated cystogenic effects in cultured mouse embryonic kidneys [80]. Collectively these data suggest that Hh signaling is a necessary component of cAMP-mediated proliferation and cystogenesis in these systems. In human ADPKD cells, elevated intracellular cAMP activates cystic fibrosis transmembrane conductance regulator (CFTR)-mediated Cl^- secretion and B-Raf/MEK/ERK signaling, causing fluid secretion and increased proliferation of cyst-lining epithelial cells, respectively [49, 52]. ADPKD cells have low homeostatic intracellular Ca^{2+}, which causes the mitogenic effect of cAMP, while augmenting intracellular Ca^{2+} in ADPKD cells counters this effect [51]. Hh inhibition may mitigate the proliferative and cystogenic effects of cAMP, FSK and EGF, by possible crosstalk between Hh and ERK signaling, which has been observed in RCC and other cancers [112, 163, 164]. Alternatively, Hh inhibition by a SMO

inhibitor, GCD-0449, has been shown to increase steady-state levels of intracellular Ca^{2+} in a lung cancer cell line [165]. Similarly, Hh inhibition might also increase intracellular Ca^{2+} in kidney epithelial cells.

Alternatively, Hh signaling and polycystin function might intersect at the primary cilium. PC2 has been indicated to be part of a complex in the cilium with adenylyl cyclases 5 and 6, and phosphodiesterase 4C, which synthesize and catabolizes cAMP, respectively, likely regulating cAMP at the primary cilium. Advanced imaging technology has enabled visualization of ciliary pools of Ca^{2+} and cAMP [40, 53]. In mouse embryonic fibroblasts, Hh activation increased ciliary Ca^{2+} [40], and decreased ciliary cAMP [53]. These studies also demonstrated that ciliary and intracellular pools of Ca^{2+} and cAMP are distinct. Since Hh inhibition by GDC-0449 increased intracellular Ca^{2+} in a lung cancer cell line [164], Hh activity may have opposing effects on ciliary and intracellular Ca^{2+}. Thus, regulation of Hh signaling on ciliary and intracellular Ca^{2+} requires further investigation.

SAG alone, but not SAG with cAMP, increased proliferation of NHK cells. This may suggest that cAMP countered the effect of SAG and inhibited Hh signaling in these cells. Yet treatment with the Hh inhibitors together with cAMP reduced cell proliferation relative to cAMP with DMSO, suggesting that proliferation of NHK cells may require a certain level of Hh signaling, which was inhibited by Gant61 and Sant2. In mouse PKD kidneys, which have high levels of cAMP, *GLI1* is increased indicating enhanced Hh signaling [80]. Thus, while cAMP might dampen the Hh pathway in certain contexts, this dampening effect may be overridden in the PKD setting.

Two studies have documented increased ciliary length in *Pkd* models [29, 55], which prompted us to examine IFT and BBS localization in ADPKD. Normal localization of IFT and

BBSome components in several ADPKD cell lines indicates that the ciliary trafficking machinery is not affected by polycystin dysfunction. Thus, other mechanisms may account for the increased ciliary length reported in these *Pkd* models. Polymorphisms in the mouse strain background may interact with the *Pkd* mutation to increase cilia length. These polymorphisms might reside in genes that regulate ciliary structure [140], cAMP [59], cytosolic tubulin, actin machinery [162], or other factor that can modulate cilia length. These genes would represent PKD modifiers.

Aside from IFT, epigenetic regulation can also result in increased GLI levels. Epigenetics has been shown to affect PKD in a preclinical model, and cancer studies have linked epigenetics to Hh regulation. Inhibition of Brd4, a BET bromodomain protein and epigenetic regulator, attenuated PKD progression in a *Pkd1* conditional knock out mouse [166]. In addition, treatment of a medulloblastoma mouse model with I-BET151, a Brd4 inhibitor, reduced *Gli1* expression, cell proliferation and tumor growth, indicating epigenetics drives Hh activation in cancer [167]. *GLI1* may be a target of BRD4 in ADPKD as well.

Since some, but not all, cyst-lining epithelial cells in ADPKD renal tissue showed increased nuclear GLI1 staining, and increased *Gli1* transcripts have been evident in kidneys of mouse models that were already cystic [80, 107, 109], we speculate that Hh signaling may increase with disease progression, and that patients with more advanced ADPKD might show a greater increase in Hh signaling than those with earlier disease. Importantly, Hh inhibitors countered the proliferative and cystogenic effects of cAMP/forskolin in patient-derived renal epithelial cells. Our findings suggest clinical relevance of the Hh pathway in ADPKD. An important experiment will be to examine whether Hh inhibition attenuates disease in an appropriate *Pkd* model *in vivo*. Hh inhibition may also serve to attenuate fibrosis[147], which is a significant component of ADPKD pathology. Still, multiple pathways are misregulated in ADPKD, and crosstalk and

feedback loops may also be present. Thus, targeting more than one pathway at different disease stages might be most effective. Interestingly, Hh and ERK signaling have been demonstrated to work cooperatively in some cancers, with inhibition of one pathway showing modest effect, but simultaneous inhibition of both pathways having a synergistic effect [168-170]. Exploring similar possibilities in appropriate *Pkd* models *in vivo* may help determine effective combinatorial therapeutic strategies against ADPKD.

Chapter Three:

Hh signaling in ADPKD mouse models

3.1 Abstract

ADPKD is among the most common fatal genetic diseases, yet therapy is limited and a cure is lacking. Proteins disrupted in ADPKD localize to the primary cilium, an antenna-like sensory organelle that mediates signaling pathways. While primary cilia dysfunction appears central to renal cystogenesis, molecular mechanisms are only beginning to emerge. Previously, we showed that downregulation of the ciliary-mediated Hh pathway attenuated renal cystic disease in mice mutant for *Thm1*, a ciliary gene and negative regulator of Hh signaling, and reduced cystogenic potential of cultured embryonic kidneys of ADPKD mouse models, *jck* and *Pkd1* mutants, suggesting a general role for increased Hh signaling in renal cystogenesis. Here we examined whether inhibition of the Hh pathway can attenuate renal cystogenesis in *jck* mutant, and *Pkd1* and *Pkd2* conditional knock-out mice *in vivo*. In *jck* mice, increased expression of GLI1, a Hh target and reporter of the Hh pathway, correlated with disease progression, and genetic inhibition of the pathway reduced kidney weight/body weight (KW/BW) ratios and BUN levels. Additionally, genetic inhibition of the Hh pathway reduced KW/BW ratios of *Pkd1* conditional knock-out (cko) mice. These data suggest Hh signaling may play a role in disease progression of ADPKD mouse models.

3.2 Introduction

Autosomal Dominant Polycystic Kidney Disease (ADPKD) affects ~1:500 individuals worldwide and is characterized by progressive growth of renal cysts that can lead to end-stage renal disease by the 6th decade of life [6]. ADPKD is caused by mutations in *PKD1* or *PKD2*, which encode polycystin-1 (PC1) and polycystin-2 (PC2) proteins, respectively. These proteins form a complex that localizes to primary cilia [139].

Primary cilia are sensory organelles that are synthesized and maintained by intraflagellar transport (IFT) or the bi-directional transport of proteins along a microtubule-based axoneme. Mutation of most *Ift* genes causes misregulation of the Hh pathway [25, 26, 144]. Further, mutation of most *Ift* and ciliary genes results in renal cystic disease [107, 121, 140, 145]. Paradoxically, genetic removal of cilia in ADPKD orthologous mouse models and pharmacological shortening of cilia in *Nek8*$^{jck/jck}$ mice attenuated PKD, leading to the proposition that a cilia-dependent signaling pathway promotes cyst formation [56, 58, 97, 141].

The mammalian Hedgehog (Hh) signaling pathway is cilia-dependent [91] and has been reported to be elevated in several renal diseases, including renal fibrosis [147], renal cell carcinoma [112, 146], and renal cystic diseases [80, 108, 148, 149]. Hh signaling is activated by ligand binding to the Patched (PTCH) receptor, leading to the ciliary enrichment and activation of the Smoothened (SMO) signal transducer and to the ultimate activation of the GLI transcription factors (GLI1, GLI2 or GLI3) [93, 97-99]. In human ADPKD kidneys, expression of Hh signaling components was increased [110, 138], and in cystic kidneys of five ADPKD mouse models, including *Nek8*$^{jck/jck}$ mutants and *Pkd1* conditional knock-out mice, expression of *Gli1*, a Hh target gene and reporter, was increased [80, 107-109]. Additionally, small molecule Hh inhibitors

reduced renal cystogenic potential of cultured embryonic kidneys of *Nek8*$^{jck/jck}$ and *Pkd*$^{m1Bei/m1Bei}$ mice [80]. Here I have sought to extend these analyses *in vivo* and downregulated Hh signaling in *Nek8*$^{jck/jck}$ mutants and *Pkd1* and *Pkd2* conditional knock-out mice.

3.3 Methods

3.3.1 Generation of *jck* mutant and *Pkd1* and *Pkd2* conditional knock-out mice

jck$^{+/-}$ mice were obtained from David Beier. *Gli2*$^{+/-}$ mice were obtained from Jonathan Eggenshwiler, courtesy of Alexandra Joyner. *Gli2*$^{flox/flox}$, *Pkd1*$^{flox/flox}$, *Pkd2*$^{flox/flox}$ and *ROSA26-Cre* mice were obtained from Jackson Laboratories (Stock numbers 007926, 010671, 017292 and 004847, respectively). Mice were intercrossed on a mixed FVB, SV129 and C57BL/J background. *ROSA26-Cre*$^{ERT/+}$ and *Gli2* floxed alleles were introduced into the lines to generate *jck*$^{+/-}$*;Gli2* $^{flox/flox}$, *Pkd1*$^{flox/flox}$*; Gli2*$^{flox/flox}$ or *Pkd2*$^{flox/flox}$; *Gli2*$^{flox/flox}$ females to mate to *jck*$^{+/-}$*; Gli2*$^{+/-}$; *ROSA26-Cre*$^{ERT/+}$, *Pkd1*$^{flox/+}$*; Gli2*$^{+/-}$, *ROSA26-Cre*$^{ERT/+}$ or *Pkd2*$^{flox/+}$*; Gli2*$^{+/-}$, *ROSA26-Cre*$^{ERT/+}$ males. *jck, Gli2*$^{flox/fox}$ (at P0), *Pkd1*$^{flox/flox}$, *Gli2*$^{flox/flox}$ (at P2) and *Pkd2*$^{flox/flox}$, *Gli2* $^{flox/flox}$ (at P0) nursing mothers were injected with tamoxifen (Sigma) at 10mg/40g mouse body weight to induce gene deletion in pups.

Since the PKD field prefers a pure strain background and to reduce variability between experiments, all mouse lines were recently backcrossed 10 generations onto a C57BL6/J background.

3.3.2 Mouse Genotyping

Mouse genotypes were determined using polymerase chain reaction (PCR) of tail genomic DNA. Primer sequences and PCR product sizes are listed in Table 3. PCR amplicon generated by *jck* primers required digestion with BseYI at 37˚C for 5h and 50 min.

3.3.3 Kidney Weight/Body Weight measurements

Mouse body weight and individual kidneys were weighed in grams using a standard weighing scale. Total kidney weights were divided by body weight for each mouse.

3.3.4 q-PCR

Trizol (Life Technologies) was used to extract RNA, according to manufacturer's protocol. One microgram of RNA was converted to cDNA using Quanta Biosciences qScript cDNA Supermix (VWR International). Quantitative PCR analysis was performed using Quanta Biosciences Perfecta qPCR Supermix (VWR International) and a Bio-Rad CFX Connect Real-Time PCR Detection System. Primers sequences are listed in Table 4. Primers were designed using the Roche Applied Science RT-qPCR Assay Design Center and synthesized by IDT Technologies.

3.3.5 BUN measurements

Mouse trunk blood was collected into Microvette CB 300 Blood Collection System tubes (Kent Scientific), and centrifuged at 1800g at 4°C for 8 minutes to collect serum. BUN was measured using the QuantiChrom Urea Assay Kit (BioAssay Systems) according to manufacturer's protocol.

3.3.6 Histology

Kidneys were extracted and renal capsules were removed. Kidneys were bisected longitudinally and fixed in Bouin's solution for several days. Tissue was dehydrated through an ethanol series, followed by xylene, and embedded in paraffin. Sections of 8μm were obtained using a microtome. Sections were deparaffinized in xylene and rehydrated through an ethanol series to distilled water and stained with hematoxylin and eosin.

3.3.7 Immunohistochemistry

Bisected kidneys were fixed in 4% paraformaldehyde for 3-7 days, then placed in 70% ethanol. Tissues were processed, embedded in paraffin, sectioned and rehydrated as described above (3.3.6). Antigen retrieval was performed by steaming tissue sections for 25 minutes in Sodium Citrate Buffer (10 mM Sodium Citrate, 0.05% Tween 20, pH 6.0). To minimize background staining, sections were treated with 3% hydrogen peroxide for 30 min, washed in PBS, then blocked with 1% BSA for 1 hour. Cells were then incubated with GLI1 antibody (1:100 dilution) (Cell Signaling) overnight at 4°C. Following 3 washes in PBS, sections were incubated with HRP-conjugated rabbit secondary antibody (Cell Signaling) for 30 minutes. Following another 3 washes in PBS, tissues were incubated with ABC reagent (Vector Laboratories), rinsed in PBS, and then incubated with SigmaFAST DAB metal enhancer (Sigma) until desired signal/color was obtained. Staining was visualized and imaged using a Nikon 80i microscope attached to a Nikon DS-Fi1 camera.

3.3.8 Drug studies

Small molecule Hh inhibitors, GDC-0449 and Itraconazole, were administered to *jck* and nursing *Pkd1* females. GDC-0449 (50mg/kg and 100mg/kg; LC laboratories) and Itraconazole (100mg/kg; Selleckchem) were reconstituted to 50mg/ml or 100mg/ml in 10% ethanol;10% cremophor;80% saline (Sigma). A 5x stock was generated weekly and diluted daily to 1x prior to administering the i.p. injection. The dose was calculated based on body weight. *jck* and control mice were injected every day with GDC-0449 or for 5 days/week with Itraconazole from P21 to P49. *Pkd1*$^{flox/flox}$ nursing moms were injected with Itraconazole every other day, from P6 to P23, to deliver treatment to *Pkd1* cko offspring. Following treatment, mice were sacrificed and kidneys were examined.

3.4 Results

3.4.1 Hh activity correlates with disease progression in *jck* mutant mice on a pure C57BL6/J background

Previously, we found *Gli1* was increased in 7-week-old *jck* mutants on a mixed strain background [80]. To reduce variability between experiments, we backcrossed our *jck* mice onto a C57BL6/J background to the 10th generation and expanded our analysis to determine if increased Hh signaling activity correlates with disease progression in *jck* mutants on this background. We harvested kidneys from control and *jck* mutant mice at 7, 13 and 18 weeks of age. Increased %KW/BW and BUN levels in older mutants confirmed that renal function declines progressively (Figure 3.1a,b). We next performed real time PCR analyses for *Gli1*, *Gli2* and *Gli3*. Our results show 18-week-old mutant kidneys have significantly increased *Gli1* and *Gli3* expression, compared to younger (7 and 13- week old) mutants. Since *Gli1* and *Gli3* are Hedgehog signaling

target genes, these results suggest Hh activity may increase with disease progression (Figure 3.1c). Additionally, immunohistochemistry revealed increased nuclear expression of GLI1 in epithelial cells lining the cysts and in cells within the interstitium of 18-week-old mutant kidneys (Figure 3.1d), indicating increased autocrine and paracrine Hh signaling, respectively. These combined data suggest that increased Hh signaling correlates with disease progression in this model.

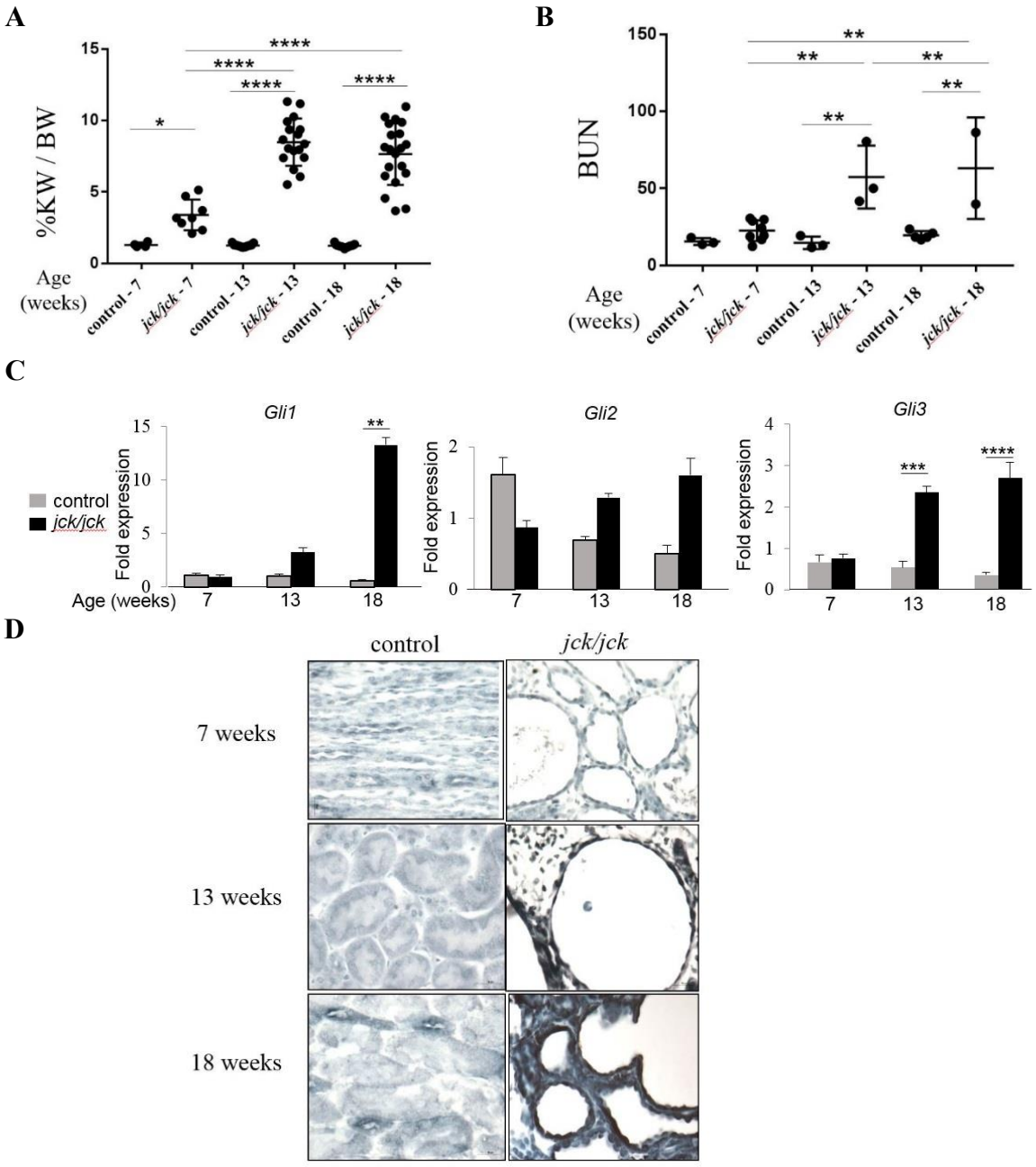

Figure 3.1: Hh activity correlates with disease progression in *jck* mutant mice
A) %KW/BW and B) BUN levels of control and *jck* mutants at 7, 13 and 18 weeks of age. C) qPCR for *Gli1*, *Gli2* and *Gli3* for control and *jck* mutant kidneys at 7- (N=3 controls, N=6 *jck*), 13- (N=3 controls; N=3 *jck*) and 18- (N=5 controls, N=3 *jck*) weeks of age. D) Representative images of control and *jck* mutants at 7, 13 and 18 weeks of age (N=3 each group). Statistical significance was determined by ANOVA. *P<0.05; **P<0.01; ****P< 0.0001.

3.4.2 Genetic downregulation of Hh signaling reduced renal cystogenesis in *jck* mice

We downregulated the Hh pathway in *jck* mice by deleting *Gli2*, the main transcriptional activator at P0 on a mixed strain background. At 7 weeks of age, *jck,Gli2* mutants showed fewer renal cysts and reduced renal size, relative to *jck* single mutants (Figure 3.2a). These data indicate that decreasing Hh signaling reduces renal cystogenesis. Additionally, *jck,Gli2* mutants showed significant reduction in kidney weight/body weight ratios (KW/BW) (Figure 3.2b). Furthermore, in the few animals tested so far, there is a trend for *jck,Gli2* mutants to show lower blood urea nitrogen (BUN) levels, suggesting downregulation of Hh signaling may improve kidney function in this model (Figure 3.2c) [159].

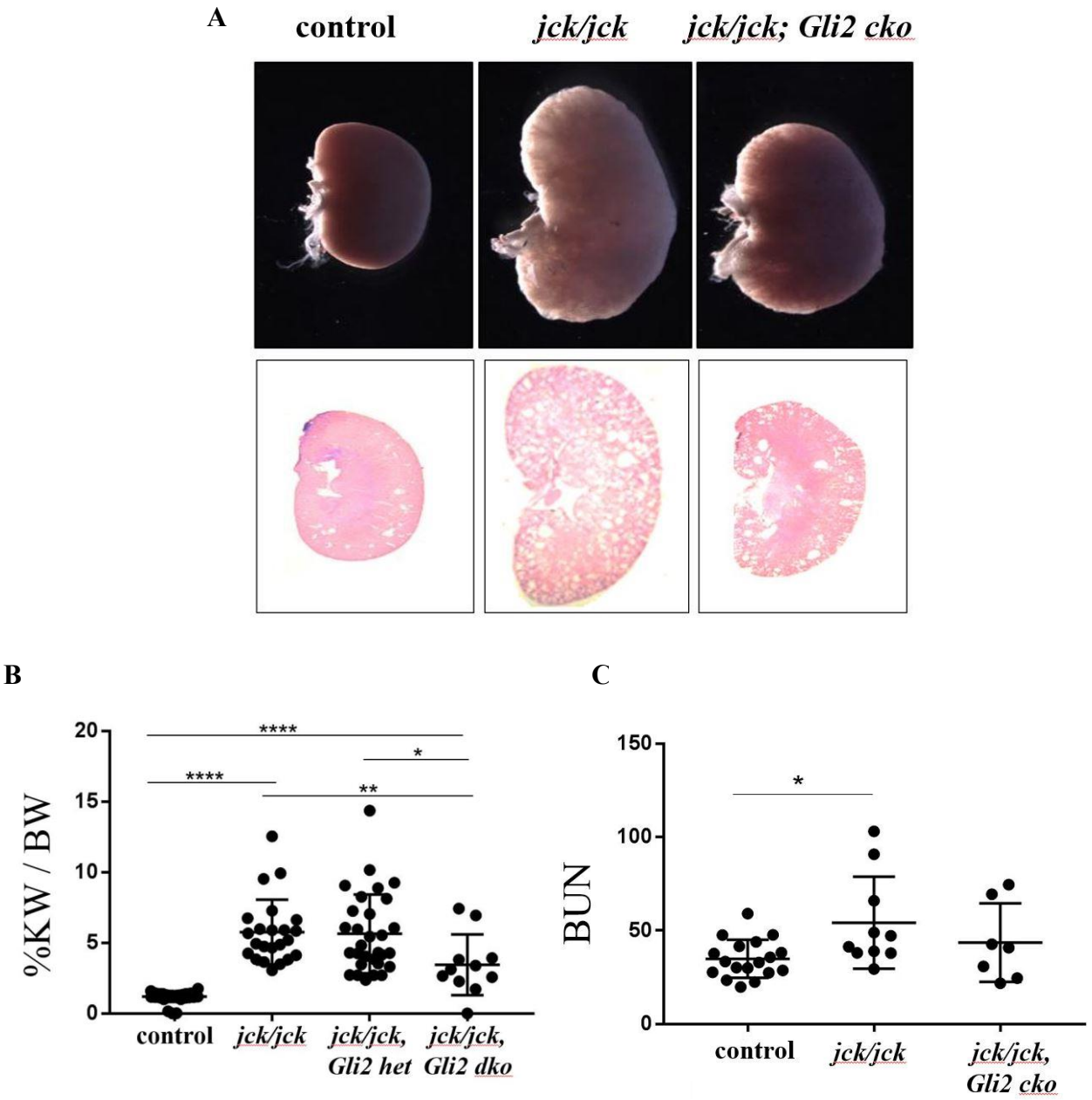

Figure 3.2: Genetic downregulation of Hh signaling reduced renal cystogenesis in *jck* mice
A) Representative images of whole-mount and histological sections of kidneys from 7-week-old control, *jck/jck* and *jck/jck;Gli2* cko mice. B) KW/BW ratios. C) BUN of 7-week-old control, *jck/jck*, *jck/jck,Gli2* het and *jck/jck;Gli2* mutant mice (N≥7). Statistical significance was determined by ANOVA. *P<0.05; **P<0.01; ****P< 0.0001

3.4.3 Genetic downregulation of Hh signaling reduced %KW/BW in *Pkd1* conditional knock-out mice

Genetic downregulation of Hh signaling by conditionally deleting *Gli2* in orthologous mouse models of ADPKD also reduced KW/BW ratios in the *Pkd1,Gli2* double knock-outs, compared to *Pkd1* mutants on a mixed strain background (Figure 3.3a). These data indicate Hh signaling may also play a role in renal cystic disease in *Pkd1* cko mouse model.

The KW/BW ratios of *Pkd2,Gli2* double mutants appeared similar to that of the *Pkd2* cko mouse (Figure 3.3b), but more numbers of *Pkd2* cko mice are required to conclude this.

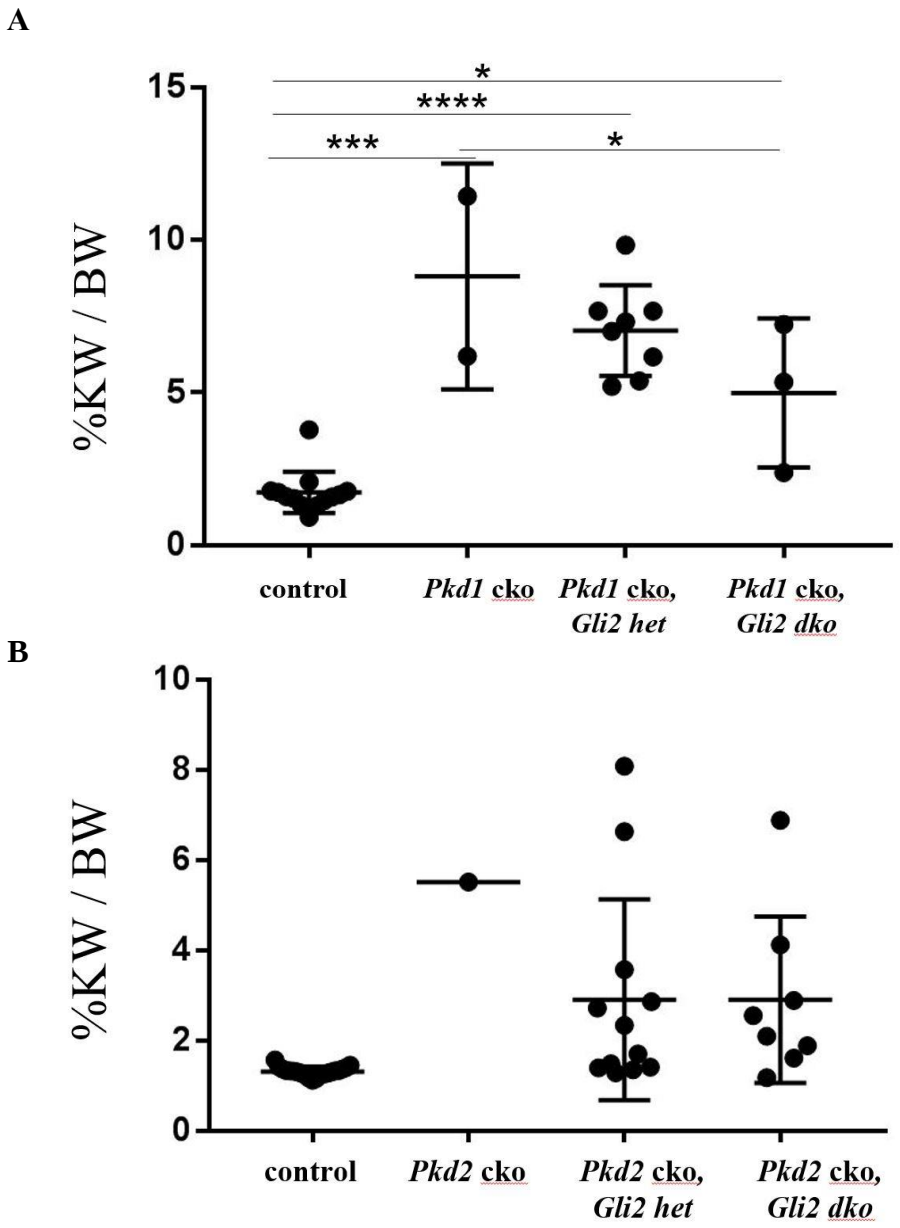

Figure 3.3: Genetic downregulation of Hh signaling (Hh) reduced %KW/BW in *Pkd1* but may not have reduce %KW/BW in *Pkd2* mutants

A) %KW/BW for control, *Pkd1 cko*, *Pkd1* cko,*Gli2* het and *Pkd1*,*Gli2 cko* mice. B) %KW/BW for control, *Pkd2 cko*, *Pkd2* cko,*Gli2* het and *Pkd2*,*Gli2 cko* mice. Statistical significance was determined by ANOVA. *P<0.05; ****P< 0.0001.

3.4.4 Pilot experiments with Hh inhibitors, GDC-0449 and Itraconazole

We sought to recapitulate the genetic experiments pharmacologically using two Hh inhibitors, GDC-0449 (50mg/kg and 100mg/kg) and Itraconazole (100mg/kg). GDC-0449 is the first FDA-approved Hh inhibitor and Itraconazole is a FDA-approved antifungal drug. Both drugs inhibit SMO [116, 164]. Mice were treated daily with GDC-0449 or 5 days/week with Itraconazole, from P21 to P63, at which time animals were dissected. Treatments with Hh inhibitors did not reduce KW/BW of *jck* mutants (Figure 3.4a-d), but further investigation is required to determine if the conditions reduced Hh signaling activity.

We also treated control and *Pkd1* mutant mice with Itraconazole. Deletion of *Pkd1* was induced at P2, resulting in rapidly progressing renal cystic disease. We administered intraperitoneal injections of either vehicle or Itraconazole every other day to the nursing female from P6 until P23. Since Itraconazole has been reported in human breast milk, we speculated that the drug would be delivered through the breastmilk to the nursing progeny [171]. At P23, KW/BW ratios were similar between saline- and Itraconazole-treated mutants (Figure 3.5a,b). Additionally, *Gli1* expression was also similar between saline- and Itraconazole-treated mutants, suggesting that the drug administration was not sufficient to reduce Hh activity (Figure 3.5c).

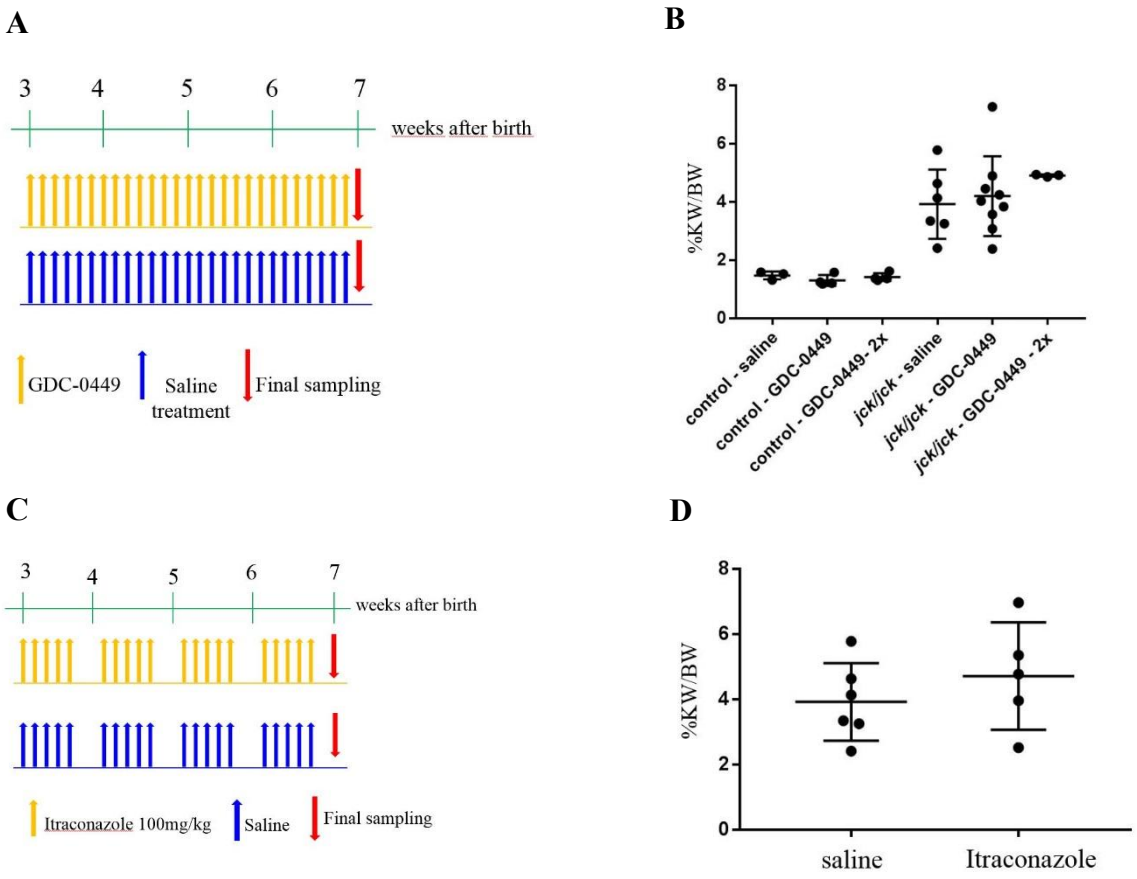

Figure 3.4: Hh inhibitors did not reduce %KW/BW in *jck* mutant mice
A) Timeline for GDC-0449 treatment. Control and mutant animals were treated with saline (N≥3 each group) or with GDC-0449 at 50mg/kg (N≥4 each group) or GDC-0449-2x at 100mg/kg (N≥3 each group). B) %KW/BW for GDC-0449 treated animals. C) Timeline for Itraconazole at 100mg/kg treatment. For the Itraconazole studies, N≥5 each group. D) %KW/BW for Itraconazole-treated animals.

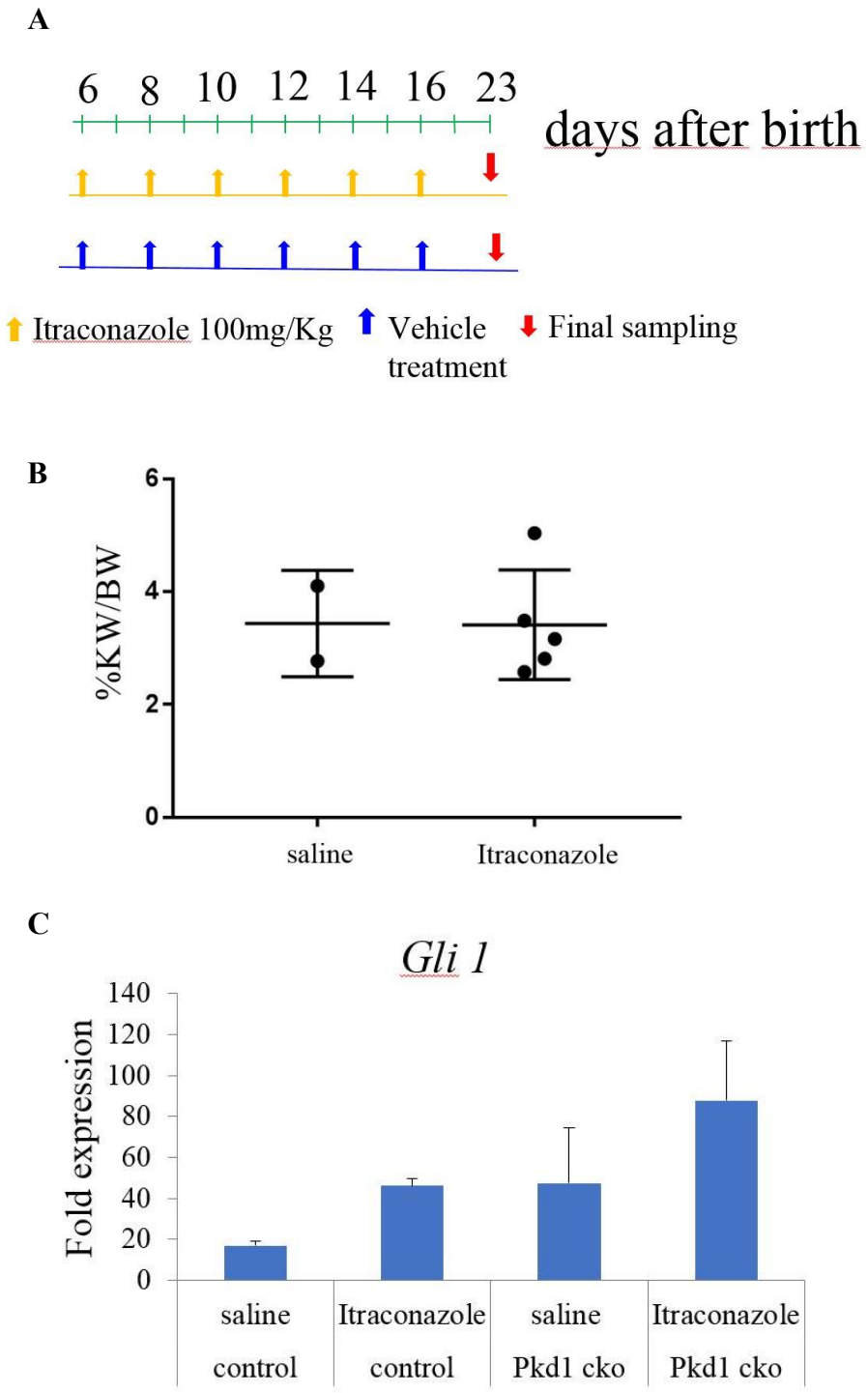

Figure 3.5: Itraconazole did not reduce %KW/BW in *Pkd1* mutant mice
A) Timeline for Itraconazole treatment. B) *Pkd1 cko* were treated with saline (N=2) or with Itraconazole (N=5) through breast milk. C) qPCR for control and mutant mice treated with saline (N=6 control, N=2 mutants) or with Itraconazole (N=4 control and N=5 mutants).

Table 3. Genotyping Primers

		Product size (bp)	
		wild-type	mutant
jck-F	5' CTT CCC ACC TGT TGC TGT TT 3'	108 and 200	308
jck-R	5' CAG TGG GCT TAC CAC CAT CT 3'		
Pkd1flox/flox-F	5' CCT GCC TTG CTC TAC TTT CC 3'	132	250
Pkd1flox/flox-R	5' AGG GCT TTT CTT GCT GGT CT 3'		
Pkd2flox/flox-F	5' GGG GTT TCC TAT GAA GAG TTC CAA G 3'	383	485
Pkd2flox/flox-R	5' CTG ACA GGC ACC TAC AGA ACA GTG 3'		
Cre-F	5' GCG GTC TGG CAG TAA AAA CTA TC 3'	none	100
Cre-R	5' GTG AAA CAG CAT TGC TGT CAC TT 3'		
Gli2+/- - F	5' AAA CAA AGC TCC TGT ACA CG 3'	none	600
Gli2+/- - R	5' ATG CCT GCT CTT TAC TGA AG 3'		
Gli2flox/flox - F	5' AGG TCC TCT TAT TGT CAG GC 3'	232	280
Gli2flox/flox - R	5' GAG ACT CCA AGG TAC TTA GC 3'		

Table 4. qPCR Primers

Ptch1–F	5’ CCT CCT GAA CCC CTG GAC 3’
Ptch1–R	5’ CAT GCC AAA GAG CTC AAC G 3’
Gli1-F	5’ CTG ACT GTG CCC GAG AGT G 3’
Gli1-R	5’ CGC TGC TGC AAG AGG ACT 3’
Gli2-F	5’ GCA GAC TGC ACC AAG GAG TA 3’
Gli2-R	5’ CGT GGA TGT GTT CAT TGT TGA 3’
Gli3-F	5’ CAC CAA AAC AGA ACA CAT TCC A 3’
Gli3-R	5’ GGG GTC TGT GTA ACG CTT G 3’
Oaz1-F	5’ GCC TGA GGG CAG TAA GGA C 3’
Oaz1-R	5’ GGA GTA GGG CGG CTC TGT 3’

3.5 Discussion

The mechanisms connecting primary cilia dysfunction to renal cystogenesis are not well understood. The Hh signaling pathway is the best characterized, cilia-mediated pathway, so we have hypothesized that misregulation of Hh signaling has a role in renal cystogenesis. Previously, increased Hh signaling was reported in human ADPKD kidneys [110, 138] and in cystic kidneys of several mouse models, including *Thm1 cko, jck* and *Pkd1* cko [80, 107, 109]. Furthermore, downregulation of Hh signaling reduced renal cystogenesis of *Thm1 cko* mice and of cultured *jck* and *Pkd1*-mutant mouse embryonic kidneys [80]. In the current studies, we expanded on the role of Hh signaling in renal cystogenesis of *jck, Pkd1* cko and *Pkd2* cko mice. Our preliminary data suggest increased Hh signaling correlates with disease progression in *jck* mutant mice and that genetic downregulation of the pathway decreases KW/BW ratios in *jck* and *Pkd1* cko mouse models.

The influence of mouse strain background on PKD severity [172-175], due to genetic modifiers interacting with the causal mutation [172], is an on-going discussion in the field. An advantage of working with a mixed strain background is better representation of the genetic heterogeneity of the human population. However, a disadvantage is the phenotypic variability that can ensue, requiring larger numbers of animals in order to obtain significance. The *cpk, pcy* and *jck* mutants are among the PKD mouse models that showed less severe disease on a C57BL/6J genetic background, compared to other background strains [175-177]. Consistent with these findings, in the current studies we show that 7-week- old *jck* mutants on a mixed background have higher %KW/BW, compared to *jck* mice on a C56BL/6J background at the same age, indicating disease is likely less severe in *jck* mice under a pure C57BL/6J background. Also, *Gli1* expression is increased at a later timepoint in *jck* mice under a C57BL/6J background shown here, while 7-

week-old mice under a mixed background already have elevated *Gli1* expression [80]. Interestingly, these results further support a role for enhanced Hh activity in disease progression.

Efforts are ongoing to increase the number of animals in the experimental groups. Recently, we have backcrossed all lines onto a C57BL/6J background to the 10^{th} generation, and crosses are underway to obtain single and double cko mice. Since our data on *jck* mice seem promising, we are continuing to examine the effect of deletion of *Gli2* in the *jck* mice. Furthermore, for *Pkd1* and *Pkd2* mice, we have generated lines to delete *Smo,* which may provide greater downregulation of the Hh pathway, than deletion of *Gli2*, since there is redundancy between the GLI transcription factors.

Our data show enhanced nuclear GLI1 staining in renal interstitial and epithelial cells of *jck* cystic tissue on a pure C57BL/6J background. Since renal tubular epithelial cells have been shown to express Hh ligand, the presence of GLI1 in the interstitium and in the epithelia suggests active paracrine and autocrine Hh signaling in this mouse model [147]. Interestingly, elevated paracrine Hh signaling has been reported in renal fibrosis, while increased autocrine Hh signaling has been shown in renal cell carcinoma (RCC) [112, 147]. Perhaps the paracrine Hh signaling in *jck* mice reflects or contributes to fibrosis, while the autocrine Hh signaling plays a role in proliferation of renal epithelial cells. Since Hh activity appeared to increase with disease progression and epithelial cells of non-dilated tubules in *jck* mutant mice did not show nuclear GLI1 staining, increased Hh signaling may have a role in disease progression, but not initiation.

Previously, genetic downregulation of Hh signaling by deleting *Gli2* attenuated renal cystogenesis in *Thm1* conditional knock-out mice [80]. Our data show that genetic downregulation of Hh signaling by deleting *Gli2* also decreases renal cystogenesis and BUN levels in *jck* mutants

and % KW/BW in *Pkd1* conditional knock-out mice, on a mixed strain background. These findings suggest increased Hh signaling may have a general role in renal cystogenesis.

Pharmacological Hh inhibitors reduced the cAMP-mediated cystogenic effects in cultured mouse embryonic kidneys [80] and also reduced cAMP-mediated cell proliferation of ADPKD primary cells [138], and thus, we anticipated that administration of pharmacological inhibitors of Hh signaling would attenuate renal cystogenesis in *jck* and *Pkd1* mutant mice, which was not the case. However, we cannot exclude the possibility that Hh pathway was not sufficiently inhibited. Thus, dosing and timing of treatment will need to be adjusted.

How Hh signaling connects to known mechanisms underlying ADPKD is unclear. ADPKD cells have decreased intracellular calcium, which together with aberrant cAMP activity induces cyst growth by stimulating fluid secretion and cell proliferation [49, 52]. Importantly, restoring calcium concentrations prevented cAMP-mediated cell proliferation of ADPKD cells *in vitro* [51]. A study suggests that Hh signaling may modulate intracellular Ca^{2+}. Smo inhibitor, GDC-0449, increased intracellular Ca^{2+} in a cancer cell line and reduced proliferation *in vitro* [164]. The mechanism(s) that lead to increased Hh activity in PKD is also not clear. *Gli1* was shown to be a target of Brd4, an epigenetic regulator, in a medulloblastoma mouse model [178], and inhibition of Brd4 in *Pkd1* cko mice slowed cystic disease progression [166]. Thus, epigenetics may be a mechanism modulating Hh signaling in the PKD mouse models used in this study.

In summary, our data suggest downregulation of the Hh pathway may attenuate renal cystic disease in ADPKD mouse models. This together with our findings that Hh signaling is increased in human ADPKD tissue and that Hh inhibitors reduced cell proliferation and microcyst formation of culture human ADPKD renal epithelial cells [138] (Chapter 2), suggest Hh signaling can be investigated further as a potential therapeutic target. Since several Hh inhibitors are already FDA-

approved or are currently under clinical trials for cancer therapy, repurposing available drugs could be an option [111]. Since ADPKD involves dysregulation of several pathways, inhibiting more than one pathway and possibly targeting different pathways at different disease stages will likely provide a more effective therapy. Our work suggests a role for ciliary-mediated Hh signaling in disease progression. What primary cilia-mediated mechanisms lead to disease initiation is another question we are invested in answering.

Chapter Four:

RNA sequencing reveals increased STAT3 signaling in pre-cystic kidneys of *Thm1* conditional knock-out mice

4.1 Abstract

Primary cilia are sensory organelles that mediate signaling pathways, and dysfunction of primary cilia leads to renal cystic disease. Multiple cellular and signaling aberrations contribute to renal cystic disease, while initiating molecular mechanisms remain unclear. In mice, perinatal global deletion of ciliary gene, *Thm1,* causes renal cysts beginning at P15. To identify molecular events that initiate renal cystogenesis in *Thm1* conditional knockout (cko) mice, RNA sequencing was performed on total RNA of pre-cystic and cystic kidneys of *Thm1* cko mice at P9 and P42, respectively. We reasoned that genes with significantly altered expression in both pre-cystic and cystic kidneys would represent early initiation events leading to cystogenesis. Approximately 10 genes - *Fos, Jun, Stat3, Endothelin 1, Vcam1, Complement C3, Ccl2, Egr2,* and *Adcy7*- met this criterion. This gene set included genes typically expressed not just by epithelial cells, but by endothelial or immune cells. Western blot analysis on whole kidney extracts showed increased P-STAT3 at P10, and upregulation of multiple components of STAT and EDN1-MAPK signaling pathways at P42. Additionally, immunohistochemistry revealed increased nuclear localization of P-STAT3 in epithelial cells of non-dilated and dilated tubules and cysts, and in interstitial cells. To study the connection between primary cilia dysfunction and upregulated STAT3 signaling, we generated *THM1* knock-down (kd) human renal 293T clonal cell lines. *THM1* kd cells have shortened primary cilia with IFT81 accumulation in a bulb-like structure at the distal tip, indicative of a retrograde ciliary protein trafficking defect. Upon treatment with IL6, *THM1* kd cells showed a more robust second wave of STAT3 activation than control cells, which was preceded by a more intense activation of ERK. Together, these data suggest that altered gene expression and signaling in renal epithelial, vascular and immune cells may potentiate renal cystogenesis, and, in particular, increased STAT3 signaling may link primary cilia dysfunction to renal cyst initiation.

4.2 Introduction

Primary cilia are signaling organelles essential for development and health [80, 140]. Genetic mutations that disrupt primary cilia function lead to ciliopathies, which manifest a plethora of clinical features, among which renal cystic diseases are very common [140]. The most common renal cystic disease is Autosomal Dominant Polycystic Kidney Disease (ADPKD), affecting ~1:500 individuals worldwide. ADPKD is caused by mutations in *PKD1* and *PKD2*, encoding polycystin-1 and polycystin-2, which function as a heterocomplex in primary cilia [6, 139]. Thus far, molecular mechanisms identified in ADPKD appear to contribute to disease progression, while initiating events remain largely obscure. Intriguingly, while ciliary dysfunction leads to renal cystogenesis, genetic ablation of primary cilia in orthologous ADPKD mouse models and pharmacological reduction of cilia length in *Nek8*$^{jck/jck}$ mice ameliorated the renal cystic disease, suggesting a ciliary-mediated signaling pathway is essential for cyst development [56, 58, 97, 141].

Primary cilia are synthesized and maintained via intraflagellar transport (IFT) or the bi-directional transport of protein cargo along a microtubular axoneme. IFT is mediated by two protein complexes: IFT complex B interacts with the kinesin motor to mediate anterograde IFT, while IFT complex A together with cytoplasmic dynein is required for retrograde IFT. IFT-A proteins are also essential for ciliary import of signaling molecules [179]. In mice, deletion of *Ift-A* or *-B* genes either perinatally or specifically in the kidney results in renal cystic disease [107, 121, 145]. However, *Ift-A* and *–B* mutants usually show contrasting ciliary phenotypes and can also show opposing signaling phenotypes, reflecting differing roles of IFT-A and –B in ciliogenesis and in regulating signaling pathways [25, 26, 107, 144]. Thus, study of both *Ift* mutant classes provides valuable insight into the various molecular mechanisms that lead to renal cysts.

Thm1 (TPR-containing Hedgehog modulator 1; also termed *Ttc21b*) encodes a component of IFT complex A, and its deletion impairs retrograde IFT, causing accumulation of proteins in bulb-like distal tips of shortened primary cilia [25]. Causative and modifying mutations in *THM1* have been identified in 5% of patients with ciliopathies, including NPHP, BBS, MKS and Jeune Syndrome [82]. In mice, deletion of *Thm1* recapitulates many of the clinical manifestations of these ciliopathies, and perinatal global deletion of *Thm1* results in renal cystic disease with renal tubular dilations beginning by P15 [25, 80]. By P42, *Thm1* cko renal cystic disease shares similarities with ADPKD, including increased cAMP and increased cell proliferation. *Thm1* cko cystic kidneys also show enhanced Hh signaling, a ciliary dependent pathway [80], which we and others have shown to be misregulated in ADPKD renal cystic tissue. In the current study, we sought to determine the signaling molecules and pathways that initiate renal cystogenesis in the *Thm1* cko mouse, using a global transcriptomics approach.

4.3 Methods

4.3.1 Generation of *Thm1* cko mice

Thm1 cko mice were generated as described [80]. Briefly, a *Thm1*-lacZ knockout mouse ($Ttc21b^{tm2a(KOMP)Wtsi}$) was purchased from KOMP (Knockout Mouse Project) [80]. The *LacZ* gene was flanked by Frt sites in intron 3 of *Thm1,* and loxP sites flanked exon 4 of *Thm1*. *Thm1*-lacZ mice were mated to FLPeR mice, expressing FLPe recombinase, to flip out the *LacZ* gene, and allow transcription from exon 3 to exon 4. Resulting $Thm1^{flox/+}$ mice were intercrossed to generate $Thm1^{flox/flox}$ mice. A tamoxifen-inducible $ROSA26Cre^{ERT}$ mouse (Jackson Laboratory – stock 004847) was mated to $Thm1^{aln/+}$mice to create $Thm1^{aln/+}$; $ROSA26Cre^{ERT/+}$ mice. Male $Thm1^{aln/+}$; $ROSA26Cre^{ERT/+}$ mice were mated with $Thm1^{flox/flox}$ females. At post-natal days 0

and 3, nursing females were injected intraperitoneally (i.p) with tamoxifen (Sigma) at 10 mg/40g mouse body weight to delete *Thm1* globally.

4.3.2 Mouse genotyping

Genotyping primers are listed in Table 5. The *aln* PCR product was digested with *Ava*II at 45 °C for 1h.

4.3.3 Kidney Weight/Body Weight measurements

Mouse body weight and individual kidneys were weighed in grams using a standard weighing scale. Total kidney weights were divided by body weight for each mouse.

4.3.4 RNA seq

RNA was extracted from whole kidneys of P9 and P42 control and *Thm1* cko mice (N=6/ each group), using QIAGEN RNeasy Mini kit according to manufacturer's instructions. Samples with RIN values >8.0, determined by the KUMC Genomics Core, were used for RNA Sequencing (HiSeq2500, Ilumina). 100-cycle paired-end reads were performed (HiSeq2500, llumina), assigning 6 multiplexed samples/lane, providing 44X coverage/sample. Data were analyzed by Dr. Sumedha Gunewardena of the KUMC Bioinformatics Core. Sequences were aligned to the mouse genome (GRCm38). Differential gene expression was calculated using Cuffdiff, and P-values were adjusted for false discovery by the Benjamini and Hochberg method.

4.3.5 Western Blot

Protein extracts were obtained by homogenizing frozen kidney tissue with Passive Lysis Buffer (Promega) containing proteinase inhibitor cocktail (Pierce) using 0.5 mm zirconium oxide PINK beads (Next Advance) and a Bullet Blender Storm (Next Advance) set at Speed 10 for approximately 10 minutes. Lysates were centrifuged at 4°C at maximum speed for 1 minute and supernatant was collected. Western blot was performed as described [80], using primary antibodies for P-STAT3, STAT3, P-ERK, ERK, P-CJUN, C-FOS, FOS-B, STAT5, STAT6, STAT1 and P-Cyclin D1 (Cell Signaling Technology), Endothelin-1 (Thermo Scientific) and VCAM1 (Abcam). Extracts from three controls and three mutants at P10 and at P42 were examined. Western Blot was quantified using ImageJ.

4.3.6 Immunohistochemistry

Kidneys were dissected and renal capsules removed. Kidneys were bisected longitudinally and placed in 4% paraformaldehyde for 3-7 days, then placed in 70% ethanol in PBS. Tissues were dehydrated through an ethanol series, embedded in paraffin and sectioned at 8μm thicknesses. Tissue sections were deparaffinized in xylene and rehydrated through an ethanol series to distilled water. Antigen retrieval was performed by steaming tissue sections for 25 minutes in Sodium Citrate Buffer (10mM Sodium Citrate, 0.05% Tween 20, pH 6.0). To minimize background staining, sections were treated with 3% hydrogen peroxide for 30 min, washed in PBS, then blocked with 1% BSA for 1 hour. Tissues were then incubated with P-STAT3 antibody (Cell Signaling) overnight at 4°C. Following 3 washes in PBS, sections were incubated with HRP-conjugated rabbit secondary antibody (Cell Signaling) for 30 minutes. Following another 3 washes in PBS, tissues were incubated with ABC reagent (Vector Laboratories), rinsed in PBS, and then

incubated with Sigma FAST DAB metal enhancer (Sigma) until desired signal/color was obtained. Staining was visualized and imaged using a Nikon 80i light/fluorescent microscope and Nikon DS-Fi1 camera.

4.3.7 Drug studies

To inhibit STAT3 signaling pharmacologically, STAT3 inhibitors, Pyrimethamine (Sigma), Stattic (Tocris) and C188-9 (Sigma), were used. Treatments began around weaning (P21) and were administered until dissection at P42. Daily gavages of pyrimethamine was administered at two doses - 12.5mg/kg and 25mg/kg. Control (N=2) and *Thm1* cko mice (N=1) received 12.5mg/kg pyrimethamine. Control (N=1) and *Thm1* cko mice (N=3) received 25mg/kg pyrimethamine. Control (N=3) and *Thm1* cko mice (N=3) received vehicle. Intraperitoneal injections of Stattic (10mg/kg) was administered every other day to control (N=4) and *Thm1* cko mice (N=3), while vehicle was administered to control (N=1) and *Thm1* cko mice (N=4). Lastly, daily intraperitoneal injections of C188-9 (50mg/kg) was administered to *Thm1* cko mice (N=4), while vehicle was administered to a *Thm1* cko mouse (N=1).

4.3.8 Immunofluorescence

Cells were washed with PBS, fixed in 4% paraformaldehyde containing 0.2% triton X-100 for 10 minutes at room temperature, washed with PBS, and blocked with 1% BSA in PBS for 1 hour, and then incubated with antibodies against IFT81 (Proteintech) and acetylated α-tubulin (Sigma) overnight at 4° C. Following 3 washes in PBS, cells were incubated with anti-rabbit secondary antibody conjugated to AF488 and anti-mouse secondary antibody conjugated to AF594 (InVitrogen Technologies) for 30 minutes at room temperature. Cells were washed 3X in PBS and

mounted with Vectashield containing 4,6-diamidino-2-phenylindole (DAPI) (Vector Laboratories). Immuno-labeled cells were viewed and imaged using a Leica TCS SPE confocal microscope configured on a DM550 Q upright microscope.

4.3.9 Cell culture

THM1 knock-down (kd) using shRNA was performed as described [25]. Briefly, pLKO.1-*THM1*-R1 plasmid was generated by cloning oligonucleotide *THM1* R1 (Table 5) annealed to its 5′-phosphorylated complementary strand into the AgeI/EcoRI sites of the pLKO.1 lentiviral vector. Subsequently, 293T cells were transfected with plasmids VSVG, delta8.2 and pLKO.1-*THM1*-R1 (pLKO.1 served as the empty control vector) for 48 h using FuGENE (Roche) to generate viruses. Medium containing the lentiviruses was filtered (0.45 μm pore size) and target 239T cells were infected with lentiviruses expressing either empty control vector or *THM1* R1 shRNA using Polybrene. Cells were then trypsinized and selected in medium containing puromycin. Lastly, clonal cell lines were generated by isolating single colonies using sterile cloning disks (Fisher), and expanding colonies.

Recombinant human IL-6 (PeproTech) was dissolved in 0.1% BSA. Control and *THM1* kd 293T renal cell lines were grown in 6-well cell culture plates until about 90% confluency. Cells were treated with IL6 (20ng/ml) for different durations (0.5h, 1h, 2h, 3h, 4h, 8, 12h, 16h and 24h). Cells that were non-treated (NT) or cultured with 0.1% BSA for 24h wells were considered controls. Cell pellets were collected at the end of each timepoint, protein was extracted, and Western Blot was performed.

4.4 Results

4.4.1 Expression of genes typically expressed by epithelial, endothelial or immune cells is increased in pre-cystic kidneys of *Thm1* cko mice

To uncover the misregulated genes and pathways that initiate *Thm1*-deficient renal cystogenesis, RNA sequencing was performed on pre-cystic and cystic whole kidney RNA extracts of *Thm1* cko mice, at P9 and P42, respectively. We hypothesized that genes with altered expression both before renal cysts have formed and during disease progression may contribute to cyst initiation as well as progression, while genes that are misregulated at P42, but not before cysts have formed, may contribute to disease progression. We identified approximately 10 genes that were significantly increased at P9 and further increased at P42. These genes included *Fos, Jun, Stat3, ET1, Vcam1, Ccl2, C3, Egr2* and *Adcy7.* We noted that while *Fos, Jun* and *Stat3* are expressed by the renal epithelium, *ET1* and *Vcam1* are often associated with endothelium, and *Ccl2, C3, Egr2* and *Adcy7* are thought to be expressed by immune cells (Figure 4.1a). These data suggest that in our global *Thm1* cko mouse, alteration of gene expression and signaling in renal epithelial, vascular and immune cells may potentiate renal cyst formation.

In contrast to the small gene set that was upregulated in both pre-cystic and cystic kidneys, P42 cystic tissues showed more than 5000 misregulated genes. In accordance with increased expression of *Fos, Jun* and *Stat3,* in the gene set described above, multiple genes of the STAT (Signal Transducer and Activator of Transcription) and MAPK (Mitogen-activated protein kinase) signaling pathways were increased. Additionally, genes of the Hedgehog (Hh) signaling pathway, *Ptch2* and *Gli3,* and of Notch signaling, *Notch3* and *Jag1,* were also increased in cystic kidneys (Figure 4.1b). *Sufu,* a negative Hh regulator, was decreased, consistent with increased Hh signaling. Further, multiple genes expressed by the immune system, and multiple genes of the

integrin, FGF, Wnt and TGF-ß signaling pathways were increased (Figure 4.1b). In contrast, multiple mitochondrial genes were downregulated. These data illustrate the molecular complexity that ensues once renal cystic disease has progressed.

A

		P9 fold change	P42 fold change
Renal Epithelium			
Fos	FBJ murine osteosarcoma viral oncogene homolog	1.7	5
Fosb	FBJ murine osteosarcoma viral oncogene homolog b	1.9	8
Jun	jun proto-oncogene	1.3	1.8
Junb	junb proto-oncogene	1.5	3.9
Stat3	signal transducer and activator of transcription 3	1.4	2.1
Endothelium			
Edn1	endothelin 1	2.5	9.5
Vcam1	vascular cell adhesion molecule 1	1.6	8.4
Immune			
Ccl2	C-C Motif Chemokine Ligand 2	2.8	28.1
C3	complement component 3 - role in inflammation	3.8	16.5
Egr2	early growth response 2 - modulator of systemic autoimmune disease	3.1	26.9
Adcy7	adenylate cyclase 7 - peripheral leukocytes	1.6	9

B

Hh		
gene	**fold- change**	**q-value**
Ptch2	1.9	5.57E-03
Gli3	3.8	4.04E-04
Sufu	-1.6	4.04E-04
Notch		
gene	**fold- change**	**q-value**
Notch3	1.5	1.11E-03
Jag1	1.8	4.04E-04

Signaling Pathways/Molecules
⬆ Immune
⬆ Integrin
⬆ TGF-Beta
⬆ MAPK
⬆ STAT
⬆ Wnt
⬆ FgF

Figure 4.1: Genes and signaling pathways significantly increased in *Thm1* cko kidneys
A) Genes significantly upregulated in both pre-cystic and cystic kidneys of P9 and P42 *Thm1* cko mice, respectively (N=6/group). B) Genes and pathways misexpressed in cystic kidneys at P42.

4.4.2 Increased STAT3 may promote renal cystogenesis in *Thm1 cko* mice

To validate the RNA Seq data, we performed Western Blot analysis on pre-cystic (P10) and cystic (P42) whole kidney extracts. We used antibodies for Endothelin-1, p-ERK, ERK, c-JUN, c-FOS and FOSB, which are components of the Endothelin-MAPK signaling pathway [180, 181] but quantification of the blot did not show a significant elevation of MAPK components amounts in pre-cystic kidneys (data not shown); indicating MAPK signaling may not play a role in renal cyst initiation in this mouse model. As expected, all the MAPK pathway components we probed for are increased in P42 kidneys, including a significant increase in FOS-B (data not shown), when renal cystic disease is already advanced (Figure 4.2a). In addition, we used antibodies for several STAT proteins (STAT1, 3, 5 and 6 are shown for P42 kidneys, while 3 and 5 are shown for P10 kidneys) and observed that these STATs are increased in cystic kidneys. Importantly, STAT3 activation (P-STAT3/STAT3) is prominently increased in pre-cystic kidneys, suggesting a role for this pathway in renal cyst initiation in this mouse model (Figure 4.2b). Further, we show increased levels of P-Cyclin D1 [182] and of inflammatory molecule, VCAM1 [183], in cystic kidneys (Figure 4.2a). Because P-STAT3/STAT3 ratios are significantly increased in pre-cystic and cystic *Thm1* cko kidneys (Figure 4.2b), we next examined subcellular localization of P-STAT3 in tissue sections. Nuclear localization of P-STAT3 indicates activation of the pathway [184]. We observed increased nuclear P-STAT3 in renal epithelial cells of non-dilated and dilated tubules at 20, and in cystic-lining epithelial cells and interstial cells at P42 (Figure 4.2c). Together, these results suggest STAT3 and MAPK signaling may initiate renal cystogenesis in *Thm1* cko mice.

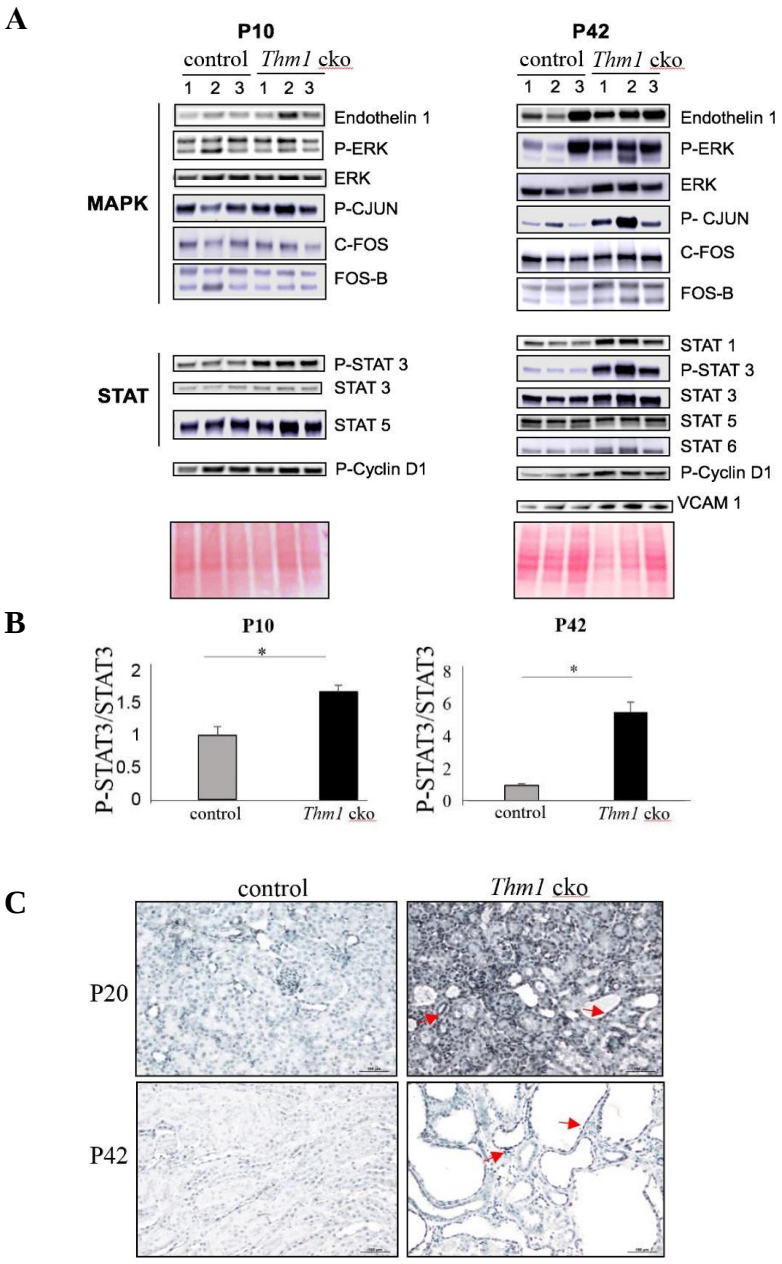

Figure 4.2: MAPK and STAT3 signaling upregulation may promote renal cystogenesis in *Thm1 cko* mice

A) Western Blot analysis shows slight increase in P-CJUN and increased STAT3 activation in pre-cystic kidneys at P10. Cystic kidneys show increase in MAPK signaling components and increased STAT1, 3 and 6. B) Western Blot quantification show increased P-STAT3/STAT3 in pre-cystic and cystic *Thm1* cko kidneys. WB was quantified using ImageJ. C) Immunohistochemistry for P-STAT3 on P20 and P42 control and *Thm1* cko kidney sections. Red arrows point to increased nuclear P-STAT3 in epithelial cells of non-dilated and dilated tubules at P20, and in interstitial and cyst-lining epithelial cells at P42.

4.4.3 IL-6 treated *THM1* kd 293T human renal cells show a stronger second wave of STAT3 activation that is preceded by increased activation of ERK

To determine the molecular mechanism by which STAT3 signaling is upregulated by the *Thm1* ciliary defect, we generated clonal *THM1* kd 293T human renal cells, with 70% less THM1 protein control cells (Figure 4.3a). *THM1* kd 293T cells have shortened cilia with accumulation of IFT81 in bulb-like distal tips, indicative of a retrograde IFT defect (Figure 4.3b). A previous report showed that IL6 treatment of colon cancer, adenocarcinoma and 293T cells caused two waves of STAT3 activation. The first wave induced EGF expression, which then induced the second wave of STAT3 activation [185]. Similarly, we treated control and *THM1* kd 293T cells with IL6 and examined STAT3 activation at different timepoints. Relative to control cells, *THM1* kd cells showed a more robust second wave of STAT3 activation, which was preceded by a more robust activation of ERK (Figure 4.3c-d). These data demonstrate that *THM1* deficiency causes aberrant activation of STAT3 and MAPK signaling in renal cells.

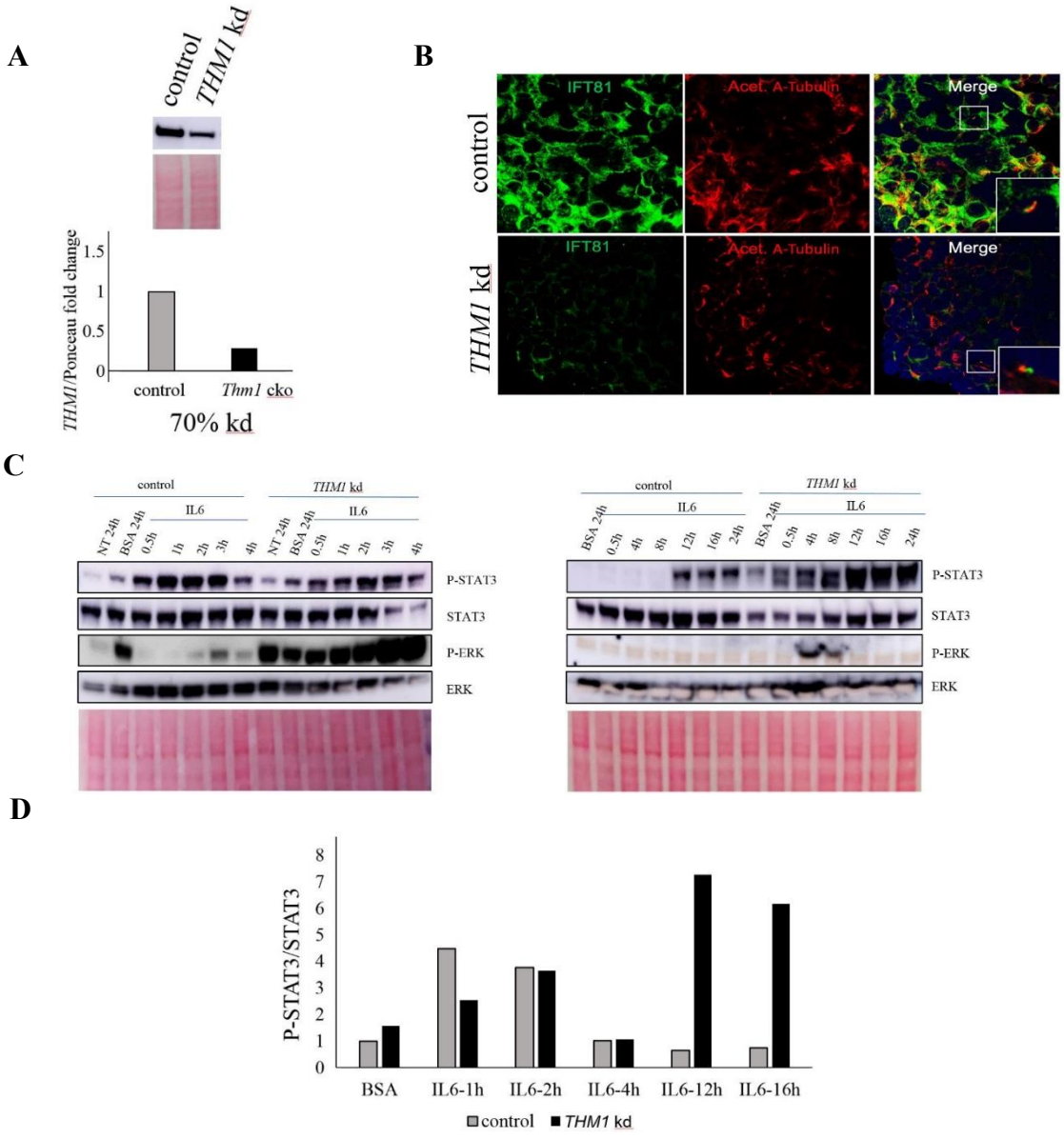

Figure 4.3: IL6-treated *THM1* kd 293T cells show a more robust second wave of STAT3 activation

A) Western Blot for THM1 on control and *Thm1* kd extracts. B) Analysis of cilia by immunostaining for IFT81 (green) and acetylated α-tubulin (red). C) Western Blot for P-STAT3/STAT3 and P-ERK/ERK on extracts of IL6-treated cells (N=2). D) Western blot quantification for P-STAT3/STAT3 include BSA and IL6 treatments (1,2,4,12 and 16h) and show more robust second wave of STAT3 activation in the *THM1* kd line. WB was quantified using ImageJ.

4.4.4 Treatment of *Thm1* cko mice with STAT3 inhibitors

To demonstrate a functional role for STAT3 signaling in *Thm1* cko renal cystic disease, we have attempted pilot experiments with several STAT3 inhibitors - Pyrimethamine at two doses (12.5mg/kg and 25mg/kg) [186], Stattic at 10mg/kg [187] and C188-9 at 50mg/kg [188]. These STAT3 inhibitors were chosen since pyrimethamine treatment of adult *Pkd1 cko* mice suppressed cyst formation and growth [186], while Stattic attenuated renal disease in a mouse model of Alport syndrome [187, 189]. Finally, C188-9 was recently identified and shown to reduce STAT3 signaling in a mouse model of hepatocellular carcinoma [190]. Administration of pyrimethamine or Stattic to *Thm1* cko mice did not reduce % KW/BW (Figures 4.4 b,d,f), and also did not reduce P-STAT3/STAT3 ratios (Figures 4.4 b,d,f). C188-9 decreased P-STAT3:STAT3 levels by about 18-46%, but did not reduce %KW/BW relative to the vehicle-treated *Thm1* cko mouse (Figure 4.4 f). However, this vehicle-treated *Thm1* cko mouse showed relatively higher levels of THM1, and an unusually low %KW/BW ratio, suggesting that this vehicle-treated *Thm1* cko mouse may not be the best representative to compare with the treated mice. Thus, more animals are required to determine the effectiveness of C188-9 in attenuating *Thm1* cko renal cystic disease.

A

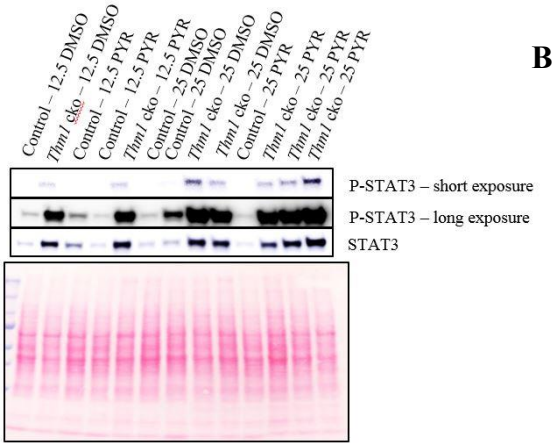

B

Thm1 cko	Treatment	%KW/BW	P-STAT3/ STAT3
1	DMSO	2.7	1
2	PYR -12.5	2.6	0.92
3	DMSO	2.7	1
4	DMSO	2.4	0.99
5	PYR - 25	2.6	1.43
6	PYR - 25	2.7	1.04
7	PYR - 25	2.8	0.8

C

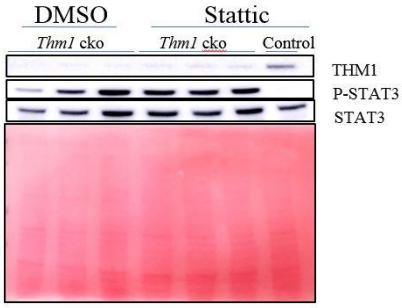

D

Thm1 cko	Treatment	%KW/BW	P-STAT3/ STAT3	THM1/ Ponceau
1	DMSO	3.5	1	1
2	DMSO	4.5	3.42	0.75
3	DMSO	2.8	3.36	0.55
4	Stattic	2.9	3.16	1
5	Stattic	3	3.92	1.04
6	Stattic	2.9	3.08	1.2

E

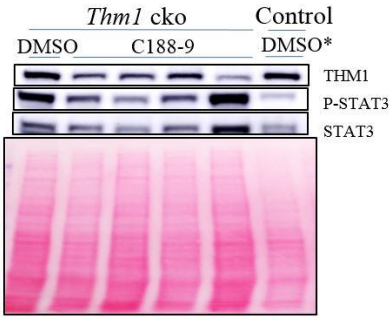

F

Thm1 cko	Treatment	%KW/BW	P-STAT3/STAT3	THM1/Ponceau
1	DMSO	1.72	1	1
2	C188-9	1.71	0.75	0.6
3	C188-9	1.8	0.56	0.6
4	C188-9	1.76	0.65	0.9
5	C188-9	2.21	0.827	0.29

Figure 4.4: Pilot experiments with STAT3 inhibitors
A/C/E) WB for P-STAT3 and THM1 for Pyrimethamine (PYR), Stattic and C188-9 treated mice. B/D/F) WB quantification and %KW/BW of *Thm1* cko mice. WB was quantified using ImageJ.

Table 5: Oligonucleotides sequences

		Product size (bp)	
		wild-type	mutant
aln-F	5’ CGC TGA TTA ACT ACT ATG GTC 3’	100	70
aln-R	5’ GCG TGG TAA AAT CGG AAG AC 3’		
Cre-F	5’ GCG GTC TGG CAG TAA AAA CTA TC 3’	none	100
Cre-R	5’ GTG AAA CAG CAT TGC TGT CAC TT 3’		
THM1 R1	5’ CCG GGA CGC TGA TTA ACT ACT ATT TCA AGA	none	none
	GAA TAG TAG TTA ATC AGC GTC TTT TTG 3’		

4.5 Discussion

We performed RNA sequencing in pre-cystic and cystic kidneys of *Thm1* cko mice to determine molecular mechanisms by which primary cilia dysfunction initiates renal cystic disease. We reasoned that genes misregulated in both pre-cystic and cystic kidneys may initiate renal cystic disease. Our data revealed genes often associated with the epithelium (*Fos, Fosb, Jun, Junb, Stat3),* with the endothelium (*Endothelin1* and *Vcam1),* and with the immune system (*Ccl2, Complement C3, Egr2* and *Adcy7*), to be upregulated in pre-cystic and cystic kidneys. These data suggest that misregulation of genes in these 3 compartments may initiate disease processes in this ciliary mouse model. These genes may also be initially expressed in renal epithelial cells, which has been reported for *Ccl2* [131]. Western blot analysis and immunohistochemistry suggest that STAT3 signaling is the most prominent pathway upregulated in pre-cystic *Thm1* cko kidneys.

Many of the molecules and pathways that are misregulated in pre-cystic (and cystic) *Thm1* cko kidneys have been reported to contribute to renal cystic disease progression, but not initiation. Increased MAPK and STAT3 signaling have been reported in mouse models of ADPKD and in human ADPKD tissue [51, 80, 107-109, 138, 184, 186, 191-193]. Endothelin 1 (ET1) is an endothelium-derived vasoconstrictor and pro-fibrotic peptide and its overexpression caused renal cysts in mice, while rat models of PKD and human ADPKD kidneys show increased ET1 [194-199]. VCAM1 is an endothelial adhesion molecule that contributes to inflammation in PKD [183]. Further, increasing *in vitro* and *in vivo* evidence suggest a role for the immune system in PKD progression [183, 200-202]. Complement C3 was found to be upregulated in urine of ADPKD patients and inhibiting C3 in a mouse model of ADPKD reduced disease progression [203]. *Ccl2,* which encodes monocyte chemoattractant protein 1 (MCP1), is the only molecule which has been reported to play a role in early renal cystic disease in a PKD mouse model. In the absence of PC1,

Ccl2 expression is increased in renal tubular epithelial cells, promoting macrophage recruitment and inflammation. *Ccl2* expression is regulated by a ciliary-localized protein complex and hence is dependent on primary cilia [131].

Since increased STAT3 activation in pre-cystic *Thm1* cko kidneys was the most prominent alteration among the proteins we queried, we focused our attention on this pathway. STAT3 is a developmental pathway with important roles in cell proliferation and in the immune system. Canonical activation of STAT3 signaling occurs when ligands, such as cytokines and growth factors, activate Janus kinases (JAK-tyrosine kinases), which in turn phosphorylate and activate STAT3, which stimulates transcription of target genes [204]. STAT3 signaling is highly active in developing kidneys, suggesting a role in renal development [184].

Increased STAT3 signaling contributes to cell proliferation and immune response in ADPKD progression, but its role in renal cyst initiation has not been reported. In the interstitium, cytokine IL-10 is released by macrophages in ADPKD and activates STAT3, contributing to disease progression [205]. In the epithelium, epidermal growth factor (which is upregulated in ADPKD) can activate STAT3. Further, STAT3 activation is increased in ADPKD human tissues [205, 206]. How STAT3 signaling leads to renal cystogenesis in our mouse model is unclear. Recently, PC1 was found to interact with Liver Kinase B1 (LKB1), a tumor suppressor kinase, which is part of a protein complex that localizes to cilia. This PC1-LKB1 signaling is thought to keep *Ccl2* expression levels low and thereby regulate inflammation through primary cilia [131]. *Pkd1*,*Ccl2* dko mice showed reduced renal cystogenesis, suggesting the immune reaction triggered by *Ccl2* may link primary cilia to renal cystic disease [131]. In a prostate cancer study, *Ccl2* was shown to be a target of STAT3 signaling [207]. Similarly, STAT3 signaling may also activate *Ccl2* expression in the kidney, contributing to renal cyst initiation in the *Thm1* cko mouse.

To determine whether increased STAT3 signaling promotes renal cystogenesis in *Thm1* cko mice, we attempted pilot studies using three pharmacological STAT3 inhibitors that have been reported to be effective in attenuating disease in mouse models. Pyrimethamine suppressed cyst formation and growth in an adult *Pkd1 cko* mouse model [186]. Stattic decreased STAT3 activity and improved renal phenotype in a mouse model of Alport syndrome, a renal disease caused by mutation in collagen type IV [187, 189]. Finally, C188-9 reduced STAT3 signaling in a mouse model of hepatocellular carcinoma [190]. Our administration of pyrimethamine and Stattic did not reduce STAT3 signaling in *Thm1* cko kidneys in our pilot studies, and therefore, a.higher dosage may be required. C188-9 reduced Stat3 signaling in *Thm1* cko kidneys, but was not effective in attenuating disease. However, since our vehicle-treated *Thm1* cko mouse showed mild cystic kidney disease and relatively high levels of THM1, we propose to expand our animal numbers and increase dose of C188-9. Alternatively, genetic downregulation of STAT3 signaling can also be performed [208].

To investigate the molecular mechanisms by which the *Thm1* defect causes upregulation of STAT3 signaling we generated *THM1* kd 293T renal cells. Cultured cell lines have both disadvantages and advantages. Cell lines do not allow for the cross-talk that may occur among different cell types and/or organs that may lead to pathway misregulation *in vivo*, and also do not represent a specific timepoint *in vivo*. Nonetheless, *in vitro* experiments allow for molecular analyses that may be difficult to carry out *in vivo*, and can reveal molecular aberrations that can be subsequently correlated with *in vivo* findings. We treated control and *THM1* kd cells with IL6, a cytokine that activates STAT3 signaling [204], and saw an aberrant response in *THM1* deficient cells, with a stronger second wave of STAT3 activation preceded by a robust activation of ERK. ERK can phosphorylate serine 727 of STAT3 [209], which may allow for easier STAT3 binding

to DNA to activate gene transcription [210], but may also prevent nuclear translocation [209]. P-CJUN, a component of MAPK signaling, is slightly increased in kidneys of pre-cystic *Thm1* cko mice, so reduced *Thm1* levels may affect regulation of ERK, and in turn, STAT3. Since P-CJUN levels were not upregulated in all pre-cystic *Thm1* cko kidneys examined, we speculate that this increase may be specific to certain cell types, and thus upregulation of MAPK signaling may be obscured in whole kidney extracts.

Another mechanism that may modulate STAT3 signaling in *Thm1* deficient cells is via PC1. PC1 regulates STAT3 activity by a dual mechanism - through JAK2 or activating STAT3 within the nucleus [206]. STAT6 is another member of JAK/STAT signaling that has been linked to PKD and can also be co-activated by PC1 [211] and localizes to cilia [211]. In contrast, the connection between STAT3 signaling and primary cilia is not known.

In addition to ERK and PC1, other components that are overexpressed in pre-cystic kidneys may also activate STAT3 signaling. For instance, ET1 induces secretion of IL6 in osteoblast-like cells [212]. Similarly, increased ET1 may induce IL6 in *Thm1* deficient kidneys, which would activate STAT3 signaling. Immune cells, such as monocytes and macrophages, can also activate STAT3 signaling in different cell-types by releasing IL6 [213]. Accordingly, macrophages are present in early renal cystic disease in Han:SPRD rats, a model of ADPKD [43]. The presence of macrophages in *Thm1* cko kidneys can also be examined.

Finally, cAMP, which is increased and has aberrant activity in ADPKD [49], activates ERK signaling, consequently inducing cell proliferation [50]. Thus, cAMP, which is also elevated in *Thm1* cko cystic kidneys, may also contribute to increased ERK and STAT3 activity in this model [80]. Future *in vitro* studies could examine the effects of cAMP on cell proliferation of *THM1* kd cells and on STAT3 activation. Other *in vitro* studies could examine the effects of MAPK and

STAT3 inhibitors to determine whether STAT3 or ERK is the first pathway to be dysregulated in *THM1* kd cells, and which pathway induces greater cell proliferation, which is essential for cyst formation [50].

In conclusion, our studies expand on the role of primary cilia in renal cyst initiation. Our analyses have led us to focus on STAT3 signaling. Future investigations will determine if STAT3 activation is mediated by primary cilia, the molecular mechanism underlying increased STAT3 signaling, and ultimately, identification of potential therapeutic targets to prevent renal cyst formation in PKD.

Chapter Five:

Discussion, Future Directions and Significance

5.1. Discussion

5.1.1 A role for increased Hedgehog signaling, a ciliary-dependent pathway, in ADPKD progression

An outstanding question in the PKD field is: What are the ciliary-mediated pathways that contribute to PKD? In Chapter 2, we are the first to show Hedgehog signaling, a ciliary-dependent pathway, plays a role in human ADPKD progression. Expression of Hh signaling components is increased in ADPKD mouse models and in human renal tissue [80, 107-110], but a functional role for increased Hh signaling in PKD had not been shown. In Chapter 2, we show enhanced nuclear GLI1 staining in interstitial and cyst-lining epithelial cells in human ADPKD renal tissue, indicating increased paracrine and autocrine Hh signaling, respectively. Increased *GLI1* levels were not evident in cultured human ADPKD cells, thus I speculate that cross-talk with other cell types or signaling molecules may cause upregulation of GLI1 observed in renal sections. Renal epithelial cells have been reported to release Hh ligands and activate Hh signaling in fibroblasts, inducing fibrosis [147], and macrophages have been reported to release and activate Hh signaling in an autocrine fashion in the liver [214]. Since fibrosis and macrophages have been reported to contribute to ADPKD progression, future investigation can examine whether fibroblasts and macrophages contribute to increased Hh signaling in ADPKD. Further, human ADPKD primary renal epithelial cells showed intact ciliary localization of IFT and BBS proteins, and intact response to SAG, an activator of Hh signaling. IFT modulates ciliary length and primary cilia are elongated in ADPKD mouse models [29, 57]. Our data suggest ciliary trafficking is not compromised in ADPKD primary cells. Thus, changes in ciliary length *in vivo* may derive from genetic modifiers or from factors produced from other cell types, which were absent in the cell culture.

Further, to investigate a functional role for Hh activity, I treated NHK and ADPKD primary renal epithelial cells with Hh modulators. Hh inhibitors decreased basal and cAMP-mediated proliferation and FSK- and EGF-induced cystogenesis of ADPKD cells. We previously observed that Hh inhibitors reduced the cAMP-mediated cystogenic effects in cultured mouse embryonic kidneys [80], and speculate that Hh signaling is a necessary component of cAMP-mediated proliferation and cystogenesis in these systems. SAG, a Hh/SMO agonist, increased proliferation, but this effect was not observed when NHK cells were treated with SAG and cAMP, suggesting that cAMP, which can inhibit the pathway by inducing GLI3 processing [215], may have countered the effect of SAG in NHK cells. However, since Hh activity and cAMP are both increased in cystic kidneys of ADPKD mouse models [80], we speculate that the regulation of cAMP on Hh signaling is altered in a diseased state.

Importantly, increased nuclear GLI1 expression was not observed in all cyst-lining epithelial cells in ADPKD renal tissue, suggesting that Hh signaling may contribute to disease progression, and not initiation.

To further demonstrate a functional role for increased Hh signaling in ADPKD, in Chapter 3, I downregulated Hh signaling [93] genetically in ADPKD mouse models, *jck*, *Pkd1* and *Pkd2* [69, 216]. My data suggest that downregulation of the Hh pathway attenuates disease, decreasing %KW/BW of *jck*, *Pkd1* and *Pkd2* mouse mutants, and decreasing BUN and cAMP levels of *jck* mutants. Additionally, immunohistochemistry for GLI1 revealed its localization to the nucleus of renal cyst-lining epithelial cells as well as of cells within the interstitium, indicating autocrine and paracrine Hh signaling, similar to human ADPKD tissues (Chapter 2). Finally, GLI1 levels/Hh activity correlated with disease progression in *jck* mice. Chapter 3 substantiates our findings in

Chapter 2, connecting increased Hh signaling with disease progression and further supporting that downregulation of Hh signaling may delay disease progression.

Together, our studies suggest enhanced Hh activity contributes to renal cyst progression in ADPKD, and thus, Hh inhibition may be a potential novel therapeutic strategy. Since several Hh inhibitors are FDA-approved in the United States, these can potentially be repurposed for ADPKD.

5.1.2 A potential role for STAT3 signaling in initiating renal cystic disease in a ciliary mouse model

In Chapters 2 and 3, we are the first to suggest Hh signaling as a mechanism that plays a role in ADPKD progression. However, what signaling pathways initiate renal cystogenesis continues to be another outstanding question in the PKD field. To uncover novel molecules that may initiate renal cystogenesis, we performed RNA sequencing in pre-cystic and cystic kidneys of *Thm1* cko mice, reasoning that genes misexpressed before cysts are formed and during disease progression may influence renal cyst initiation. With this reasoning, our data suggest that increased expression of *Stat3, Fos, Jun, Endothelin1, Vcam1, Ccl2, Complement C3, Egr2* and *Adcy7* may initiate renal cystic disease. In my validation of these molecules at the protein level, I have shown that STAT3 signaling activity is significantly increased in pre-cystic and cystic kidneys. STAT3 signaling has been reported to contribute to PKD progression [205, 206], but we are the first to suggest a role for STAT3 signaling in renal cyst initiation. To investigate the molecular mechanisms by which *Thm1* deficiency causes upregulation of STAT3 signaling, I treated control and *THM1* kd 293T human renal cells with IL6, a cytokine that activates STAT3 signaling [204]. Relative to control cells, *THM1* kd cells showed a stronger second wave of STAT3

activation that is preceded by robust ERK activation. These data indicate that THM1 regulates ERK and STAT3 signaling.

The other nine molecules identified by RNA seq to be upregulated in pre-cystic and cystic *Thm1* cko kidneys may also contribute to renal cyst initiation, either independently or by converging on STAT3 signaling. Several reports show a very influential role of the immune system on renal cystogenesis in ADPKD, including via STAT3 signaling [183, 200-202]. Our RNA Seq data revealed several immune-related genes, including *Ccl2*/*Mcp1,* to be upregulated in pre-cystic kidneys. Recently, polycystin-1 was reported to interact with ciliary-localized LKB1 to decrease CCL2/MCP1 and consequently regulate inflammation through primary cilia [131]. *Pkd1*,*Ccl2* double knock-out mice showed reduced renal cystogenesis, indicating the immune reaction triggered by CCL2 may link primary cilia to renal cystic disease [131]. These data suggest that the increased expression of *Ccl2* in our mouse model may also contribute to renal cyst formation. Interestingly, *Ccl2* has been shown to be a target of STAT3 signaling in prostate cancer [207]. A similar mechanism may also occur in the kidney connecting STAT3 signaling to CCL2 and renal cyst initiation.

In summary, our study has identified molecules and pathways, particularly STAT3 signaling, that are misexpressed before cysts are formed. We propose that these molecules play a role in renal cyst initiation.

5.2 Future Directions

5.2.1 Expanding the knowledge of Hh signaling in ADPKD progression

5.2.1.1 Correlate Hh signaling and cilia length with ADPKD severity

In Chapter 2, my findings suggest increased Hh signaling plays a role in human ADPKD progression. To expand on these findings, we can correlate Hh signaling with age and disease severity of ADPKD kidney samples, and anticipate that upregulation of Hh signaling in the kidney will increase in patients with worsening prognosis. In addition to a role for Hh signaling in renal epithelial cells [138, 149], increased Hh signaling in fibroblasts has previously shown to contribute to fibrosis [147] and may also stimulate fibrosis in ADPKD. Future experiments can examine the role of Hh signaling in fibrosis, beginning with co-immunostaining interstitial cells, such as fibroblasts, with GLI1. Finally, since cilia length may associate with disease severity in mice [29, 55], we can quantify cilia length in ADPKD renal tissue using immunostaining and ImageJ for quantification to examine if ADPKD renal tissue has longer primary cilia than NHK renal tissue. I did not observe cilia length differences between NHK and ADPKD primary renal epithelial cells, however, extraction and culture of cells could have influenced cilia length. Similarly, increased Hh signaling was not observed in ADPKD primary renal epithelial cells, in contrast to the immunohistochemistry findings on ADPKD renal sections.

5.2.1.2 Examine interconnection between Hh and Ca^{2+} signaling

Additionally, in Chapter 2, Hh inhibitors reduced basal and cAMP-mediated cell proliferation and cyst formation of ADPKD cells *in vitro*. The combination of decreased intracellular Ca^{2+} levels and aberrant cAMP activity leads to increased cell proliferation of ADPKD cells, which in turn, facilitates cyst growth [49, 52]. Importantly, increasing intracellular calcium reverts the abnormal activity of cAMP [51]. To determine if Hh inhibitors reduce ADPKD cell proliferation by increasing intracellular Ca^{2+}, we can treat cells with DMSO or Hh inhibitors and use commercially available sensors, such as a genetically-encoded Ca^{2+} indicator (GECO) to

examine Ca^{2+} levels in the cytosol. We can also treat cells with ionomycin, a calcium ionophore that increases Ca^{2+} in the cytosol and in cilia and compare the effects of ionomycin and of Hh inhibitors on cAMP-induced proliferation [40]. To further support that Hh inhibitors increase intracellular Ca^{2+}, we may treat ADPKD cells with high concentrations of ionomycin, which should induce a substantial increase in intracellular Ca^{2+}, and compare cell proliferation to cells treated with low concentrations of ionomycin combined with low concentrations of Hh inhibitors. If Hh inhibitors are modulating calcium, combinatory treatment would result in similar proliferation behavior to higher ionomycin alone. To examine cAMP, we can use the cADDis cAMP Sensor BacMam kits to determine if Hh inhibitors affect ciliary or cytosolic cAMP levels.

Additionally, we can determine which Ca^{2+} pool - ciliary or cytosolic - drives proliferation of ADPKD cells. We can treat ADPKD cells with cAMP in combination with various Ca^{2+} modulators, such as fenoldopam, ionomycin and thrombin [86]. Fenoldopam increases ciliary Ca^{2+} only. Ionomycin elevates ciliary and cytosolic Ca^{2+} and thrombin increases Ca^{2+} in the cytosol only [86]. If fenoldopam reduces cell proliferation, this would suggest ciliary Ca^{2+} reverses cAMP-stimulated proliferation of ADPKD cells. If thrombin decreases cell proliferation, this would indicate cytosolic Ca^{2+} is more important to regulate cAMP-induced cell proliferation. Finally, if ionomycin is the only treatment that counteracts the increased cell proliferation, this would suggest that both ciliary and cytosolic Ca^{2+} modulate cell proliferation of ADPKD cells.

Another gap in knowledge we can address is whether the converse regulation exists. Does Ca^{2+} regulate Hh signaling? And is this regulation compromised in ADPKD? To determine this, we can stimulate Hh signaling by treating ADPKD cells with SAG, alone, and in combination with Ca^{2+} channel blockers, gadolinium or verapamil. Gadolinium prevents cytosolic Ca^{2+} from being released, while verapamil prevents both ciliary and cytosolic Ca^{2+} from being released [28, 217].

If activation of the pathway depends on ciliary Ca^{2+}, treatment with verapamil will inhibit Hh signaling. However, if both treatments inhibit Hh activity, then this would suggest the cytosolic Ca^{2+} pool is the most important for activation of the pathway.

5.2.1.3 Examine epigenetics as a regulator of Hh signaling

Alternatively, epigenetics may cause upregulation of Hh signaling in ADPKD tissues. In cultured medulloblastoma and basal cell carcinoma mouse-tumor-derived cells, inhibition of Brd4, an epigenetic regulator, reduced *Gli1* expression [178]. In addition, treatment of a medulloblastoma mouse model with I-BET151, a Brd4 inhibitor, reduced *Gli1* expression and tumor growth [167]. Further, I-BET151 treatment attenuated PKD progression in a *Pkd1* cko mouse [166]. To examine whether epigenetics also targets the Hh pathway in ADPKD, we can treat ADPKD primary cells with SAG together with I-BET151 or with I-BET51 alone. If epigenetics is regulating the Hh pathway, then resulting Hh gene expression and cell proliferation should be comparable to the effects of the Hh inhibitors reported in Chapter 2.

5.2.1.4 Connecting Hh and ERK signaling

Finally, Hh and ERK pathways have been reported to synergize in some cancers [168-170]. We can examine if these pathways also synergize in ADPKD by comparing the effects of treating primary cells with Hh and ERK inhibitors, individually, and in combination. If these pathways synergize in ADPKD, I expect that treating cells with both Hh and ERK inhibitors will further decrease cell proliferation.

Combined these experiments will further connect primary cilia and Hh signaling to ADPKD biology and may provide further support of Hh signaling as a potential therapeutic target for ADPKD.

5.2.2 Expanding investigation of Hedgehog signaling in disease progression in ADPKD mouse models

In Chapter 3, we show promising data suggesting that genetic downregulation of Hh signaling in ADPKD mouse models, *jck* and *Pkd1*, ameliorates renal cystic disease. Future directions will include obtaining statistical significance for reduction in %KW/BW, cAMP, BUN and cystic index. Additionally, we will validate downregulation of Hh signaling by examining *Gli1* expression either through qPCR or Western Blot. Cell proliferation and fibrosis can also be examined. We can also address if ciliary length was altered by downregulation of Hh signaling as *jck* and *Pkd1* mutants were reported to have increased ciliary length that may contribute to disease [29, 55, 57]. Lastly, because cooperation between Hh and ERK signaling has previously been reported in cancer studies [168-170], we can determine if Hh inhibitors also modulated ERK signaling, which would indicate a connection between these two pathways in PKD. The results of the suggested experiments will further support Hh inhibitors as potential components for therapy against ADPKD.

5.2.3 Expanding knowledge of ciliary mechanisms that contribute to renal cyst initiation

5.2.3.1 Examine subcellular localization of STAT3 signaling components

Chapter 4 suggests elevated STAT3 signaling contributes to renal cyst initiation in *Thm1* cko mice. Future experiments will determine whether STAT3 signaling is mediated by primary

cilia. Subcellular localization of STAT3, P-STAT3, and JAK2, a kinase that phosphorylates and activates STAT3 [204], can be examined in *THM1* kd and control 293T cells using immunofluorescence. If STAT3 signaling components localize to primary cilia, we can examine whether ciliary-localized PC1 may be activating STAT3 signaling in this *in vitro* system. A proximity ligation assay can be performed to determine whether THM1, STAT3, JAK2 and/or PC1 form a complex in cilia. Additionally, since STAT6 is a cilia-localized protein that can be activated by PC1 [211] and is upregulated in cystic kidneys of *Thm1 cko* mice, we can perform similar experiments for STAT6 as well.

Since we show that *THM1* kd 293T cells have increased activation of ERK and STAT3 signaling when treated with IL-6, we can determine if the regulation of these pathways is dependent on primary cilia, by treating cells with chloral hydrate, which removes primary cilia from cells [85, 218]. If regulation of ERK and STAT3 signaling relies on primary cilia, I would expect reduced activation of these pathways by IL-6, in cells treated with chloral hydrate.

5.2.3.2 Connect STAT3, ERK and cAMP signaling in *THM1* kd cells

To broaden the signaling network, we can then examine the connection between cAMP, STAT3 and ERK signaling. cAMP is increased in the kidneys of *Thm1 cko* mice, and treating *THM1* kd 293T cells with cAMP might increase ERK and STAT3 activation and cell proliferation, recapitulating the *in vivo* events. We can also combine treatment of cAMP with IL6 to determine if this causes even greater cell proliferation than either treatment alone, and conversely, combine treatment of cAMP with a STAT3 inhibitor, such as Stattic, to determine if this decreases cAMP-induced cell proliferation, suggesting cAMP may act in part via STAT3 signaling. To address potential cross-talk between ERK and STAT3 signaling in this system, we can treat cells with

different combinations of cAMP, a specific MEK inhibitor, like PD098059 [209], and a STAT3 inhibitor, such as Stattic, and examine cell proliferation. Since ERK signaling is upregulated in cystic kidneys of *Thm1* cko mice and in IL6-treated *THM1* kd 293T cells (Chapter 4), we expect ERK inhibition to decrease cell proliferation. If ERK signaling has a more influential role than STAT3 signaling in inducing proliferation of *THM1*-deficient cells, ERK inhibitor may show a greater decrease in cell proliferation, compared to Stattic-treated cells. If ERK and STAT3 signaling are both essential in inducing cell proliferation, treating *THM1* kd cells with both ERK and STAT3 inhibitors may provide a greater reduction in cell proliferation, compared to treatment with a single inhibitor.

To demonstrate that increased STAT3 signaling is causative of *Thm1* cko renal cystic disease, we will continue to pursue treatments with C188-9, which showed the most promising reduction of STAT3 signaling *in vivo*. We will increase the dose of C188-9 and expand mouse numbers. We will then determine %KW/BW ratios, cystic index, BUN, and examine fibrosis and cell proliferation in tissue sections. Alternatively, we can genetically delete *Stat3*, either specifically in kidneys or globally in a time-dependent manner, using a Cre-ROSA26^{ERT} allele, in our mouse model [208].

Finally, to determine if other molecules that are upregulated in pre-cystic kidneys of *Thm1* cko mice contribute to renal cyst initiation, we can treat 293T cells with these molecules and examine STAT3 and ERK activation and cell proliferation. Interestingly, endothelin-1 (ET-1) induces secretion of IL-6 in osteoblast-like cells [212], and may similarly contribute to upregulation of STAT3 pathway in *Thm1*-deficient kidneys. Another molecule we are interested in is CCL2. CCL2 was recently reported to contribute to early renal cystic disease via a ciliary-mediated mechanism [131]. *Ccl2* has also been shown to be a target of STAT3 signaling in

prostate cancer [207]. We can examine *Ccl2* expression in kidneys of our mutant mice, as well as in our *THM1* kd 293T cells, to validate whether *Thm1* deficiency increases *Ccl2*, as suggested by our RNA seq data, and may in turn contribute to the renal cystic phenotype in our model.

5.2.3.3 Examine PC1 function in *THM1*-deficient cilia

Another way to further our knowledge of the ciliary mechanisms that contribute to renal cyst initiation in *Thm1* cko mice is to determine whether PC1 functions properly in *Thm1*-deficient cilia. PC1 activates the Calcineurin/NFAT (Nuclear Factor of Activated T cells) signaling pathway by sustaining increased intracellular calcium levels [219]. To determine whether the *THM1* cilia defect affects PC1 function, we can use calcineurin/NFAT signaling pathway as a read-out. We can transfect *THM1* kd and control 293T cells with PC1 C-tail or a control construct and examine NFAT signaling before and after caffeine treatment, which stimulates an increase in intracellular calcium [219]. If primary cilia dysfunction affects PC1 activity, the control transfected 293T cells will sustain increased calcium levels, while the *THM1* kd cells will not. We can also treat cells with CSA, a calcineurin inhibitor, as a negative control [219]. We expect that *THM1* kd cells will be unable to sustain calcium levels, and therefore will not show calcineurin-dependent NFAT activation, reflective of defective PC1 function.

The PC1 C-tail can also activate STAT3 signaling [206], and thus, may activate STAT3 signaling in *THM1* kd 293T cells. To determine this, we can examine whether levels of PC1 C-tail are increased in *Thm1* cko pre-cystic kidneys [211]. We can also transfect *THM1* kd and control 293T cells with PC1 C-tail alone and in combination with IL-6 to activate STAT3 signaling, or with Stattic to inhibit STAT3 signaling, and examine STAT3 activation using Western blot. The expected results would show further upregulation of STAT3 signaling in *THM1* kd cells

transfected with PC1 C-tail, indicating PC1 tail has ability to activate STAT3 signaling. Treatment with Stattic will reduce STAT3 activity. Combined, these experiments will help determine if PC1 activity is dysregulated by *Thm1* deficiency.

5.2.4 Examine effect of *Thm1* deletion on a renal cystic disease background

Genetic removal of primary cilia rescued the cystic phenotype in *Pkd1* and *Pkd2* mouse models, suggesting an event or mechanism within primary cilia is essential to renal cystogenesis in PKD [58]. Deletion of *Thm1* does not ablate primary cilia, but shortens primary cilia and affects protein trafficking within cilia. *Thm1* deletion can also have opposing effects on signaling pathways than deletion of genes essential for cilia formation [25]. Furthermore, a role for IFT-B has been shown in ADPKD mouse models [58], but a role for IFT-A in ADPKD mouse models has not been reported. This prompted us to investigate the effects of deletion of *Thm1*, an IFT-A gene, on renal cystic disease in *Pkd1* cko mice. We conditionally deleted both genes at 5 weeks of age, resulting in a slowly progressing model of renal cystic disease. We dissected animals at 6 months of age (Figure 5.2.4.1A). At 4 months of age (data not shown), renal cysts in *Pkd1* cko mice are beginning to appear. At 6-months of age, *Pkd1* cko mice show moderate disease progression, and double-mutants show reduced %KW/BW and BUN level, indicating deletion of *Thm1* reduced renal cystogenic potential and improved renal function (Figure 5.2.4.1B,C). The cysts in double-mutant kidneys derive from collecting ducts, and cell proliferation is reduced in *Pkd1*,*Thm1* kidneys, compared to single mutants (Figure 5.2.4.2 and Figure 5.2.4.3).

Additionally, we examined fibrosis using immunofluorescence for smooth-muscle actin (SMA) antibody on kidney sections. However, not a lot of fibrosis was detected by this method in either the single or double mutant kidneys (Figure 5.2.4.4), suggesting that the main effect of

deleting *Thm1* together with *Pkd1* is reduction of renal cystogenesis. We performed Western Blot analysis on whole kidney extracts and observed that STAT3 and ERK signaling activity correlates with disease severity, with *Pkd1*,*Thm1* dko kidneys showing less ERK and STAT3 activation than *Pkd1* cko kidneys (Figure 5.2.4.5). Since increased ciliary length has been reported in the $Pkd1^{RC/RC}$ mouse model [29, 55], we also examined cilia phenotype in collecting ducts by immunostaining kidney sections using antibodies against acetylated α-tubulin, a ciliary marker, together with DBA lectin staining. *Pkd1* cko kidneys have strikingly longer primary cilia than wild-type kidneys (Figure 5.2.4.6), while *Pkd1*,*Thm1* dko kidneys have shorter primary cilia than *Pkd1* cko kidneys, similar to wild-type (Figure 5.2.4.6). Combined, these data are the first to demonstrate that IFT-A is essential to renal cystogenesis and dysregulated ciliogenesis in *Pkd1* cko mice. Increased cilia length has been reported in other ADPKD mouse models and may alter signaling pathways leading to renal cystogenesis. Further ciliary analyses will be performed to determine if the *Pkd1*,*Thm1* dko cilia have a similar phenotype to *Thm1* cko cilia or have a rescued cilia phenotype.

Future directions will address the mechanisms underlying the striking attenuation of renal cystic disease in *Pkd1*,*Thm1* cko mice. For instance, we can perform single-cell RNA Sequencing to compare collecting duct-derived cells from control, *Pkd1* cko and *Pkd1*,*Thm1* dko mice and suggest novel molecules that we can investigate as therapeutic targets. In addition to signaling molecules, we can also look for genes that are known to regulate ciliogenesis as misregulation of these genes could cause differences in cilia length between single and double-mutant renal cells. Additionally, we can generate primary renal cells from the single and double knock-out mutants or knock-down the genes in 293T renal cells and analyze localization and expression of ciliary components that regulate ciliary length. These analyses could reveal defects in ciliogenesis, cilia

disassembly and/or ciliary entry of membrane proteins, which could reveal additional mechanisms that lead to enhanced or rescued renal cystogenesis.

Additionally, we can examine the ciliary-dependent LKB1-*Ccl2* pathway in *Thm1* cko and *Pkd1, Thm1* dko kidneys, as this pathway has been shown to be misregulated in *Pkd1* cko mice and rescued by deletion of cilia [131]. Since THM1 is an IFT protein, THM1 may play a role in the transport of molecules that regulate *Ccl2*, such as the ciliary LKB1- NEK7-ANKS3-NPHP1 complex. Future experiments will include immunofluorescence and proximity ligation assays using THM1, LKB1 and ANKS3 antibodies to determine if THM1 interacts with any of these proteins within cilia of 293T human renal cells. If THM1 interacts with these proteins and this interaction is compromised in *THM1* deficient cells, this would suggest that THM1 is important in CCL2 regulation in the presence of intact cilia. Our RNA seq data revealed increased *Ccl2* in pre-cystic kidneys of *Thm1* cko mice, generated by deleting *Thm1* cko at P0. Of note, however, these *Pkd1,Thm1* dko mice were generated by deleting the genes at 5 weeks of age. Thus, these experiments may reveal whether the effect of THM1 on LKB1-*Ccl2* signaling differs in rapidly-progressing vs. slowly progressing renal cystic disease models.

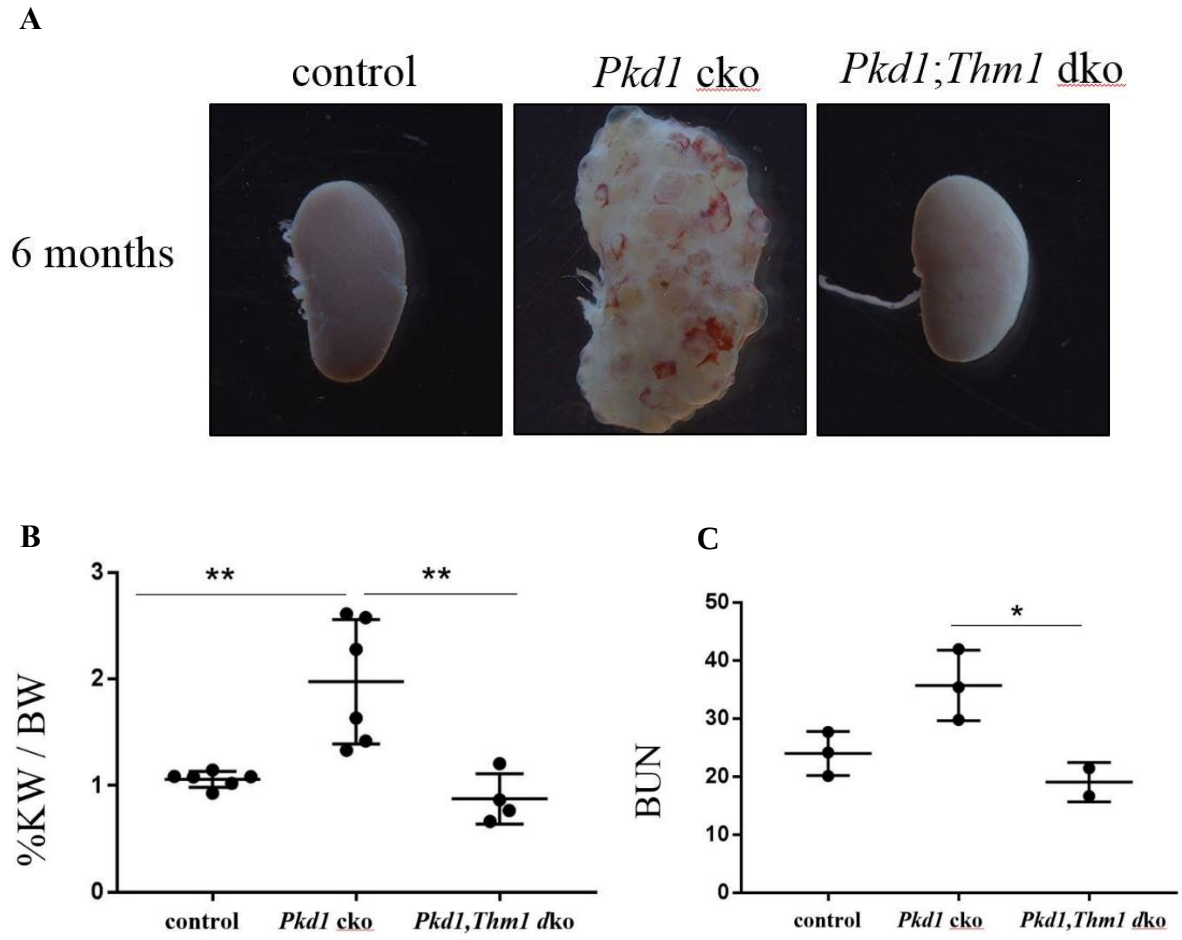

Figure 5.2.4.1: Deletion of *Thm1* ameliorates renal cystic disease in *Pkd1* cko mice.
A) Whole kidney images show *Pkd1,Thm1* dko have smaller kidneys, compared to *Pkd1* cko mice. B) *Pkd1,Thm1* dko mice have lower %KW/BW and BUN levels. Statistical significance was determined by ANOVA. **P<0.005

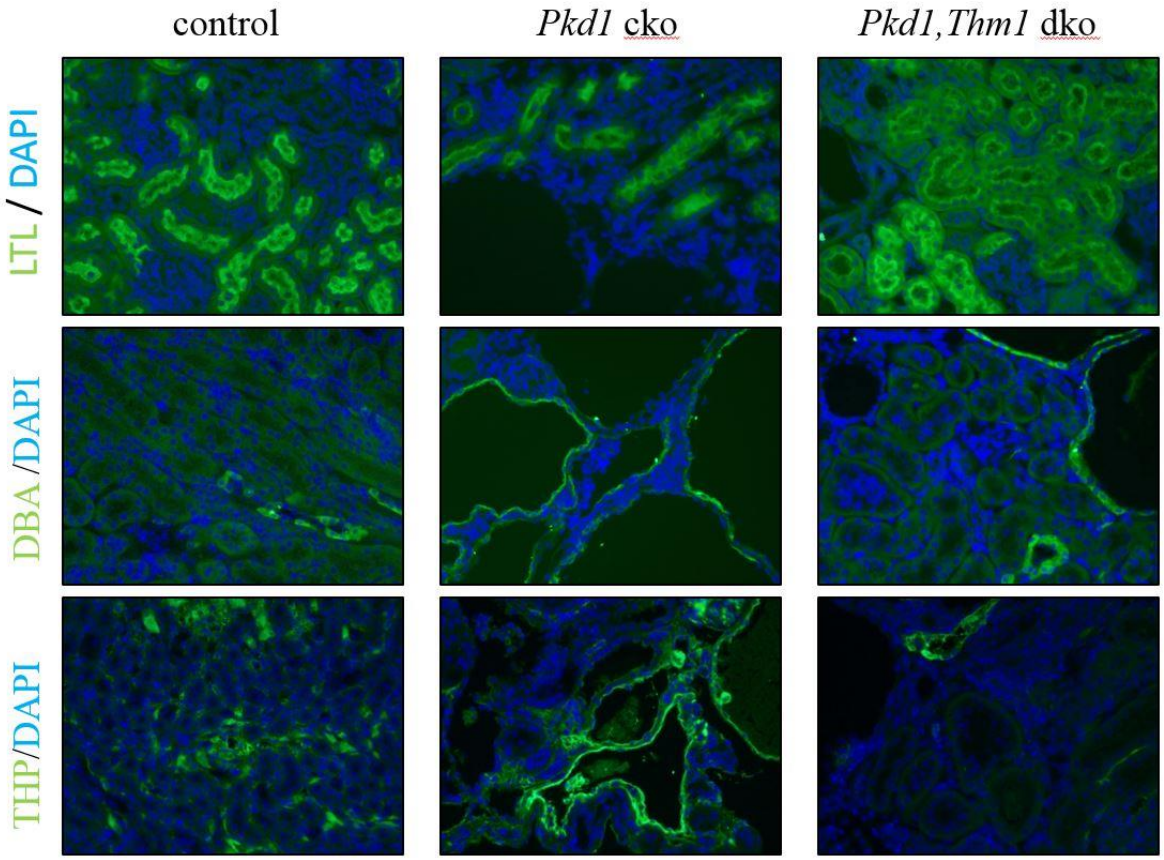

Figure 5.2.4.2: *Pkd1,Thm1* dko kidneys show cysts that derive from collecting duct.
Staining for proximal tubule (LTL), collecting duct (DBA), and loop of Henle (THP) renal tubules.

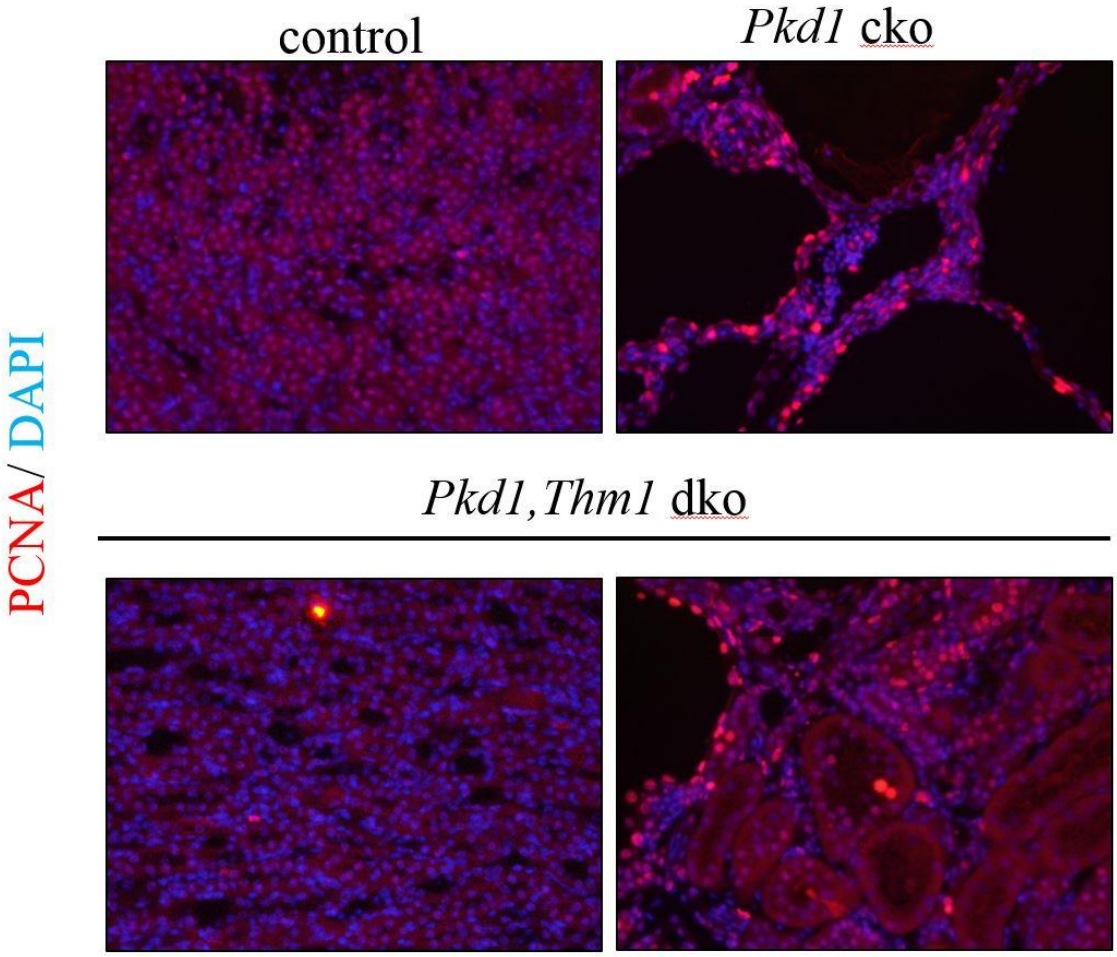

Figure 5.2.4.3: *Pkd1,Thm1* dko kidneys show less cell proliferation than *Pkd1* cko kidneys. Staining for cell proliferation (PCNA).

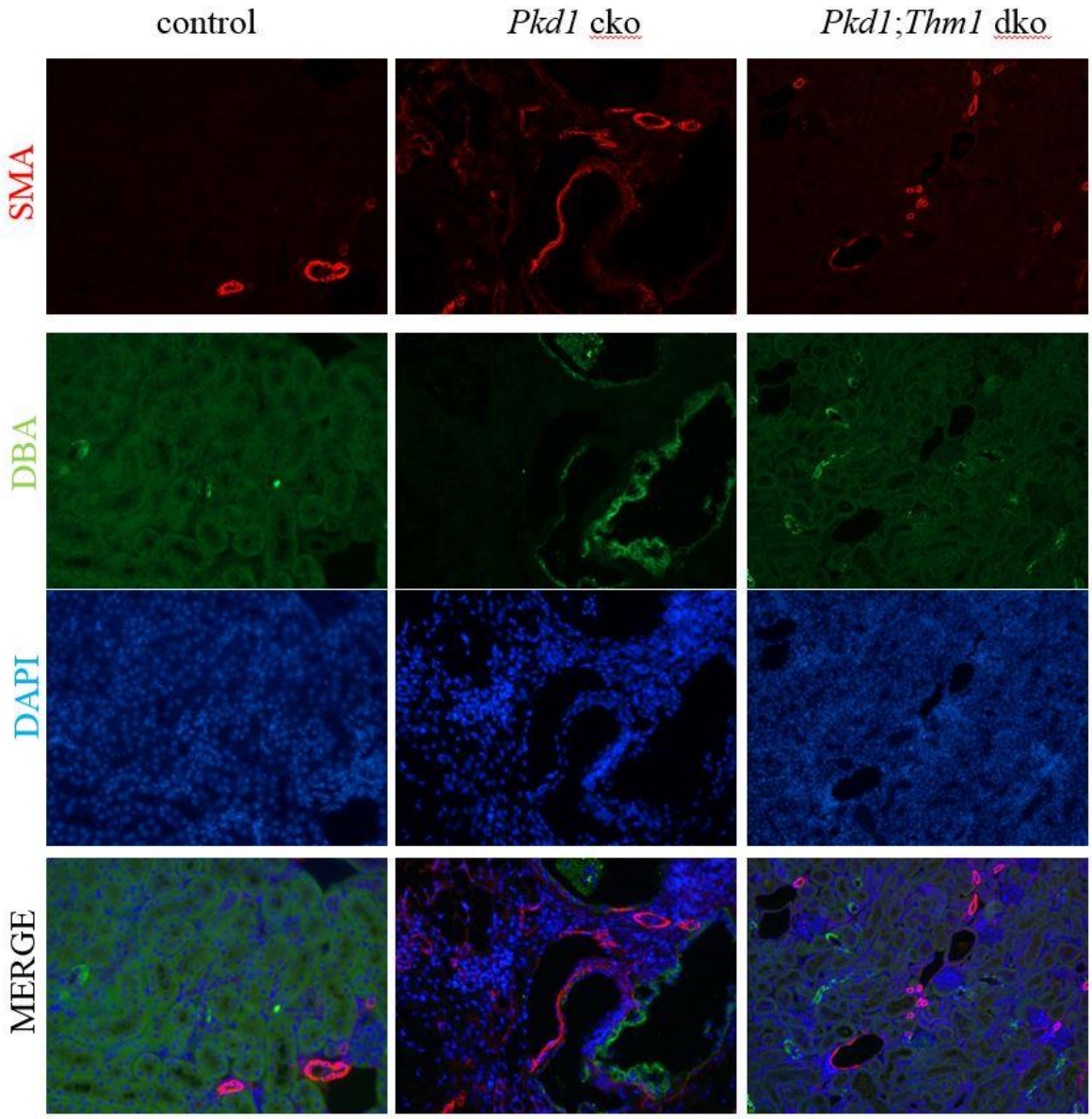

Figure 5.2.4.4: *Pkd1,Thm1* dko and *Pkd1* cko kidneys do not show much fibrosis.
Immunostaining for SMA, a marker of fibrosis, combined with DBA lectin staining for collecting duct.

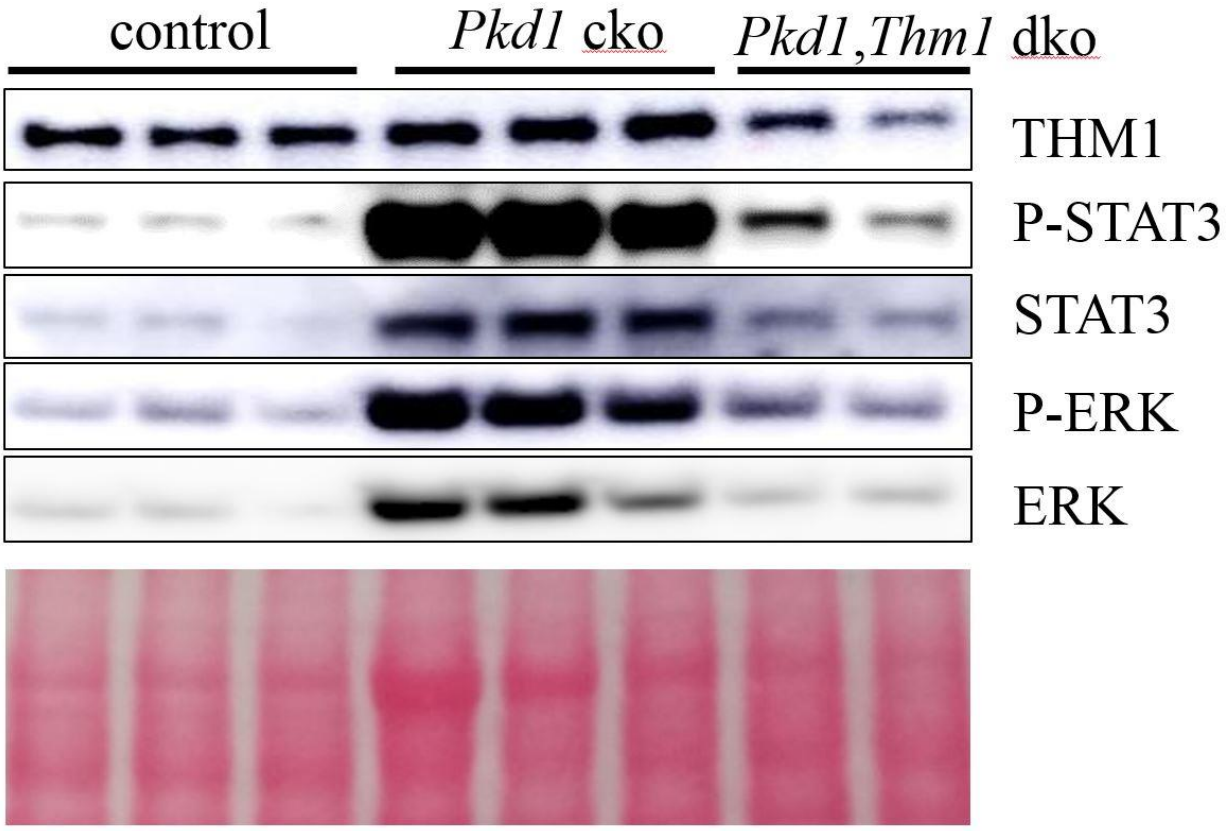

Figure 5.2.4.5: STAT3 and ERK signaling activity correlates with disease severity in *Pkd1,Thm1* dko and *Pkd1* cko kidneys.
Western Blot on whole kidney extracts.

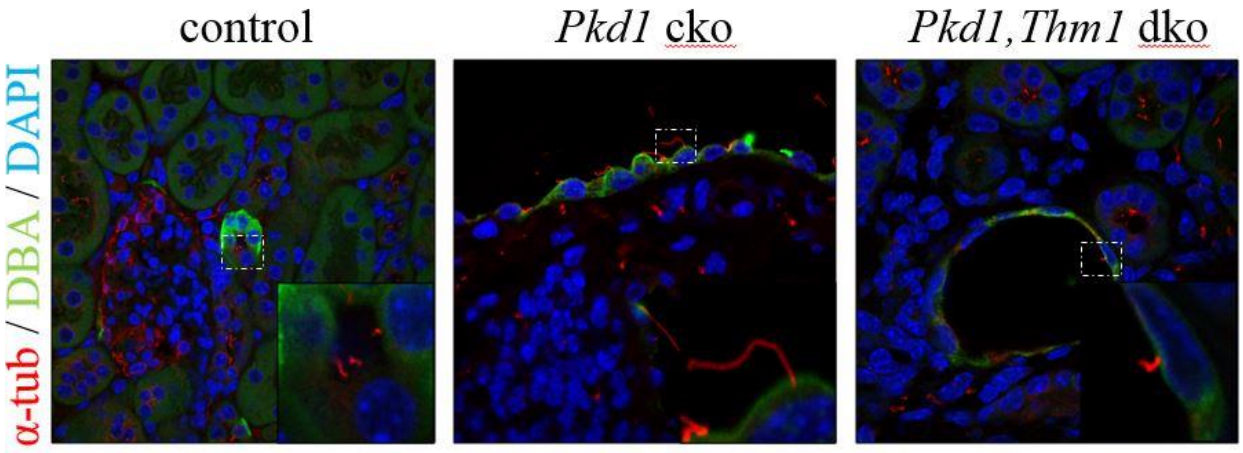

Figure 5.2.4.6: Deletion of *Thm1* rescues lengthened cilia in *Pkd1* cko mice.
Immunofluorescence using acetylated α-tubulin as a ciliary marker and DBA as a collecting duct marker. *Pkd1* cko collecting ducts show increased ciliary length.

5.3 Significance of these studies

ADPKD is a genetic disease that affects 1:500 people worldwide, leading to compromised renal function [35]. With limited therapy and no cure, ADPKD results in over a billion dollars spent every year in health care around the world [132]. Primary cilia appear to play a central role in the pathogenesis of ADPKD [35], yet the mechanisms by which primary cilia contribute to renal cystogenesis are not well-established. We proposed to uncover the ciliary-mediated pathway(s) that are dysregulated and contribute to cyst growth. We used *in vitro* and *in vivo* systems and are the first to suggest cilia-mediated Hh signaling plays a role in ADPKD progression, and increased STAT3 signaling may play a role in renal cyst initiation. There are FDA-approved Hh and STAT3 inhibitors, which can be potentially repurposed and investigated as components of combinatorial therapies against ADPKD.

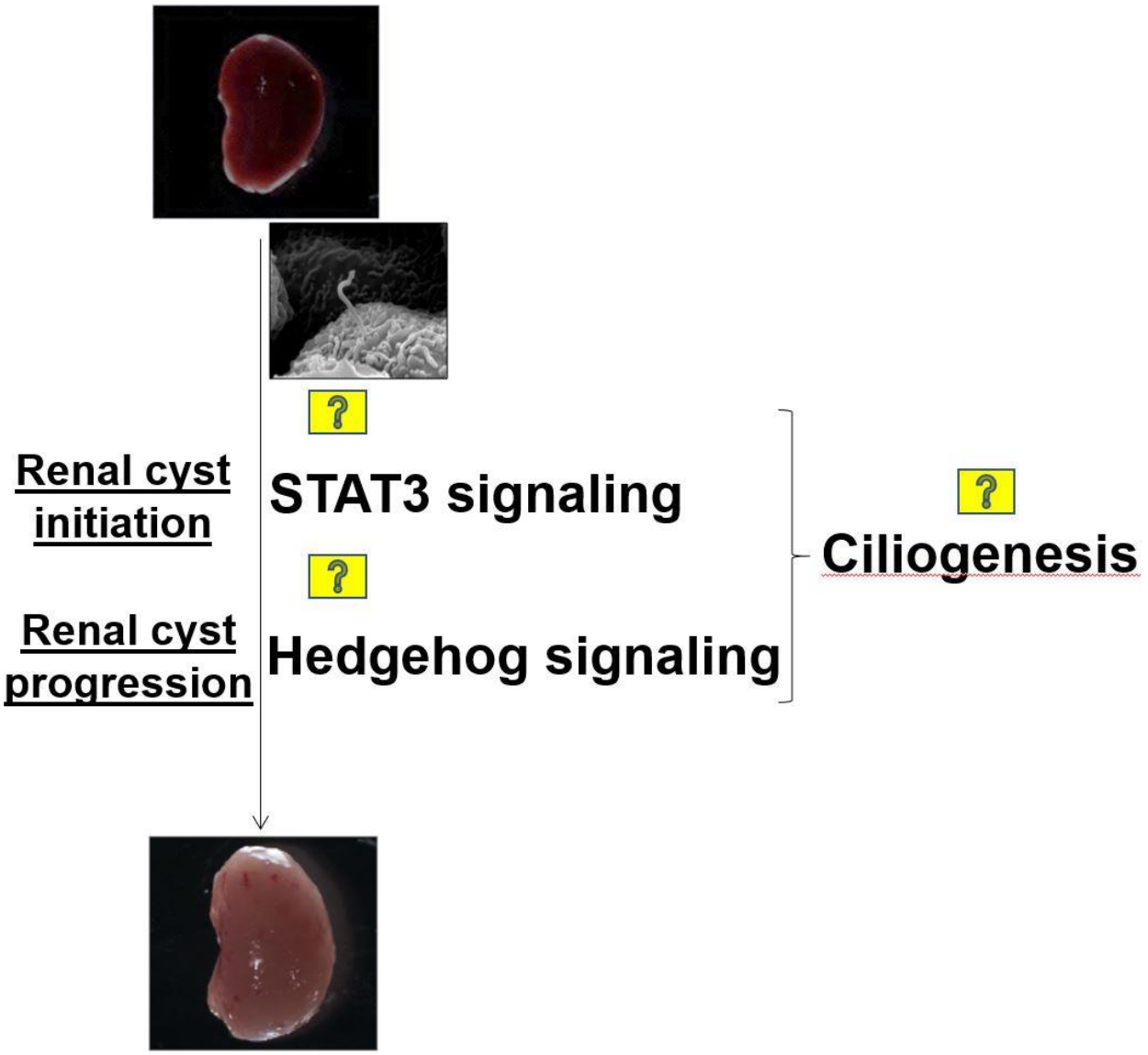

Figure 5.3: Summary of findings.
Our research aims to understand the mechanisms connecting primary cilia to renal cystogenesis in PKD. Our findings suggest STAT3 signaling may initiate renal cystogenesis in a ciliary mouse model, and that Hh signaling plays a role in renal cystic disease progression in human ADPKD and ADPKD mouse models. The link between primary cilia and STAT3 signaling, and STAT3 signaling and Hh signaling require further investigation.

References

1. Plotnikova, O.V., E.N. Pugacheva, and E.A. Golemis, *Primary cilia and the cell cycle.* Methods Cell Biol, 2009. **94**: p. 137-60.
2. Gilula, N.B. and P. Satir, *The ciliary necklace. A ciliary membrane specialization.* J Cell Biol, 1972. **53**(2): p. 494-509.
3. Utrilla, J.C., et al., *Comparative study of the primary cilia in thyrocytes of adult mammals.* J Anat, 2015. **227**(4): p. 550-60.
4. Kathem, S.H., A.M. Mohieldin, and S.M. Nauli, *The Roles of Primary cilia in Polycystic Kidney Disease.* AIMS Mol Sci, 2014. **1**(1): p. 27-46.
5. Goetz, S.C. and K.V. Anderson, *The primary cilium: a signalling centre during vertebrate development.* Nat Rev Genet, 2010. **11**(5): p. 331-44.
6. Waters, A.M. and P.L. Beales, *Ciliopathies: an expanding disease spectrum.* Pediatr Nephrol, 2011. **26**(7): p. 1039-56.
7. Satir, P. and S.T. Christensen, *Overview of structure and function of mammalian cilia.* Annu Rev Physiol, 2007. **69**: p. 377-400.
8. Garcia-Gonzalo, F.R. and J.F. Reiter, *Scoring a backstage pass: mechanisms of ciliogenesis and ciliary access.* J Cell Biol, 2012. **197**(6): p. 697-709.
9. Nigg, E.A. and T. Stearns, *The centrosome cycle: Centriole biogenesis, duplication and inherent asymmetries.* Nat Cell Biol, 2011. **13**(10): p. 1154-60.
10. Paridaen, J.T., M. Wilsch-Brauninger, and W.B. Huttner, *Asymmetric inheritance of centrosome-associated primary cilium membrane directs ciliogenesis after cell division.* Cell, 2013. **155**(2): p. 333-44.
11. Malicki, J.J. and C.A. Johnson, *The Cilium: Cellular Antenna and Central Processing Unit.* Trends Cell Biol, 2017. **27**(2): p. 126-140.
12. Pedersen, L.B. and J.L. Rosenbaum, *Intraflagellar transport (IFT) role in ciliary assembly, resorption and signalling.* Curr Top Dev Biol, 2008. **85**: p. 23-61.
13. Nachury, M.V., et al., *A core complex of BBS proteins cooperates with the GTPase Rab8 to promote ciliary membrane biogenesis.* Cell, 2007. **129**(6): p. 1201-13.
14. Valente, E.M., et al., *Primary cilia in neurodevelopmental disorders.* Nature Reviews Neurology, 2013. **10**: p. 27.
15. Rahmouni, K., et al., *Leptin resistance contributes to obesity and hypertension in mouse models of Bardet-Biedl syndrome.* J Clin Invest, 2008. **118**(4): p. 1458-67.
16. Arsov, T., et al., *Fat aussie--a new Alstrom syndrome mouse showing a critical role for ALMS1 in obesity, diabetes, and spermatogenesis.* Mol Endocrinol, 2006. **20**(7): p. 1610-22.
17. Ruiz-Perez, V.L., et al., *Evc is a positive mediator of Ihh-regulated bone growth that localises at the base of chondrocyte cilia.* Development, 2007. **134**(16): p. 2903-12.
18. Tobin, J.L. and P.L. Beales, *The nonmotile ciliopathies.* Genet Med, 2009. **11**(6): p. 386-402.
19. Krakow, D. and D.L. Rimoin, *The skeletal dysplasias.* Genet Med, 2010. **12**(6): p. 327-41.
20. Bastos, A.P. and L.F. Onuchic, *Molecular and cellular pathogenesis of autosomal dominant polycystic kidney disease.* Braz J Med Biol Res, 2011. **44**(7): p. 606-17.

21. Avasthi, P., R.L. Maser, and P.V. Tran, *Primary Cilia in Cystic Kidney Disease.* Results Probl Cell Differ, 2017. **60**: p. 281-321.
22. Huangfu, D., et al., *Hedgehog signalling in the mouse requires intraflagellar transport proteins.* Nature, 2003. **426**(6962): p. 83-7.
23. Liu, A., B. Wang, and L.A. Niswander, *Mouse intraflagellar transport proteins regulate both the activator and repressor functions of Gli transcription factors.* Development, 2005. **132**(13): p. 3103-11.
24. Houde, C., et al., *Hippi is essential for node cilia assembly and Sonic hedgehog signaling.* Dev Biol, 2006. **300**(2): p. 523-33.
25. Tran, P.V., et al., *THM1 negatively modulates mouse sonic hedgehog signal transduction and affects retrograde intraflagellar transport in cilia.* Nat Genet, 2008. **40**(4): p. 403-410.
26. Qin, J., et al., *Intraflagellar transport protein 122 antagonizes Sonic Hedgehog signaling and controls ciliary localization of pathway components.* Proc Natl Acad Sci U S A, 2011. **108**(4): p. 1456-61.
27. Zhou, J., *Polycystins and primary cilia: primers for cell cycle progression.* Annu Rev Physiol, 2009. **71**: p. 83-113.
28. Jin, X., et al., *L-type calcium channel modulates cystic kidney phenotype.* Biochim Biophys Acta, 2014. **1842**(9): p. 1518-26.
29. Hopp, K., et al., *Functional polycystin-1 dosage governs autosomal dominant polycystic kidney disease severity.* J Clin Invest, 2012. **122**(11): p. 4257-73.
30. Skalicka, K., et al., *Genetic defects in ciliary genes in autosomal dominant polycystic kidney disease.* World J Nephrol, 2018. **7**(2): p. 65-70.
31. Srivastava, A. and N. Patel, *Autosomal dominant polycystic kidney disease.* Am Fam Physician, 2014. **90**(5): p. 303-7.
32. Pei, Y., et al., *Bilineal disease and trans-heterozygotes in autosomal dominant polycystic kidney disease.* Am J Hum Genet, 2001. **68**(2): p. 355-63.
33. Porath, B., et al., *Mutations in GANAB, Encoding the Glucosidase IIalpha Subunit, Cause Autosomal-Dominant Polycystic Kidney and Liver Disease.* Am J Hum Genet, 2016. **98**(6): p. 1193-1207.
34. Brown, J.A., *Images in clinical medicine. End-stage autosomal dominant polycystic kidney disease.* N Engl J Med, 2002. **347**(19): p. 1504.
35. Torres, V.E. and P.C. Harris, *Mechanisms of Disease: autosomal dominant and recessive polycystic kidney diseases.* Nat Clin Pract Nephrol, 2006. **2**(1): p. 40-55; quiz 55.
36. Cai, Y., et al., *Altered trafficking and stability of polycystins underlie polycystic kidney disease.* J Clin Invest, 2014. **124**(12): p. 5129-44.
37. Lemos, F.O. and B.E. Ehrlich, *Polycystin and calcium signaling in cell death and survival.* Cell Calcium, 2018. **69**: p. 37-45.
38. Su, Q., et al., *Structure of the human PKD1-PKD2 complex.* Science, 2018. **361**(6406).
39. Nauli, S.M., et al., *Polycystins 1 and 2 mediate mechanosensation in the primary cilium of kidney cells.* Nat Genet, 2003. **33**(2): p. 129-37.
40. Delling, M., et al., *Primary cilia are specialized calcium signalling organelles.* Nature, 2013. **504**(7479): p. 311-4.
41. DeCaen, P.G., et al., *Direct recording and molecular identification of the calcium channel of primary cilia.* Nature, 2013. **504**(7479): p. 315-8.

42. Raychowdhury, M.K., et al., *Characterization of single channel currents from primary cilia of renal epithelial cells.* J Biol Chem, 2005. **280**(41): p. 34718-22.
43. Abdul-Majeed, S. and S.M. Nauli, *Polycystic Diseases in Visceral Organs.* Obstetrics and Gynecology International, 2011. **2011**: p. 7.
44. Harris, P.C., *What is the role of somatic mutation in autosomal dominant polycystic kidney disease?* J Am Soc Nephrol, 2010. **21**(7): p. 1073-6.
45. Lea, W.A., et al., *Human-Specific Abnormal Alternative Splicing of Wild-Type PKD1 Induces Premature Termination of Polycystin-1.* J Am Soc Nephrol, 2018.
46. Qian, F., et al., *The molecular basis of focal cyst formation in human autosomal dominant polycystic kidney disease type I.* Cell, 1996. **87**(6): p. 979-87.
47. Piontek, K., et al., *A critical developmental switch defines the kinetics of kidney cyst formation after loss of Pkd1.* Nat Med, 2007. **13**(12): p. 1490-5.
48. Magenheimer, B.S., et al., *Early embryonic renal tubules of wild-type and polycystic kidney disease kidneys respond to cAMP stimulation with cystic fibrosis transmembrane conductance regulator/Na(+),K(+),2Cl(-) Co-transporter-dependent cystic dilation.* J Am Soc Nephrol, 2006. **17**(12): p. 3424-37.
49. Wallace, D.P., *Cyclic AMP-mediated cyst expansion.* Biochim Biophys Acta, 2011. **1812**(10): p. 1291-300.
50. Yamaguchi, T., et al., *Cyclic AMP activates B-Raf and ERK in cyst epithelial cells from autosomal-dominant polycystic kidneys.* Kidney Int, 2003. **63**(6): p. 1983-94.
51. Yamaguchi, T., et al., *Calcium restriction allows cAMP activation of the B-Raf/ERK pathway, switching cells to a cAMP-dependent growth-stimulated phenotype.* J Biol Chem, 2004. **279**(39): p. 40419-30.
52. Yamaguchi, T., et al., *Calcium restores a normal proliferation phenotype in human polycystic kidney disease epithelial cells.* J Am Soc Nephrol, 2006. **17**(1): p. 178-87.
53. Moore, B.S., et al., *Cilia have high cAMP levels that are inhibited by Sonic Hedgehog-regulated calcium dynamics.* Proc Natl Acad Sci U S A, 2016. **113**(46): p. 13069-13074.
54. Ou, Y., et al., *Adenylate cyclase regulates elongation of mammalian primary cilia.* Exp Cell Res, 2009. **315**(16): p. 2802-17.
55. Jin, X., et al., *L-type calcium channel modulates cystic kidney phenotype.* Biochim Biophys Acta, 2014.
56. Smith, L.A., et al., *Development of polycystic kidney disease in juvenile cystic kidney mice: Insights into pathogenesis, ciliary abnormalities, and common features with human disease.* Journal of the American Society of Nephrology, 2006. **17**(10): p. 2821-2831.
57. Husson, H., et al., *Reduction of ciliary length through pharmacologic or genetic inhibition of CDK5 attenuates polycystic kidney disease in a model of nephronophthisis.* Hum Mol Genet, 2016. **25**(11): p. 2245-2255.
58. Ma, M., et al., *Loss of cilia suppresses cyst growth in genetic models of autosomal dominant polycystic kidney disease.* Nat Genet, 2013. **45**(9): p. 1004-12.
59. Besschetnova, T.Y., et al., *Identification of signaling pathways regulating primary cilium length and flow-mediated adaptation.* Curr Biol, 2010. **20**(2): p. 182-7.
60. Verghese, E., et al., *Renal cilia display length alterations following tubular injury and are present early in epithelial repair.* Nephrol Dial Transplant, 2008. **23**(3): p. 834-41.
61. Verghese, E., et al., *Renal primary cilia lengthen after acute tubular necrosis.* J Am Soc Nephrol, 2009. **20**(10): p. 2147-53.

62. Bastos, A.P., et al., *Pkd1 haploinsufficiency increases renal damage and induces microcyst formation following ischemia/reperfusion.* J Am Soc Nephrol, 2009. **20**(11): p. 2389-402.
63. Prasad, S., et al., *Pkd2 dosage influences cellular repair responses following ischemia-reperfusion injury.* Am J Pathol, 2009. **175**(4): p. 1493-503.
64. Happé, H. and D.J.M. Peters, *Translational research in ADPKD: lessons from animal models.* Nature Reviews Nephrology, 2014. **10**: p. 587.
65. Abremski, K. and R. Hoess, *Phage P1 Cre-loxP site-specific recombination. Effects of DNA supercoiling on catenation and knotting of recombinant products.* J Mol Biol, 1985. **184**(2): p. 211-20.
66. Atala, A., et al., *Juvenile cystic kidneys (jck): a new mouse mutation which causes polycystic kidneys.* Kidney Int, 1993. **43**(5): p. 1081-5.
67. Liu, S., et al., *A defect in a novel Nek-family kinase causes cystic kidney disease in the mouse and in zebrafish.* Development, 2002. **129**(24): p. 5839-46.
68. Stewart, J.H., *End-stage renal failure appears earlier in men than in women with polycystic kidney disease.* Am J Kidney Dis, 1994. **24**(2): p. 181-3.
69. Mahjoub, M.R., M.L. Trapp, and L.M. Quarmby, *NIMA-related kinases defective in murine models of polycystic kidney diseases localize to primary cilia and centrosomes.* J Am Soc Nephrol, 2005. **16**(12): p. 3485-9.
70. Watnick, T. and G. Germino, *From cilia to cyst.* Nat Genet, 2003. **34**(4): p. 355-6.
71. Sohara, E., et al., *Nek8 regulates the expression and localization of polycystin-1 and polycystin-2.* J Am Soc Nephrol, 2008. **19**(3): p. 469-76.
72. Bowers, A.J. and J.F. Boylan, *Nek8, a NIMA family kinase member, is overexpressed in primary human breast tumors.* Gene, 2004. **328**: p. 135-42.
73. Zalli, D., R. Bayliss, and A.M. Fry, *The Nek8 protein kinase, mutated in the human cystic kidney disease nephronophthisis, is both activated and degraded during ciliogenesis.* Human Molecular Genetics, 2012. **21**(5): p. 1155-1171.
74. Choi, H.J., et al., *NEK8 links the ATR-regulated replication stress response and S phase CDK activity to renal ciliopathies.* Mol Cell, 2013. **51**(4): p. 423-39.
75. Otto, E.A., et al., *NEK8 mutations affect ciliary and centrosomal localization and may cause nephronophthisis.* J Am Soc Nephrol, 2008. **19**(3): p. 587-92.
76. Stokman, M., M. Lilien, and N. Knoers, *Nephronophthisis,* in *GeneReviews((R))*, M.P. Adam, et al., Editors. 1993: Seattle (WA).
77. Carter, H., et al., *Prioritization of driver mutations in pancreatic cancer using cancer-specific high-throughput annotation of somatic mutations (CHASM).* Cancer Biol Ther, 2010. **10**(6): p. 582-7.
78. Natoli, T.A., et al., *Pkd1 and Nek8 mutations affect cell-cell adhesion and cilia in cysts formed in kidney organ cultures.* Am J Physiol Renal Physiol, 2008. **294**(1): p. F73-83.
79. Herron, B.J., et al., *Efficient generation and mapping of recessive developmental mutations using ENU mutagenesis.* Nat Genet, 2002. **30**(2): p. 185-9.
80. Tran, P.V., et al., *Downregulating hedgehog signaling reduces renal cystogenic potential of mouse models.* J Am Soc Nephrol, 2014. **25**(10): p. 2201-12.
81. Jacobs, D.T., et al., *Dysfunction of intraflagellar transport-A causes hyperphagia-induced obesity and metabolic syndrome.* Dis Model Mech, 2016. **9**(7): p. 789-98.

82. Davis, E.E., et al., *TTC21B contributes both causal and modifying alleles across the ciliopathy spectrum.* Nat Genet, 2011. **43**(3): p. 189-96.
83. Driver, A.M., C. Shumrick, and R.W. Stottmann, *Ttc21b Is Required in Bergmann Glia for Proper Granule Cell Radial Migration.* J Dev Biol, 2017. **5**(4).
84. Huynh Cong, E., et al., *A homozygous missense mutation in the ciliary gene TTC21B causes familial FSGS.* J Am Soc Nephrol, 2014. **25**(11): p. 2435-43.
85. Praetorius, H.A. and K.R. Spring, *Bending the MDCK cell primary cilium increases intracellular calcium.* J Membr Biol, 2001. **184**(1): p. 71-9.
86. Jin, X., et al., *Cilioplasm is a cellular compartment for calcium signaling in response to mechanical and chemical stimuli.* Cell Mol Life Sci, 2014. **71**(11): p. 2165-78.
87. Su, S., et al., *Genetically encoded calcium indicator illuminates calcium dynamics in primary cilia.* Nat Methods, 2013. **10**(11): p. 1105-7.
88. Delling, M., et al., *Primary cilia are not calcium-responsive mechanosensors.* Nature, 2016. **531**(7596): p. 656-60.
89. Nauli, S.M., R. Pala, and S.J. Kleene, *Calcium channels in primary cilia.* Curr Opin Nephrol Hypertens, 2016. **25**(5): p. 452-8.
90. Pala, R., N. Alomari, and S.M. Nauli, *Primary Cilium-Dependent Signaling Mechanisms.* Int J Mol Sci, 2017. **18**(11).
91. Ingham, P.W., Y. Nakano, and C. Seger, *Mechanisms and functions of Hedgehog signalling across the metazoa.* Nat Rev Genet, 2011. **12**(6): p. 393-406.
92. Wilson, C.W. and P.T. Chuang, *Mechanism and evolution of cytosolic Hedgehog signal transduction.* Development, 2010. **137**(13): p. 2079-94.
93. Goetz, S.C., P.J. Ocbina, and K.V. Anderson, *The primary cilium as a Hedgehog signal transduction machine.* Methods Cell Biol, 2009. **94**: p. 199-222.
94. Mann, R.K. and P.A. Beachy, *Novel lipid modifications of secreted protein signals.* Annu Rev Biochem, 2004. **73**: p. 891-923.
95. Gallet, A., *Hedgehog morphogen: from secretion to reception.* Trends Cell Biol, 2011. **21**(4): p. 238-46.
96. Wong, S.Y. and J.F. Reiter, *The primary cilium at the crossroads of mammalian hedgehog signaling.* Curr Top Dev Biol, 2008. **85**: p. 225-60.
97. Sasaki, H., et al., *Regulation of Gli2 and Gli3 activities by an amino-terminal repression domain: implication of Gli2 and Gli3 as primary mediators of Shh signaling.* Development, 1999. **126**(17): p. 3915-24.
98. Aza-Blanc, P., et al., *Proteolysis that is inhibited by hedgehog targets Cubitus interruptus protein to the nucleus and converts it to a repressor.* Cell, 1997. **89**(7): p. 1043-53.
99. Bai, C.B., D. Stephen, and A.L. Joyner, *All mouse ventral spinal cord patterning by hedgehog is Gli dependent and involves an activator function of Gli3.* Dev Cell, 2004. **6**(1): p. 103-15.
100. Niewiadomski, P., et al., *Gli protein activity is controlled by multisite phosphorylation in vertebrate Hedgehog signaling.* Cell Rep, 2014. **6**(1): p. 168-181.
101. Brennan, D., et al., *Noncanonical Hedgehog signaling.* Vitam Horm, 2012. **88**: p. 55-72.
102. Liem, K.F., Jr., et al., *The IFT-A complex regulates Shh signaling through cilia structure and membrane protein trafficking.* J Cell Biol, 2012. **197**(6): p. 789-800.
103. Christensen, S.T. and C.M. Ott, *Cell signaling. A ciliary signaling switch.* Science, 2007. **317**(5836): p. 330-1.

104. Fabian, S.L., et al., *Hedgehog-Gli pathway activation during kidney fibrosis.* Am J Pathol, 2012. **180**(4): p. 1441-53.
105. Hu, M.C., et al., *GLI3-dependent transcriptional repression of Gli1, Gli2 and kidney patterning genes disrupts renal morphogenesis.* Development, 2006. **133**(3): p. 569-78.
106. Cain, J.E., et al., *GLI3 repressor controls nephron number via regulation of Wnt11 and Ret in ureteric tip cells.* PLoS One, 2009. **4**(10): p. e7313.
107. Jonassen, J.A., et al., *Disruption of IFT complex A causes cystic kidneys without mitotic spindle misorientation.* J Am Soc Nephrol, 2012. **23**(4): p. 641-51.
108. Attanasio, M., et al., *Loss of GLIS2 causes nephronophthisis in humans and mice by increased apoptosis and fibrosis.* Nat Genet, 2007. **39**(8): p. 1018-24.
109. Li, Y., et al., *Deletion of ADP Ribosylation Factor-Like GTPase 13B Leads to Kidney Cysts.* J Am Soc Nephrol, 2016. **27**(12): p. 3628-3638.
110. Song, X., et al., *Systems biology of autosomal dominant polycystic kidney disease (ADPKD): computational identification of gene expression pathways and integrated regulatory networks.* Hum Mol Genet, 2009. **18**(13): p. 2328-43.
111. Gupta, S., N. Takebe, and P. Lorusso, *Targeting the Hedgehog pathway in cancer.* Ther Adv Med Oncol, 2010. **2**(4): p. 237-50.
112. Dormoy, V., et al., *The sonic hedgehog signaling pathway is reactivated in human renal cell carcinoma and plays orchestral role in tumor growth.* Mol Cancer, 2009. **8**: p. 123.
113. Heretsch, P., L. Tzagkaroulaki, and A. Giannis, *Modulators of the hedgehog signaling pathway.* Bioorg Med Chem, 2010. **18**(18): p. 6613-24.
114. Taipale, J., et al., *Effects of oncogenic mutations in Smoothened and Patched can be reversed by cyclopamine.* Nature, 2000. **406**(6799): p. 1005-9.
115. Wang, Y., et al., *Selective translocation of intracellular Smoothened to the primary cilium in response to Hedgehog pathway modulation.* Proc Natl Acad Sci U S A, 2009. **106**(8): p. 2623-8.
116. Kim, J., et al., *Itraconazole, a commonly used antifungal that inhibits Hedgehog pathway activity and cancer growth.* Cancer Cell, 2010. **17**(4): p. 388-99.
117. Proctor, A.E., L.A. Thompson, and C.L. O'Bryant, *Vismodegib: an inhibitor of the Hedgehog signaling pathway in the treatment of basal cell carcinoma.* Ann Pharmacother, 2014. **48**(1): p. 99-106.
118. Kim, E.J., et al., *Pilot clinical trial of hedgehog pathway inhibitor GDC-0449 (vismodegib) in combination with gemcitabine in patients with metastatic pancreatic adenocarcinoma.* Clin Cancer Res, 2014. **20**(23): p. 5937-5945.
119. Lauth, M., et al., *Inhibition of GLI-mediated transcription and tumor cell growth by small-molecule antagonists.* Proc Natl Acad Sci U S A, 2007. **104**(20): p. 8455-60.
120. Simons, M., et al., *Inversin, the gene product mutated in nephronophthisis type II, functions as a molecular switch between Wnt signaling pathways.* Nat Genet, 2005. **37**(5): p. 537-43.
121. Lin, F., et al., *Kidney-specific inactivation of the KIF3A subunit of kinesin-II inhibits renal ciliogenesis and produces polycystic kidney disease.* Proc Natl Acad Sci U S A, 2003. **100**(9): p. 5286-91.
122. Ocbina, P.J., M. Tuson, and K.V. Anderson, *Primary cilia are not required for normal canonical Wnt signaling in the mouse embryo.* PLoS One, 2009. **4**(8): p. e6839.

123. Boehlke, C., et al., *Primary cilia regulate mTORC1 activity and cell size through Lkb1.* Nat Cell Biol, 2010. **12**(11): p. 1115-22.
124. Shillingford, J.M., et al., *The mTOR pathway is regulated by polycystin-1, and its inhibition reverses renal cystogenesis in polycystic kidney disease.* Proc Natl Acad Sci U S A, 2006. **103**(14): p. 5466-71.
125. Tao, Y., et al., *Rapamycin markedly slows disease progression in a rat model of polycystic kidney disease.* J Am Soc Nephrol, 2005. **16**(1): p. 46-51.
126. Wahl, P.R., et al., *Inhibition of mTOR with sirolimus slows disease progression in Han:SPRD rats with autosomal dominant polycystic kidney disease (ADPKD).* Nephrol Dial Transplant, 2006. **21**(3): p. 598-604.
127. Takiar, V., et al., *Activating AMP-activated protein kinase (AMPK) slows renal cystogenesis.* Proc Natl Acad Sci U S A, 2011. **108**(6): p. 2462-7.
128. Serra, A.L., et al., *Sirolimus and kidney growth in autosomal dominant polycystic kidney disease.* N Engl J Med, 2010. **363**(9): p. 820-9.
129. Walz, G., et al., *Everolimus in patients with autosomal dominant polycystic kidney disease.* N Engl J Med, 2010. **363**(9): p. 830-40.
130. Ruggenenti, P., et al., *Effect of Sirolimus on Disease Progression in Patients with Autosomal Dominant Polycystic Kidney Disease and CKD Stages 3b-4.* Clin J Am Soc Nephrol, 2016. **11**(5): p. 785-94.
131. Viau, A., et al., *Cilia-localized LKB1 regulates chemokine signaling, macrophage recruitment, and tissue homeostasis in the kidney.* EMBO J, 2018. **37**(15).
132. Ong, A.C., et al., *Autosomal dominant polycystic kidney disease: the changing face of clinical management.* Lancet, 2015. **385**(9981): p. 1993-2002.
133. Torres, V.E., et al., *Angiotensin blockade in late autosomal dominant polycystic kidney disease.* N Engl J Med, 2014. **371**(24): p. 2267-76.
134. Caroli, A., et al., *Effect of longacting somatostatin analogue on kidney and cyst growth in autosomal dominant polycystic kidney disease (ALADIN): a randomised, placebo-controlled, multicentre trial.* Lancet, 2013. **382**(9903): p. 1485-95.
135. Meijer, E., et al., *Rationale and design of the DIPAK 1 study: a randomized controlled clinical trial assessing the efficacy of lanreotide to Halt disease progression in autosomal dominant polycystic kidney disease.* Am J Kidney Dis, 2014. **63**(3): p. 446-55.
136. Barnawi, R.A., et al., *Is the light at the end of the tunnel nigh? A review of ADPKD focusing on the burden of disease and tolvaptan as a new treatment.* Int J Nephrol Renovasc Dis, 2018. **11**: p. 53-67.
137. El-Damanawi, R., et al., *Randomised controlled trial of high versus ad libitum water intake in patients with autosomal dominant polycystic kidney disease: rationale and design of the DRINK feasibility trial.* BMJ Open, 2018. **8**(5): p. e022859.
138. Silva, L.M., et al., *Inhibition of Hedgehog signaling suppresses proliferation and microcyst formation of human Autosomal Dominant Polycystic Kidney Disease cells.* Sci Rep, 2018. **8**(1): p. 4985.
139. Yoder, B.K., X. Hou, and L.M. Guay-Woodford, *The polycystic kidney disease proteins, polycystin-1, polycystin-2, polaris, and cystin, are co-localized in renal cilia.* J Am Soc Nephrol, 2002. **13**(10): p. 2508-16.
140. Quinlan, R.J., J.L. Tobin, and P.L. Beales, *Modeling ciliopathies: Primary cilia in development and disease.* Curr Top Dev Biol, 2008. **84**: p. 249-310.

141. Husson, H., et al., *Reduction of ciliary length through pharmacologic or genetic inhibition of CDK5 attenuates polycystic kidney disease in a model of nephronophthisis.* Hum Mol Genet, 2016.
142. Corbit, K.C., et al., *Vertebrate Smoothened functions at the primary cilium.* Nature, 2005. **437**(7061): p. 1018-21.
143. Rohatgi, R., L. Milenkovic, and M.P. Scott, *Patched1 regulates hedgehog signaling at the primary cilium.* Science, 2007. **317**(5836): p. 372-6.
144. Eggenschwiler, J.T. and K.V. Anderson, *Cilia and developmental signaling.* Annu Rev Cell Dev Biol, 2007. **23**: p. 345-73.
145. Yoder, B.K., et al., *Polaris, a protein disrupted in orpk mutant mice, is required for assembly of renal cilium.* Am J Physiol Renal Physiol, 2002. **282**(3): p. F541-52.
146. D'Amato, C., et al., *Inhibition of Hedgehog signalling by NVP-LDE225 (Erismodegib) interferes with growth and invasion of human renal cell carcinoma cells.* Br J Cancer, 2014. **111**(6): p. 1168-79.
147. Zhou, D., et al., *Sonic Hedgehog Is a Novel Tubule-Derived Growth Factor for Interstitial Fibroblasts after Kidney Injury.* J Am Soc Nephrol, 2014.
148. Chan, S.K., et al., *Corticosteroid-induced kidney dysmorphogenesis is associated with deregulated expression of known cystogenic molecules, as well as Indian hedgehog.* Am J Physiol Renal Physiol, 2010. **298**(2): p. F346-56.
149. Li, B., et al., *Increased hedgehog signaling in postnatal kidney results in aberrant activation of nephron developmental programs.* Hum Mol Genet, 2011. **20**(21): p. 4155-66.
150. Reif, G.A., et al., *Tolvaptan inhibits ERK-dependent cell proliferation, Cl- secretion, and in vitro cyst growth of human ADPKD cells stimulated by vasopressin.* American Journal of Physiology-Renal Physiology, 2011. **301**(5): p. F1005-F1013.
151. Pei, Y., *Practical Genetics for Autosomal Dominant Polycystic Kidney Disease.* Nephron Clinical Practice, 2011. **118**(1): p. C19-C30.
152. Mangoo-Karim, R., et al., *Renal epithelial fluid secretion and cyst growth: the role of cyclic AMP.* FASEB J, 1989. **3**(14): p. 2629-32.
153. Neufeld, T.K., et al., *In vitro formation and expansion of cysts derived from human renal cortex epithelial cells.* Kidney Int, 1992. **41**(5): p. 1222-36.
154. Davidow, C.J., et al., *The cystic fibrosis transmembrane conductance regulator mediates transepithelial fluid secretion by human autosomal dominant polycystic kidney disease epithelium in vitro.* Kidney Int, 1996. **50**(1): p. 208-18.
155. Wallace, D.P., J.J. Grantham, and L.P. Sullivan, *Chloride and fluid secretion by cultured human polycystic kidney cells.* Kidney Int, 1996. **50**(4): p. 1327-36.
156. Su, X., et al., *Bardet-Biedl syndrome proteins 1 and 3 regulate the ciliary trafficking of polycystic kidney disease 1 protein.* Hum Mol Genet, 2014. **23**(20): p. 5441-51.
157. Xu, Q., et al., *BBS4 and BBS5 show functional redundancy in the BBSome to regulate the degradative sorting of ciliary sensory receptors.* Sci Rep, 2015. **5**: p. 11855.
158. Yamaguchi, T., et al., *cAMP stimulates the in vitro proliferation of renal cyst epithelial cells by activating the extracellular signal-regulated kinase pathway.* Kidney Int, 2000. **57**(4): p. 1460-71.

159. Yamaguchi, T., et al., *Renal accumulation and excretion of cyclic adenosine monophosphate in a murine model of slowly progressive polycystic kidney disease.* Am J Kidney Dis, 1997. **30**(5): p. 703-9.
160. Keady, B.T., et al., *IFT25 links the signal-dependent movement of Hedgehog components to intraflagellar transport.* Dev Cell, 2012. **22**(5): p. 940-51.
161. Liew, G.M., et al., *The intraflagellar transport protein IFT27 promotes BBSome exit from cilia through the GTPase ARL6/BBS3.* Dev Cell, 2014. **31**(3): p. 265-78.
162. Nager, A.R., et al., *An Actin Network Dispatches Ciliary GPCRs into Extracellular Vesicles to Modulate Signaling.* Cell, 2017. **168**(1-2): p. 252-263 e14.
163. Rovida, E. and B. Stecca, *Mitogen-activated protein kinases and Hedgehog-GLI signaling in cancer: A crosstalk providing therapeutic opportunities?* Semin Cancer Biol, 2015. **35**: p. 154-67.
164. Tian, F., et al., *The hedgehog pathway inhibitor GDC-0449 alters intracellular Ca2+ homeostasis and inhibits cell growth in cisplatin-resistant lung cancer cells.* Anticancer Res, 2012. **32**(1): p. 89-94.
165. Choi, Y.H., et al., *Polycystin-2 and phosphodiesterase 4C are components of a ciliary A-kinase anchoring protein complex that is disrupted in cystic kidney diseases.* Proc Natl Acad Sci U S A, 2011. **108**(26): p. 10679-84.
166. Zhou, X., et al., *Therapeutic targeting of BET bromodomain protein, Brd4, delays cyst growth in ADPKD.* Hum Mol Genet, 2015. **24**(14): p. 3982-93.
167. Long, J., et al., *The BET bromodomain inhibitor I-BET151 acts downstream of smoothened protein to abrogate the growth of hedgehog protein-driven cancers.* J Biol Chem, 2014. **289**(51): p. 35494-502.
168. Stecca, B., et al., *Melanomas require HEDGEHOG-GLI signaling regulated by interactions between GLI1 and the RAS-MEK/AKT pathways.* Proc Natl Acad Sci U S A, 2007. **104**(14): p. 5895-900.
169. Schnidar, H., et al., *Epidermal growth factor receptor signaling synergizes with Hedgehog/GLI in oncogenic transformation via activation of the MEK/ERK/JUN pathway.* Cancer Res, 2009. **69**(4): p. 1284-92.
170. Seto, M., et al., *Regulation of the hedgehog signaling by the mitogen-activated protein kinase cascade in gastric cancer.* Mol Carcinog, 2009. **48**(8): p. 703-12.
171. McNamara, P.J. and M. Abbassi, *Neonatal exposure to drugs in breast milk.* Pharm Res, 2004. **21**(4): p. 555-66.
172. Montagutelli, X., *Effect of the genetic background on the phenotype of mouse mutations.* J Am Soc Nephrol, 2000. **11 Suppl 16**: p. S101-5.
173. Woo, D.D., et al., *Genetic identification of two major modifier loci of polycystic kidney disease progression in pcy mice.* J Clin Invest, 1997. **100**(8): p. 1934-40.
174. Upadhya, P., et al., *Genetic modifiers of polycystic kidney disease in intersubspecific KAT2J mutants.* Genomics, 1999. **58**(2): p. 129-37.
175. Iakoubova, O.A., H. Dushkin, and D.R. Beier, *Genetic analysis of a quantitative trait in a mouse model of polycystic kidney disease.* Am J Respir Crit Care Med, 1997. **156**(4 Pt 2): p. S72-7.
176. Fry, J.L., Jr., et al., *A genetically determined murine model of infantile polycystic kidney disease.* J Urol, 1985. **134**(4): p. 828-33.

177. Takahashi, H., et al., *A hereditary model of slowly progressive polycystic kidney disease in the mouse.* J Am Soc Nephrol, 1991. **1**(7): p. 980-9.
178. Tang, Y., et al., *Epigenetic targeting of Hedgehog pathway transcriptional output through BET bromodomain inhibition.* Nat Med, 2014. **20**(7): p. 732-40.
179. Fu, W., et al., *Role for the IFT-A Complex in Selective Transport to the Primary Cilium.* Cell Rep, 2016. **17**(6): p. 1505-1517.
180. Touyz, R.M., et al., *Angiotensin II and endothelin-1 regulate MAP kinases through different redox-dependent mechanisms in human vascular smooth muscle cells.* J Hypertens, 2004. **22**(6): p. 1141-9.
181. Plotnikov, A., et al., *The MAPK cascades: signaling components, nuclear roles and mechanisms of nuclear translocation.* Biochim Biophys Acta, 2011. **1813**(9): p. 1619-33.
182. Weinberg, R.A., *The retinoblastoma protein and cell cycle control.* Cell, 1995. **81**(3): p. 323-30.
183. Merta, M., et al., *Cytokine profile in autosomal dominant polycystic kidney disease.* Biochemistry and Molecular Biology International, 1997. **41**(3): p. 619-624.
184. Weimbs, T. and J.J. Talbot, *STAT3 Signaling in Polycystic Kidney Disease.* Drug Discov Today Dis Mech, 2013. **10**(3-4): p. e113-e118.
185. Wang, Y., et al., *STAT3 activation in response to IL-6 is prolonged by the binding of IL-6 receptor to EGF receptor.* Proc Natl Acad Sci U S A, 2013. **110**(42): p. 16975-80.
186. Takakura, A., et al., *Pyrimethamine inhibits adult polycystic kidney disease by modulating STAT signaling pathways.* Hum Mol Genet, 2011. **20**(21): p. 4143-54.
187. Schust, J., et al., *Stattic: a small-molecule inhibitor of STAT3 activation and dimerization.* Chem Biol, 2006. **13**(11): p. 1235-42.
188. Gavino, A.C., et al., *STAT3 inhibition prevents lung inflammation, remodeling, and accumulation of Th2 and Th17 cells in a murine asthma model.* Allergy, 2016. **71**(12): p. 1684-1692.
189. Yokota, T., et al., *STAT3 inhibition attenuates the progressive phenotypes of Alport syndrome mouse model.* Nephrol Dial Transplant, 2018. **33**(2): p. 214-223.
190. Jung, K.H., et al., *Multifunctional Effects of a Small-Molecule STAT3 Inhibitor on NASH and Hepatocellular Carcinoma in Mice.* Clin Cancer Res, 2017. **23**(18): p. 5537-5546.
191. Idowu, J., et al., *Aberrant Regulation of Notch3 Signaling Pathway in Polycystic Kidney Disease.* Sci Rep, 2018. **8**(1): p. 3340.
192. Le, N.H., et al., *Increased activity of activator protein-1 transcription factor components ATF2, c-Jun, and c-Fos in human and mouse autosomal dominant polycystic kidney disease.* J Am Soc Nephrol, 2005. **16**(9): p. 2724-31.
193. Omori, S., et al., *Extracellular signal-regulated kinase inhibition slows disease progression in mice with polycystic kidney disease.* J Am Soc Nephrol, 2006. **17**(6): p. 1604-14.
194. Yanagisawa, M., et al., *A novel potent vasoconstrictor peptide produced by vascular endothelial cells.* Nature, 1988. **332**(6163): p. 411-5.
195. Simonson, M.S., *Endothelins: multifunctional renal peptides.* Physiol Rev, 1993. **73**(2): p. 375-411.
196. Barton, M. and M. Yanagisawa, *Endothelin: 20 years from discovery to therapy.* Can J Physiol Pharmacol, 2008. **86**(8): p. 485-98.

197. Ong, A.C., L.J. Newby, and M.R. Dashwood, *Expression and cellular localisation of renal endothelin-1 and endothelin receptor subtypes in autosomal-dominant polycystic kidney disease.* Nephron Exp Nephrol, 2003. **93**(2): p. e80.
198. Hocher, B., et al., *Endothelin-1 transgenic mice develop glomerulosclerosis, interstitial fibrosis, and renal cysts but not hypertension.* J Clin Invest, 1997. **99**(6): p. 1380-9.
199. Hocher, B., et al., *Renal endothelin system in polycystic kidney disease.* J Am Soc Nephrol, 1998. **9**(7): p. 1169-77.
200. Karihaloo, A., et al., *Macrophages promote cyst growth in polycystic kidney disease.* J Am Soc Nephrol, 2011. **22**(10): p. 1809-14.
201. Swenson-Fields, K.I., et al., *Macrophages promote polycystic kidney disease progression.* Kidney Int, 2013. **83**(5): p. 855-64.
202. Mrug, M., et al., *Overexpression of innate immune response genes in a model of recessive polycystic kidney disease.* Kidney Int, 2008. **73**(1): p. 63-76.
203. Su, Z., et al., *Excessive activation of the alternative complement pathway in autosomal dominant polycystic kidney disease.* J Intern Med, 2014. **276**(5): p. 470-85.
204. Levy, D.E. and J.E. Darnell, Jr., *Stats: transcriptional control and biological impact.* Nat Rev Mol Cell Biol, 2002. **3**(9): p. 651-62.
205. Peda, J.D., et al., *Autocrine IL-10 activation of the STAT3 pathway is required for pathological macrophage differentiation in polycystic kidney disease.* Dis Model Mech, 2016. **9**(9): p. 1051-61.
206. Talbot, J.J., et al., *Polycystin-1 regulates STAT activity by a dual mechanism.* Proc Natl Acad Sci U S A, 2011. **108**(19): p. 7985-90.
207. Lin, T.H., et al., *Anti-androgen receptor ASC-J9 versus anti-androgens MDV3100 (Enzalutamide) or Casodex (Bicalutamide) leads to opposite effects on prostate cancer metastasis via differential modulation of macrophage infiltration and STAT3-CCL2 signaling.* Cell Death Dis, 2013. **4**: p. e764.
208. Chapman, R.S., et al., *Suppression of epithelial apoptosis and delayed mammary gland involution in mice with a conditional knockout of Stat3.* Genes Dev, 1999. **13**(19): p. 2604-16.
209. Chung, J., et al., *STAT3 serine phosphorylation by ERK-dependent and -independent pathways negatively modulates its tyrosine phosphorylation.* Mol Cell Biol, 1997. **17**(11): p. 6508-16.
210. Zhang, X., et al., *Requirement of serine phosphorylation for formation of STAT-promoter complexes.* Science, 1995. **267**(5206): p. 1990-4.
211. Low, S.H., et al., *Polycystin-1, STAT6, and P100 function in a pathway that transduces ciliary mechanosensation and is activated in polycystic kidney disease.* Dev Cell, 2006. **10**(1): p. 57-69.
212. Matsuno, M., et al., *Involvement of protein kinase C activation in endothelin-1-induced secretion of interleukin-6 in osteoblast-like cells.* Cell Signal, 1998. **10**(2): p. 107-11.
213. Tanaka, T., M. Narazaki, and T. Kishimoto, *IL-6 in inflammation, immunity, and disease.* Cold Spring Harb Perspect Biol, 2014. **6**(10): p. a016295.
214. Pereira, T.A., et al., *Macrophage-derived Hedgehog ligands promotes fibrogenic and angiogenic responses in human schistosomiasis mansoni.* Liver Int, 2013. **33**(1): p. 149-61.

215. Wang, B., J.F. Fallon, and P.A. Beachy, *Hedgehog-regulated processing of Gli3 produces an anterior/posterior repressor gradient in the developing vertebrate limb.* Cell, 2000. **100**(4): p. 423-34.
216. Lee, S.H. and S. Somlo, *Cyst growth, polycystins, and primary cilia in autosomal dominant polycystic kidney disease.* Kidney Res Clin Pract, 2014. **33**(2): p. 73-8.
217. Malone, A.M., et al., *Primary cilia mediate mechanosensing in bone cells by a calcium-independent mechanism.* Proc Natl Acad Sci U S A, 2007. **104**(33): p. 13325-30.
218. Eichenlaub-Ritter, U. and I. Betzendahl, *Chloral hydrate induced spindle aberrations, metaphase I arrest and aneuploidy in mouse oocytes.* Mutagenesis, 1995. **10**(6): p. 477-86.
219. Puri, S., et al., *Polycystin-1 activates the calcineurin/NFAT (nuclear factor of activated T-cells) signaling pathway.* J Biol Chem, 2004. **279**(53): p. 55455-64.